

Co-targeting among MicroRNAs is Widespread and Enriched in the Brain

by

Jennifer M. Cherone

B.A. Molecular and Cell Biology
with an emphasis in Genetics, Genomics, and Development
University of California, Berkeley (2011)

Submitted to the Department of Biology
in Partial Fulfillment of the Requirements for the Degree of

DOCTOR OF PHILOSOPHY

at the

MASSACHUSETTS INSTITUTE OF TECHNOLOGY

February 2019

© 2019 Massachusetts Institute of Technology.
All rights reserved.

Signature of Author:

Signature redacted

Department of Biology
November 16, 2018

Certified by:

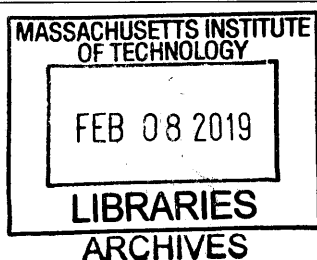
Signature redacted

Christopher B. Burge
Professor of Biology
Thesis Supervisor

Accepted by:

Signature redacted

Amy E. Keating
Professor of Biology
Chair, Biology Graduate Committee





77 Massachusetts Avenue
Cambridge, MA 02139
<http://libraries.mit.edu/ask>

DISCLAIMER NOTICE

Due to the condition of the original material, there are unavoidable flaws in this reproduction. We have made every effort possible to provide you with the best copy available.

Thank you.

The images contained in this document are of the best quality available.

Co-targeting among MicroRNAs is Widespread and Enriched in the Brain

by

Jennifer M. Cherone

Submitted to the Department of Biology on November 17, 2018 in Partial Fulfillment of the Requirements for the Degree of Doctor of Philosophy in Biology

Abstract

MicroRNAs (miRNAs) play roles in diverse developmental processes and cellular differentiation. Distinct miRNAs have hundreds to thousands of conserved binding sites in mRNAs, but typically exert only modest repression on a single site. Co-targeting of individual mRNAs by multiple different miRNAs could be commonly used to achieve stronger and more complex patterns of repression. Comparing target sets of different miRNAs, we identified hundreds of pairs of miRNAs that share more mRNA targets than expected (often ~2-fold or more) relative to stringent controls. For one co-targeting pair, miR-138 and miR-137, we validated functional overlap in neuronal differentiation. Clustering of the pairing relationships revealed a group of 9 predominantly brain-enriched miRNAs that share many targets. In reporter assays, subsets of these miRNAs together repressed gene expression by 5- to 10-fold or more, sometimes exhibiting cooperative repression. Our results uncover an unexpected pattern in which certain combinations of miRNAs can collaborate to strongly repress particular targets, and suggest important developmental roles.

Thesis Supervisor:

Christopher B. Burge, Professor of Biology

To my grandparents:

Julie and Tony Cherone

&

Betty and Eugene Millard

*For always considering me a “smart investment”
and having boundless pride.*

Acknowledgements

My journey to where I am today – graduating with my PhD from MIT – has been both a difficult and fortunate one. I never would have thought in my wildest dreams growing up that I could achieve this, and I have many people to thank for helping me to get here.

I grew up in a family of five with two sisters. My father was a mechanic and worked long hard days in the school bus yard. My mother worked various jobs throughout my childhood to help with the family finances. When I was very young she ran a family daycare business, and I can remember our house always being full of other children. When I was in elementary school, she started working nights as a waitress – I remember missing her profoundly at bedtime. In later years, she was lucky to get work in the school district to better match the schedule of my sisters and I – first as a lunch lady and then as a school health assistant – always quick to correct people that she was not a nurse. My parents worked hard to make sure they could provide for us and give us as much as they could. They never took vacations or spent money in any frivolous way. My parents provided an early example to me of how even with very little, hard work and a strong will can get you very far. I can remember from the time I was in elementary school, my mother would tell me that I could and would go to college, but that I needed to work very hard so that I could get lots of scholarships – getting it in your head that you belong is half the battle.

I was sandwiched in the middle of my sisters Danielle and Rebecca. They will always be two of my best friends, and they have both supported and encouraged me more than I can say. I fully credit Danielle with teaching me how to write – I can remember the night still when I was struggling to write an essay for my high school English class, and with Danielle’s guidance something clicked. Those principles have guided my writing since and have been crucial to my success. Rebecca is the kind soul of our family. She calls everyone weekly, just because she wants to ‘hear your voice.’ During the many times in graduate school when I felt too busy and stressed to talk to anyone, Rebecca never let that happen. I am so grateful to have them both in my life.

My grandparents have also been very influential in my life. On my mother’s side, my grandmother Betty passed away when I was a toddler from breast cancer. While I have few memories of her, I can see my mother’s undying love for her daily – and this served as an early motivator for me to want to do research. My grandfather Eugene would always give me a great big bear hug when he would see me, and with his prickly, stubbled face brushing my cheek, he would whisper into my ear, “I am *so* proud of you.” I never really knew exactly what he was proud of, but it made me feel very special and loved...and like I was capable of making someone proud. It made me want to work harder – to keep making him proud.

On my father’s side, my grandmother Julie was a fiery spirit with a fight inside her, not so unlike myself. She was the first in her family to graduate from high school when her mother did not even know how to read or write. I lived with my grandparents in Cambria, CA for the summer between my sophomore and junior years in high school and worked at Hearst Castle. My grandmother would pick me up from work and make me go out to eat in my State Parks uniform. I was mortified to be seen in these green high-waisted puckering pants and oversized khaki shirt with state park badges on each sleeve. But my grandmother was proud, and I believe she wanted

to teach me to never be ashamed or embarrassed of myself. My grandfather, Tony, always expressed an interest in my research and would tell me how impressed he was. This was really special and motivating for me.

My partner in life, Peter McCullagh, has supported me in every imaginable way. When I decided to go to MIT for graduate school, he picked up his life and moved with me. He has always put my dreams and goals above his own, and I am grateful for his eternal belief in me. In my early days of graduate school, I was always stressed and worried about what I didn't know. Peter would stop me and say, 'Of course you don't know everything. You're a student, and you are here to learn.' I didn't always like hearing this because I didn't always believe it, but it became a sort of mantra for me in tough times – *I am a student. I am here to learn.* In the last couple years of my PhD when I begin coming into lab seven days a week, Peter took care of me in every way – he cooked me breakfast and dinner nearly every day, did all of the laundry, cleaned the house. I am not sure I could have done it without his support.

During my time at UC Berkeley, I became an early version of the scientist I am today. In my sophomore year I got two work-study jobs in different labs. In one, I would make stock reagents and change the trash, and in the other, I would split cells for hours, helping to maintain more than 40 cell lines for the Berkeley campus. It is funny to think back to how much I loved just splitting cells all day, but I felt immensely lucky and I am still grateful to Ann Fischer for giving me the job and teaching me the best possible sterile technique.

In my junior year at Berkeley, I begin doing research at with my professor, Fyodor Urnov, at Sangamo Biosciences. I had been so impressed and inspired by his lectures, I wrote to him asking if he had any research opportunities available, not even fully understanding that he was a senior scientist at a biotech company and not at Berkeley. I don't know why he answered my email out of all of the student emails he received and decided to give me a chance at Sangamo, but I am eternally grateful, as my time at Sangamo came to define me more than any other experience. At Sangamo, I worked hard – I stacked all of my classes on Tuesday and Thursday, and I worked M/W/F at Sangamo for about 30 hours a week. Because of this, I learned an immense amount. At Sangamo, I worked directly under Bryan Zeitler. Bryan taught me the basis of everything I know in the wet lab. Thanks to him, I became a proficient experimentalist, which was key to my success in graduate school. My lab mates are constantly impressed with all of my tips and tricks – and they are all from Bryan. Bryan was also an avid photographer and rock climber, as well as a father, and he demonstrated to me the importance of having a balanced life.

Fyodor was by far one of the biggest influencers in my life. He literally taught me how to pipette. On my first day at Sangamo, he sent me home with a 50mL falcon tube, so that I could practice opening and closing it with just my left hand. During my time at Sangamo, I fell in love with research and was inspired by everything that was possible to do with science – and Fyodor's undying passion and enthusiasm was a major driver behind that. Maybe most importantly, Fyodor made me see value and possibility in myself. He was one of the first people to believe in me and tell me I was talented, and I cannot say how important that was for me. I keep one lesson from Fyodor close to my heart and have shared it with others in tough times, he told me, "Jennifer, everyone fails – what matters is how you respond to that failure." I am eternally grateful for Fyodor's mentorship.

At MIT, I was very lucky to be able to join Chris Burge's lab. Chris has some sort of magical power to build the most welcoming yet scientifically rigorous lab environment. Coming out of graduate school, I truly believe that the people you are around influence your growth more than anything else, and in Chris's lab, I can say without a doubt I was around the best. My lab mates were friendly and kind and always willing to take the time to help me or to explain something, and they were brilliant – I am so impressed with each and every one of them and their abilities. I hesitate to list names because I don't want to leave anyone out, but I want to recognize a couple actions that meant so much. Thank you to Peter Sudmant and Danny Dominguez for sitting down with me and helping me figure out how to organize my research into something that could begin to look like a story and a manuscript. Thank you to Maria Alexis for always being willing to talk about statistics or how to code something – you are the MVP in the lab. Thank you to Bridget Begg for transforming our lab into one where everyone talked and conversed much more than before you got there. And thank you Maria and Bridget for being my graduate student support and friends when things were tough. Thank you to Marvin Jens for your enthusiasm about my project and constant excitement – you brought me back up when I felt down. Thank you Ana Fiszbein and Athma Pai for being phenomenal role models of successful women in science. Thank you all for teaching me how to give a good talk – this is a tough skill and one I will have forever.

Chris provided an excellent space for me to experiment and grow as a scientist. I am grateful for the freedom he gave me to try different things while always supporting my endeavors even when things were not working. His guidance on the computational aspects of this work was crucial to the project's success and rigor. Chris fosters a special way to think and do science in the lab. I will forever know what it means to 'follow the data.' I have truly grown so much since I joined the lab, and I am immensely grateful for this.

My committee members, David Sabatini, Phil Sharp, and Myriam Heiman, were an tremendous help to me throughout my time at MIT. Committee meetings often resulted in pivotal shifts in my project and focus thanks to their insightful thoughts and suggestions. I would also like to thank Frank Slack for joining as my external committee member for my thesis defense.

I am grateful for my friends and classmates who did not let us drift apart even when I isolated myself in the lab. Gina Mawla, Justin Chen, and Hannah Wirtshafter – I am so glad that we could share our experience at MIT together and thank you for all of the support over the years. Thank you Hannah for being there for me when I broke all those bones in my face – I will never forget your kindness. To my very best friends from Berkeley, Jocelynn Pearl and Albert Luong, thank you for all of the visits and support over the years. I am so proud of you both and everything you have achieved, and I hope that we can continue to grow together.

And a huge *thank you* to everyone else that I did not have the space to mention.

Table of Contents

Abstract	3
Acknowledgements	5
Table of Contents	8
Chapter 1: Introduction	10
Overview	11
A brief history and the mechanics of microRNAs	11
Initial discovery and large-scale identification of miRNA genes	11
Biogenesis	13
Target recognition	15
Mechanisms of repression	18
Factors that influence targeting efficacy	20
miRNAs working together	25
Combinatorial activity by miRNAs	25
Examples of synergism by miRNAs	27
miRNAs in the brain	28
miR-124 in neuronal differentiation	29
Additional roles of neuronal miRNAs	30
References	33
Chapter 2: Cotargeting among microRNAs is widespread, and is highly enriched in the brain	45
Abstract	46
Introduction	47
Results	50
Co-targeting by distinct miRNA pairs is prevalent	50
The co-targeting miRNAs miR-138 and miR-137 coordinately increase across neuronal differentiation	52
<i>mir-138</i> is required for the differentiation of CAD cells	55

miR-137 can rescue a block in neuronal differentiation caused by loss of <i>mir-138</i>	61
Groups of miRNAs preferentially share targets with one another.....	66
Groups of brain cluster miRNAs can collaborate to exert strong repression	67
Co-targeting miRNA sites with close spacing act cooperatively	74
Co-targeting miRNAs direct potent and complex patterns of repression	75
Discussion	80
Acknowledgements	83
Author contribution.....	83
Supplemental figures	84
Methods.....	89
References.....	98
Chapter 3: Conclusions	103
Implications	104
Future Directions	107
References.....	109
Appendix I: Supplemental Tables to Chapter 2	111
Table I-S1.....	112
Table I-S2.....	118
Table I-S3.....	120
Table I-S4.....	124
Biographical Note	130

Chapter 1:

Introduction

Overview

microRNAs (miRNAs) are small non-coding RNAs that repress expression of specific target genes through recognition of a sequence complementary to the seed (nucleotides 2 - 8) of the miRNA. Collectively, the hundreds of confidently annotated miRNAs are predicted to target over 60% of protein coding genes in the mammalian genome (Friedman et al., 2008), yielding a profound amount of regulatory potential en masse. Research over the past two decades has revealed roles for miRNAs in a multitude of diverse cellular processes and their contribution to disease pathogenesis (Bartel, 2018). Here, I will review what we have learned about miRNAs since their initial discovery in 1993 in an effort to connect this to how we think miRNAs function to meaningfully impact gene regulation and the questions that have yet to be answered in the field.

A brief history and overview of microRNAs

Initial discovery and large-scale identification of miRNA genes

The first microRNA (miRNA) gene, *lin-4*, was identified in *C. Elegans* as an essential regulator of the developmental timing of early larval development. Victor Ambros and colleagues discovered that *lin-4* did not encode a protein but rather two RNA transcripts of approximately 22 and 61 nt in size and proposed that the shorter product may be processed from the from the longer one, later defined as the mature and precursor miRNAs (Lee et al., 1993). These small RNA species contained antisense complementarity to a sequence element found repeated in the 3' untranslated region (UTR) of *lin-14* mRNA, which was shown to be necessary for the regulation of *lin-14* by *lin-4* (Wightman et al., 1993). The true gravity of this finding would come to be understood several years later with the discovery of *let-7* in *C. Elegans*, an

essential regulator of *lin-41* in the transition from late larval development to adult cell fates (Reinhart et al., 2000; Slack et al., 2000). And more consequential, *let-7* homologs were identified across a range of bilaterian animal species, including vertebrates, ascidian, hemichordates, and others (Pasquinelli et al., 2000). In the year to follow, small RNA cloning and sequencing experiments in worms, flies, and mammals revealed over a hundred similar short non-coding RNAs, defining a new conserved class of small regulatory RNAs that would be named miRNAs after their small size and unknown function (Lagos-Quintana et al., 2001; Lau et al., 2001; Lee and Ambros, 2001).

The field experienced a rapid expansion in the number and types of studies, defining hundreds of additional miRNA sequences in more than 200 species using both experimental and computational methods (Kozomara and Griffiths-Jones, 2014; Lai et al., 2003; Lim et al., 2003). Sequencing of miRNAs in different mammalian tissues and cell types revealed tissue-specific signatures of miRNA expression (Houbaviy et al., 2003; Lagos-Quintana et al., 2003; 2002; Landgraf et al., 2007), suggesting roles for miRNAs in the definition or maintenance of particular cell types (discussed further in a later section.) High throughput sequencing of small RNAs paired with stringent criteria for defining a miRNA gene (Lu et al., 2005; Ruby et al., 2006) puts current estimates of confidently annotated canonical miRNAs at 147 in *C. Elegans* (Jan et al., 2011), 164 in *Drosophila* (Fromm et al., 2015), 475 in mouse (Chiang et al., 2010), and 519 in human (Fromm et al., 2015). These miRNAs can be grouped into seed families with one another on the basis of sharing the same seed sequence and thus likely recognizing and regulating the same set of targets. Of the aforementioned 519 human miRNA genes, 296 fall within 177 seed families conserved among placental mammals, 200 fall within 89 seed families conserved among vertebrates, and 75 fall within 27 seed families conserved to the bilaterian

common ancestor of humans, flies, and nematodes (Bartel, 2018), revealing sets of both deeply conserved and more newly evolved miRNAs.

Biogenesis

miRNAs are encoded in both intergenic regions under the control of their own promoter and within introns of pre-mRNAs, the latter constituting about a quarter of conserved miRNAs and more than half of all poorly conserved mammalian miRNAs (Chiang et al., 2010). These primary miRNA (pri-miRNA) sequences are transcribed by RNA Polymerase II (Pol II) and contain an imperfect hairpin from which the mature miRNA will be processed (Lee et al., 2004). Pri-miRNAs transcribed from intergenic regions are 5' capped and often polyadenylated (Cai et al., 2004), while those contained in introns can be spliced out of the pre-mRNA or transcribed independently but are most commonly co-expressed with the host gene (Baskerville and Bartel, 2005; Rodriguez et al., 2004). Many miRNAs are clustered in the genome and are expressed as a single polycistronic pri-miRNA from which multiple different miRNAs can be processed, allowing the co-expression of these miRNAs upon transcriptional activation (Lee et al., 2002).

In the canonical pathway, miRNA hairpins are processed out of the pri-miRNA by Microprocessor, a heterotrimeric complex containing one molecule of the Drosha endoribonuclease and two molecules of its double stranded RNA-binding cofactor DGCR8. Drosha, which contains two RNase III domains, makes two asymmetric cuts approximately 11 bp from the basal ssRNA-dsRNA junction (an interaction which is stabilized and made accurate by the interaction of DGCR8 with the stem and apical junction) producing a ~66 nt stem-loop structure called the precursor miRNA (pre-miRNA), which bears a 5' monophosphate (MP) and a 2 nt 3' overhang (Lee et al., 2003; Nguyen et al., 2015). The pre-miRNA is exported from

nucleus to the cytoplasm by the nuclear export factor, exportin-5, in a RanGTP-dependent manner (Bohnsack et al., 2004; Lund et al., 2004; Yi et al., 2003). Once in the cytoplasm, the pre-miRNA is further processed by Dicer, an endonuclease that makes two cuts to generate the miRNA duplex with ~2 nt 3' overhangs on each end (Zhang et al., 2004). Later studies revealed some sequence specificity beyond the known structural requirements that can enhance the efficiency of processing: GHG motif near the base of the stem (positions 7 - 9) with the central base mismatched (Fang and Bartel, 2015), UG at the 5' base of the stem, UGU at the 5' end of the apical loop, and CNNC 5 nt 3' of the stem (Auyeung et al., 2013). The sequence and structural specificity for miRNA processing has helped to define rules for miRNA gene discovery and can instruct de novo design of miRNA hairpins.

The miRNA duplex is loaded into Argonaute (AGO), which lies at the heart of the RNA-Induced Silencing Complex (RISC), with the help from two chaperone proteins, HSC70/HSP90, that shift AGO to an open conformation permissive of the miRNA duplex, in an ATP-dependent manner (Iwasaki et al., 2010; Kawamata and Tomari, 2010). One of the strands of the miRNA duplex is preferentially selected as the guide strand, which stays in AGO, and the other becomes the passenger strand, which is removed from the complex and degraded. The strand selection is based on the original orientation of duplex loading: AGO favors the strand with the thermodynamically less stable 5'-terminal pairing as the guide strand (Khvorova et al., 2003; Schwarz et al., 2003), in addition to preference for an AMP or UMP at the 5' end which permits a more optimal fit into the phosphate-binding pocket at the junction of the MID and PIWI domains of AGO (Frank et al., 2010; Suzuki et al., 2015). The miRNA-loaded RISC is equipped and ready to carry out sequence-specific regulation of target genes.

Target recognition

For newly discovered miRNAs, aptly named for their small size but unknown function when first identified, accurate target predictions were key to understanding what functions they might serve in a cell. The complementarity observed between *lin-4* or *let-7* and sequences in the 3' UTR of each miRNA's respective target, *lin-28* or *lin-41*, provided the first indications as to how miRNAs target specific mRNAs (Lee et al., 1993; Reinhart et al., 2000; Wightman et al., 1993). The most defining feature for predicting targets of a miRNA is Watson-Crick pairing through the seed region (nucleotides 2 – 7) at the 5' end of the miRNA (Lewis et al., 2003). This helps to explain why the 5' end of the miRNA is the most conserved region of metazoan miRNA genes (Lim et al., 2003). Preferential conservation of the canonical target site, defined by uninterrupted pairing to the miRNA seed, vastly improved target predictions (Brennecke et al., 2005; Krek et al., 2005; Lewis et al., 2005). Bases opposite position 1 and 8 of the miRNA were also strongly conserved. While the base opposite position 8 showed a strong bias to provide additional Watson-Crick pairing, the base opposite position 1 had a strong bias for adenosine, regardless of the base in the miRNA (Lewis et al., 2005). The majority of miRNAs actually begin with a U (Lau et al., 2001), but for miRNAs that do not, requiring an A at position 1 is a better predictor of targeting than Watson-Crick pairing at this position (Baek et al., 2008; Nielsen et al., 2007). This is because the A does not pair with the miRNA but is inserted into a binding pocket of Argonaute which serves to further stabilize the miRNA:target interaction (Schirle et al., 2014). Based on these principles, several canonical target site types were defined; these include: the 8mer, 7mer-m8, 7mer-A1, and 6mer site (sites are listed in order of decreasing preferential conservation and repressive ability). It should be noted that 6mer sites typically

confer regulation barely over that of background, so these sites are generally not considered in most analyses (Agarwal et al., 2015; Grimson et al., 2007; Nielsen et al., 2007).

Supplementary pairing to the 3' end of the miRNA does not strongly increase target site effectiveness (Baek et al., 2008; Grimson et al., 2007). A present but modest effect, possessing higher preferential conservation and conferring greater target repression, is only observed for supplementary pairing centered on miRNA bases 13 to 16 (Grimson et al., 2007), thus the term “3' supplementary pairing” refers to this specific form of pairing to the 3' region. Structural studies support that bases 13 – 16 are special. After target binding is initiated through guide nucleotides 2 to 5, AGO undergoes a conformational change exposing nucleotides 6 – 8 and 13 – 16 (Schirle et al., 2014), thus it is logical that this 3' region would be the most instructive for target binding after the seed itself. These 3' supplementary sites, containing both 3' supplementary pairing and full complementarity to the seed, are atypical, ~5% of canonical conserved target sites (Friedman et al., 2008), and have a modest impact on the levels of target repression (Grimson et al., 2007) and target affinity (Salomon et al., 2015; Wee et al., 2012), or if the supplementary pairing does increase affinity, it appears to be specific to only some miRNAs (Salomon et al., 2015).

3' supplementary pairing can help compensate for a mismatch or bulge in the miRNA seed – this is called a 3' compensatory site. This site type requires more extensive complementarity to the 3' region, at least 9 consecutive bases in all experimentally validated examples, and is rarely under selective pressure to be conserved, constituting 1% of preferentially conserved sites in mammals (Brennecke et al., 2005; Friedman and Burge, 2013; Lewis et al., 2005). However, 3' compensatory sites can have functional reasons for evolving, such as *let-7* targeting of *lin-41*. *Lin-41* contains two highly conserved 3' compensatory sites for

let-7, so why conserve these sites so strongly if they are less effective and more difficult to conserve? The reason lies in that *let-7* has several family members in worm, which contain the same seed sequence but have distinct sequence otherwise (Lau et al., 2001; Lim et al., 2003). These paralogs are expressed at earlier stages in development than *let-7*, and so if these family members were able to target every site in *lin-41*, they might drive down *lin-41* expression too quickly and trigger early differentiation (Abbott et al., 2005; Reinhart et al., 2000). Cleverly, these sites develop imperfect pairing in the seed and extensive pairing to the 3' region to disrupt effective targeting and only restore targeting for specific paralogs with extensive 3' complementarity (Brennecke et al., 2005; Lewis et al., 2005).

Other forms of non-canonical binding may be more prevalent. High throughput sequencing of RNAs that crosslinked with AGO revealed high levels of AGO binding with no canonical 6mer target site, making up about 25-50% of all crosslink events (Chi et al., 2012; 2009; Grosswendt et al., 2014; Hafner et al., 2010; Helwak et al., 2013; Loeb et al., 2012). These studies characterized new non-canonical site types, such as pivot pairing which contains a bulged nt in the seed between position 5 and 6 (Chi et al., 2012), and found evidence that some these sites are quite prevalent, under purifying selection, and repressed but to a lesser extent than canonical motifs (Chi et al., 2012; Grosswendt et al., 2014; Helwak et al., 2013; Loeb et al., 2012). In contrast, other studies have found that these noncanonical AGO-bound mRNAs do not confer detectable levels of repression in experiments where miRNA expression is altered (Agarwal et al., 2015). McGeary and colleagues, using a new *in vitro* method to assess relative binding affinities of AGO loaded with different miRNAs (based off of the RNA Bind-n-Seq protocol (Lambert et al., 2014)), identified instances of strong binding to non-canonical sites with affinities that could exceed those of 7mer-m8 and 7mer-A1 canonical binding in some

instances (McGeary et al.). Many of these non-canonical sites are miRNA-specific, which could explain why these features of non-canonical targeting were not identified with earlier more global searches for features. For miR-124 (which had the largest number of high affinity non-canonical sites), there were 5 non-canonical sites higher affinity than the 7mer-m8, and 29 non-canonical sites with higher affinity than the 7mer-A1 sites (McGeary et al.). Many of the high affinity non-canonical sites have no seed at all but instead extensive pairing to the 3' region of the miRNA (McGeary et al.). Current models of AGO binding will need to be expanded to explain these new site types; perhaps AGO has more than one binding mode allowing it to accommodate both. Because non-canonical affinities are miRNA-specific, performing AGO-RBNS on additional miRNAs will strengthen future predictions, and in addition, modification of the technique to allow evaluation of miRNA-specific 3' supplementary effects in the presence of a canonical site could provide more accurate prediction of expected repression from individual sites.

Mechanisms of repression

miRNA-mediated repression in animals acts primarily via mRNA destabilization. Upon target recognition and binding by RISC, AGO recruits the adaptor protein TNRC6 (GW182 in flies and AIN-1/2 in nematodes) (Ding et al., 2005; Rehwinkel et al., 2005) that interacts with the Poly(A)-binding protein (PABPC) in the poly(A) tail and recruits the deadenylase complexes: the PAN2-PAN3 complex and the CCR4-NOT complex (Jonas and Izaurralde, 2015). These complexes cause shortening of the poly(A) tail, leading to mRNA destabilization through 5' decapping by the Decapping protein 2 (DCP2) and rapid 5'-to-3' decay by the exonuclease XRN1 (Chen and Shyu, 2011).

miRNAs can also act to inhibit translation through the recruitment of DDX6, a helicase that binds the decapping complex, by the CCR4-NOT complex (Chu and Rana, 2006; Jonas and Izaurralde, 2015). DDX6 also interacts with the EIF4E transporter 4E-T, which normally competes with EIF4G for binding to EIF4E, further enhancing both translational repression and mRNA destabilization (Kamenska et al., 2014; 2016; Nishimura et al., 2015; Ozgur et al., 2015). Kinetic studies of miRNA regulation revealed that translational inhibition occurs very soon after RISC binding to the target transcript, which is followed by deadenylation, decapping, and degradation of the bound mRNA target (Béthune et al., 2012; Djuranovic et al., 2012).

While early characterization focused on the effect of miRNAs on translation, later studies, which compared mRNA levels with protein expression or translational efficiency upon overexpression or depletion of a miRNA, demonstrated that decreases at the level of mRNA could explain the majority (66 - 90%) of the steady state repression by mammalian miRNAs (Baek et al., 2008; Eichhorn et al., 2014; Guo et al., 2010; Hendrickson et al., 2009). This result not only had important mechanistic implications for understanding miRNA regulation, but also had practical implications – the effects of a miRNA could be faithfully measured using RNA sequencing. However, an exception to this result lies in the cells of early embryos, in which translational repression serves as the primary mode of regulation (Bazzini et al., 2012; Subtelny et al., 2014). A notable example, miR-430 targets maternal mRNAs in the early zebrafish embryos, acting first by strongly repressing translation and only triggering decay of target mRNAs at later stages (Bazzini et al., 2012). Poly(A)-tail shortening appears to have very different consequences in the early embryo compared to post-gastrulation cells after zygotic transcription is activated. In early embryonic cells, poly(A)-tail shortening reduces translational efficiency with little effect on mRNA stability, but inversely, poly(A)-tail shortening has strong

destabilizing effects on mRNA with little effect on translational efficiency in cells post-gastrulation (Subtelny et al., 2014).

Alternatively, if a target has sufficiently extensive pairing through the center of the miRNA, AGO2, the only mammalian Argonaute to retain slicing activity (Liu et al., 2004; Meister et al., 2004), can catalyze cleavage of the target transcript (Hutvagner and Zamore, 2002; Yekta et al., 2004). In one model, substantial pairing across the target initiates a second site of nucleation at nucleotides 13-16 of the miRNA, eventually releasing the 3' end of the miRNA from its binding pocket and initiating a conformational change in AGO that brings the target in close proximity to the activated DEDH catalytic tetrad core and cleaves the target at the phosphodiester bond opposite nucleotides 10 and 11 of the miRNA (Bartel, 2018). The 5' and 3' products are then degraded by the exosome and XRN1 respectively. While this is the major mode of miRNA-mediated repression in plants (Jones-Rhoades et al., 2006), target slicing rarely occurs in mammals and has only been observed in a total of twenty-one mammalian transcripts (Davis et al., 2005; Hansen et al., 2011; Shin et al., 2010; Yekta et al., 2004).

Factors that influence targeting efficacy

Early experiments revealed that miRNA targeting was widespread – hundreds of mammalian genes were repressed following exogenous miRNA overexpression (Lim et al., 2005). Conversely, inhibiting or ablating an endogenous miRNA also had widespread effects on the transcriptome (Giraldez et al., 2006; Krützfeldt et al., 2005; Rodriguez et al., 2007). While widespread, the effects were quite modest – often repression of any given target is about 20% (Baek et al., 2008; Selbach et al., 2008). These experiments revealed the extensive regulatory effect miRNAs have on the transcriptome, but also urged the question of how to accurately

predict which targets will be regulated, and which targets will be regulated most strongly. There are additional factors beyond the presence of the 7 or 8 nt seed sequence that influence targeting efficacy. Because the study of miRNAs even still today often requires sets of predicted targets to identify direct versus indirect effects of the miRNA, target prediction remains very important.

Conservation generally serves as a good predictor of effective targeting, in addition to being an indicator of biological significance in which a gain in fitness drives the selective maintenance of the target sites (Baek et al., 2008; Brennecke et al., 2005; Krek et al., 2005; Lewis et al., 2005; Neilson et al., 2007). Mammalian miRNAs conserved through vertebrates have an average of more than 300 conserved targets containing 7 or 8mer sites (more than 400 if 6mer sites are included) – overall, more than half of all protein-coding genes are under selective pressure to maintain sites in the 3' UTR for pairing with miRNAs (Friedman et al., 2008). While conservation selects for sites that more likely to be regulated, non-conserved sites can also confer repression (Farh et al., 2005). There are an astounding 10x more poorly conserved 7mer sites than preferentially conserved sites (Farh et al., 2005). Given the huge number of non-conserved sites, one might assume that some fraction of these could exert repressive function and wreak havoc on the regulatory systems, but these non-conserved sites are mostly found in genes expressed primarily in tissues where the cognate miRNA is not expressed (Farh et al., 2005). Thus, sites can accumulate in particular 3' UTR regions (where the gene and miRNA are not co-expressed) without any detrimental effect to the organism, but sites are selectively avoided in 3' UTR regions where the gene and miRNA are both highly expressed because this would otherwise confer unwanted repression. The “selective avoidance” for sites in highly co-expressed transcripts is so robust that it is possible to accurately predict the expression patterns of miRNAs based on depleted 7 nt motifs in the 3' UTRs of transcripts that are preferentially expressed in

particular tissues (Farh et al., 2005). The most highly expressed genes contain on average about half as many non-conserved 7 nt sites than would be expected by chance (Farh et al., 2005), and provides a reasoning as to why highly expressed “house keeping” genes in animals typically have shorter 3' UTRs in general and compared to orthologs in plants and fungi which do not have extensive 3' UTR targeting – reducing 3' UTR length can be a regulatory strategy to avoid spurious targeting and repression (Farh et al., 2005; Stark et al., 2005). The combination of conservation and selective avoidance of target sites makes the evolution of almost all mammalian mRNAs under the influence of miRNAs. For the non-conserved target sites that are not selectively avoided (i.e. mRNAs containing non-conserved sites and the targeting miRNA are co-expressed), some of these may represent newly evolving, species-specific regulation, but many could also lack efficient repressive ability due to non-optimal context features.

Sites are more effective, i.e. drive stronger repression, when A/U-rich sequences flank the seed sequence (Grimson et al., 2007; Neilson et al., 2007). Recent biochemical work from the Bartel Lab also underscores the importance of flanking di-nucleotide (di-nt) content, finding that the two bases immediately upstream and downstream of the seed can alter site affinity more than changing the site type itself (McGeary et al.). The presence of an A or U in these positions enhances affinity, a G reduces affinity, and a C is somewhat neutral. In addition, the 5' flanking di-nt appears to be about 2x more important than the 3' flanking sequence (McGeary et al.), affirming earlier observations that an A/U nt opposite miRNA position 9 gives the strongest repression enhancement (Neilson et al., 2007). With the presence of two 5' flanking A's, a miR-124 site with a bulge in the seed between nucleotides 5 and 6 is almost just as strong as a perfect 8mer target site (McGeary et al.). These context preferences likely reflect an underlying preference for reduced secondary structure, in which flanking A/U bases help to ensure that the

site remains in an unpaired state, which is supported by analyses of several independent measures of structure and accessibility (Grimson et al., 2007; McGeary et al.; Robins et al., 2005).

The location of the target site within the transcript also matters. While 7mer and 8mer miRNA seed match sites can be found in the 5' UTR and in the coding sequence (CDS), sites generally only confer repression when located in the 3' UTR. Further, these sites must be at least 15 nt downstream of the stop codon, likely for the same reason that sites in the CDS do not confer repression – it is hypothesized that the ribosome prevents efficient binding by knocking off proteins in its path (Grimson et al., 2007). Target sites are also generally more effective if they are located near the start or end of the 3' UTR (Grimson et al., 2007), as more complex folded structures in the center of a long 3' UTR may occlude the site or distance it from interaction with relevant proteins like the PABPC.

Target sites also tend to be more effective if they reside in close proximity to sites for other co-expressed miRNAs (Grimson et al., 2007). This observation is likely due to the fact that target sites can be cooperative (i.e. yield more repression than expected from each site individually) if they lie within a defined distance from one another, typically 15 to 35 nt between seed starts (Doench and Sharp, 2004; Grimson et al., 2007; Saetrom et al., 2007). Early evidence suggests that TNRC6 (GW182 in flies) may contribute to this observed cooperative effect. TNRC6 is composed of an unstructured N-terminal/Ago-binding domain (ABD) and a C-terminal/silencing domain. In humans, the ABD domain contains more than 30 glycine-tryptophan (GW/WG) repeats, of which three have been shown to mediate an interaction with AGO (Lazzaretti et al., 2009; Lian et al., 2009; Takimoto et al., 2009; Till et al., 2007). While AGO can only bind a single GW motif, TNRC6 can bind up to three AGO proteins at once

(Elkayam et al., 2017). The presence of multiple guide-primed AGOs and auxiliary target sites in close proximity could result in increased dwell time on the target transcript and help to explain the cooperative effect.

Based on the occurrence of a miRNA target site in the transcriptome, miRNAs will have different target abundances, which has been proposed to alter miRNA activity (Arvey et al., 2010). The effective target abundance is defined as the number of target sites that must be added into a cell to achieve half-maximal de-repression of targets (Denzler et al., 2014). miRNAs often have limited expression compared to the many conserved and non-conserved target sites they recognize in hundreds to thousands of mRNAs. One of the most highly expressed miRNAs liver-specific miR-122, which constitutes 72% of the total miRNA in hepatocytes at 135,000 copies per cell, has an even higher effective target abundance (Chang et al., 2004; Denzler et al., 2014; 2016). This means that miRNA levels are rarely saturating and targets will remain responsive to changes in miRNA expression allowing them to dynamically regulate levels of repression through their own abundance. The finding that all effective target abundances are quite high also means that the competing endogenous RNA (ceRNA) hypothesis, which posited that fluxes in target abundances from gene expression changes could serve to regulate the activity of a miRNA, is very unlikely (Salmena et al., 2011). Extending back to our example of miR-122, 1.5×10^5 sites per cell had to be added to begin to see de-repression of miR-122 targets (Denzler et al., 2014). This value, and those calculated for additional miRNAs, exceeds the physiological expression of any one gene and is more than the sum of all predicted targets that change in a disease state, thus any changes from competing endogenous miRNAs would be small and likely inconsequential (Denzler et al., 2014; 2016).

The availability of target sites themselves can be regulated, thus turning miRNA regulation on or off for a particular gene. The usage of different 3'UTR isoforms, alternative last exons (ALEs) or tandem 3' UTRs, can be dynamically regulated and has been shown to lead to the gain or loss of miRNA target sites (Mayr and Bartel, 2009; Miura et al., 2013; Sandberg et al., 2008). For example, highly proliferative cells, like cancer cells, tend to use upstream alternative polyadenylation sites thus shortening the 3' UTR and potentially removing any miRNA-mediated repression that was encoded in that sequence. RNA editing, such as adenosine-to-inosine editing catalyzed by adenosine deaminases that act on double-stranded RNA (ADAR), could also disrupt or introduce a site for miRNA binding. One study found that 20% of A-to-I editing events were in miRNA seed sites (Borchert et al., 2009; Peng et al., 2012). Lastly, RNA binding proteins (RBPs) can compete for binding and occlude miRNA-loaded RISC binding when an RBP motif is overlapping that of a miRNA site or if the RBP footprint would sterically hinder RISC binding.

miRNAs working together

Combinatorial activity by miRNAs

The regulatory logic of miRNAs is incompletely understood – miRNAs often regulate hundreds of targets but confer only a small amount of repression, often ~20%, to each seed match site (Baek et al., 2008; Selbach et al., 2008). However, genes usually contain multiple conserved seed match sites in their 3' UTRs, with an average of 4.2 target sites per targeted 3' UTR (Friedman et al., 2008). While a gene can develop multiple sites to the same miRNA (Mayr et al., 2007), it is much more common to have sites to different miRNA families with only 7% of genes containing one or more conserved site for the same miRNA, and 72% of genes contain

more than one conserved site for any miRNA family (Friedman et al., 2008). The genes most highly targeted by all miRNAs are enriched for transcriptional regulators and nuclear factors (Hon and Zhang, 2007), which may hint that miRNAs are more likely to co-target genes in key gene regulatory networks. The repression conferred by two individual sites is multiplicative (also referred to as log-additive), so theoretically, five target sites that individually repress an mRNA to 80% of its prior level could together repress expression to $(0.8)^5 = \sim 33\%$ of its prior level (Grimson et al., 2007; Neilson et al., 2007). Two sites can confer greater repression together than they can individually if the sites lie within a cooperative distance from one another, most optimally when there is 13-35 nt between seed starts (Doench and Sharp, 2004; Grimson et al., 2007; Saetrom et al., 2007). This cooperative effect can yield stronger, more responsive tuning of gene expression, particularly where miRNAs have differences in temporal expression or varying levels across cell types.

Some early studies selected candidate genes to test for the ability for more than one miRNA to regulate it. However, the results were underwhelming with no more than 2-fold repression for two or three sites in a 3' UTR (Grimson et al., 2007; Krek et al., 2005), and in one case, no repression was observed for three sites until the authors moved the sites artificially closer to one another into a cooperative distance which also would have impacted the entire context they had evolved in (Saetrom et al., 2007). The idea of co-targeting has also been explored on a more global level, but in a limited number of studies. However, it was observed that miRNAs expressed from the same polycistronic clusters, and thus co-expressed, had target sets with overlapping genes as well as enrichments for similar pathways (Tsang et al., 2010). This demonstrated that miRNAs expressed in the same fashion have the potential to develop co-targeting relationships, possibly with a stronger and more detectable relationship than pairs of

miRNAs who do not correlate as strongly in their expression patterns. In another study, Obermayer and colleagues found that particular pairs of miRNAs had an enriched number of sites that were co-conserved in a 3' UTR together, suggesting that co-targeting can be a conserved mechanism of regulation (Obermayer and Levine, 2014).

Examples of synergism between miRNAs

Several examples of miRNAs that have synergistic effects or possible co-targeting relationships are known. For some of these, it has not been investigated where the underlying synergy is coming from – a wider breadth of targets or co-targeting a core set transcripts to drive larger levels of repression – something that may be an important distinction to make as the regulatory logic of miRNAs is investigated. For example, the neuronal miRNAs miR-9 and miR-124 can drive the direct conversion of fibroblasts to neurons in combination but not alone (Yoo et al., 2011). In another study, the role of a trio of miRNAs, miR-124, miR-128 and miR-137, in the differentiation of neural stem cells was explored, specifically by knocking down each miRNA and performing RNA-sequencing to attain a list of semi-validated targets for each miRNA (Santos et al., 2016). Their de-repressed targets sets had a striking amount of overlap leading to the possibility that they synergistically promote differentiation through their large co-targeting network which appears to converge on Sp1 (Santos et al., 2016). In another instance, Riley and colleagues identified a co-targeting relationship between Epstein-Barr virus (EBV) and highly expressed human host miRNAs of both viral and human genes involved in cell cycle and apoptosis (Riley et al., 2012). They validated some of these co-targets with luciferase assays, and for one viral RNA target BHFR1, containing 2 sites for a viral miRNA and one site for miR-142, they observed about 4-fold repression (Riley et al., 2012).

miRNAs in the brain

miRNA expression profiling has revealed high and specific/enriched expression of many miRNAs in the brain (Landgraf et al., 2007; Sempere et al., 2004) and temporal patterns of expression during development or neuronal differentiation (Krichevsky et al., 2003; Miska et al., 2004; Sempere et al., 2004), suggesting a specific role for many miRNAs in the brain. The temporal regulation and tissue-specificity of miRNA expression has long suggested that miRNAs may play a role in cellular differentiation and maintenance. In an early experiment, overexpression of either miR-124 or miR-1 in HeLa cells resulted in repression of targets specific to each miRNA but also globally shifted the transcriptome to look more like that of the tissue the transfected miRNA is primarily expressed in, brain and muscle respectively (Lim et al., 2005), demonstrating the role miRNAs can play in shaping the gene expression program of cells.

When Giraldez and colleagues generated maternal zygotic mutants of zebrafish Dicer, ablating the miRNA-processing pathway, they observed gross defects in early brain patterning and morphogenesis, demonstrating that miRNAs are essential for proper brain development (Giraldez et al., 2005). Similar severe phenotypes of defective brain patterning and neuronal differentiation were observed in mammalian systems using conditional knockouts of Dicer or other miRNA biogenesis factors (Choi et al., 2008; Cuellar et al., 2008; Damiani et al., 2008; Davis et al., 2008; Kim et al., 2007). Subsequent studies have revealed prominent roles for miRNAs in many fundamental processes of the brain, including neuronal progenitor expansion, differentiation and migration, in addition to the establishment of synaptic connections and activity-dependent plasticity of these connections (Hu and Li, 2017; Rajman and Schratt, 2017).

miR-124 in neuronal differentiation

Many miRNAs have been shown to play critical roles in neuronal differentiation through diverse cellular mechanisms (Rajman and Schratt, 2017). Here, I will highlight what is known about one of these miRNAs, miR-124, which is one of the most highly expressed, neuron-specific miRNAs (Lagos-Quintana et al., 2002), as well as one of the most well-studied miRNAs. The overexpression of miR-124 in a variety of systems, including neuronal progenitors, embryonic stem cells, glioma cells and fibroblasts, results in forced neuronal differentiation (Krichevsky et al., 2006; Silber et al., 2008; Xia et al., 2012; Yoo et al., 2011).

One mechanism by which miR-124 drives differentiation is through targeting the small C-terminal phosphatase domain 1 (CTDSP1), which phosphorylates and stabilizes RE1 silencing transcription factor (REST) (Nesti et al., 2014; Visvanathan et al., 2007). REST binds upstream of neuronal genes and strongly represses their expression, and thus REST must be repressed for neuronal differentiation to occur (Ballas et al., 2005). Interestingly, REST represses the expression of miR-124, among other neuronal miRNAs, forming a double-negative feedback loop to strongly drive differentiation in a switch-like fashion (Visvanathan et al., 2007). Because REST represses the expression of many neuronal miRNAs, it has also been proposed that there may be a larger network of miRNAs that target multiple different components of the REST complex to help drive neuronal differentiation and stabilize neuronal gene expression (Wu and Xie, 2006).

miR-124 also impacts alternative splicing through targeting polypyrimidine-tract-binding protein (PTBP1), a splicing factor which is expressed in non-neuronal cells and suppresses the inclusion of neuron-specific exons (Makeyev et al., 2007). PTBP1 negatively regulates the

expression of the neuron-enriched homolog, PTBP2, by causing exon skipping and producing a nonsense-mediated decay (NMD) isoform (Makeyev et al., 2007). As PTBP1 is repressed and PTBP2 is activated, the cells transition to a neuronal splicing program. The importance of this regulatory connection is highlighted by the finding that knocking down PTBP1 alone can drive the conversion of fibroblasts to neurons (Xue et al., 2013).

miR-124 regulates the switch to neuron-specific ATP-dependent chromatin remodeling complexes, nBAF, by down-regulating the BAF53a subunit found in non-neural and neural progenitor cells, and allowing replacement by the homologous neuron-specific BAF53b (Yoo et al., 2009). BAF complexes regulate nucleosome mobility and chromosome accessibility, and nBAF is essential for many post-mitotic functions including dendritic development (Wu et al., 2007). There is also strong evidence that both strands of miR-9 repress BAF53a (Yoo et al., 2009).

The Notch pathway controls neural progenitor cell maintenance and inhibits neuronal differentiation (Louvi and Artavanis-Tsakonas, 2006). When the Notch ligand Jagged1 (Jag1) binds the Notch transmembrane receptor, neural stem cell self-renewal is promoted and neuronal differentiation is blocked (Imayoshi and Kageyama, 2011). miR-124 targets Jag1 to turn off Notch signaling and allow differentiation to proceed (Cheng et al., 2009; Liu et al., 2011).

Additional roles of neuronal miRNAs

Following neuronal cell specification, miRNAs have also been shown to play an important role in the migration of neurons through targets like doublecortin, Foxp2, and N-cadherin (Clovis et al., 2012; Gaughwin et al., 2011; Rago et al., 2014). As neurons migrate they polarize, often having to convert from a multipolar to bipolar morphology after they reach their

final location, which once they reach, they begin to grow axons and dendrites – miRNAs are implicated in regulating each level of this (Rajman and Schratt, 2017). Axon guidance through the growth cone is dependent on local translation, and multiple miRNAs have been implicated in the regulation of this process (Rajman and Schratt, 2017). Lastly, synapse development and maintenance depends on the presence of particular miRNAs in the dendritic spine for control of local translation (Rajman and Schratt, 2017). For example, miR-134 negatively regulates dendritic spine size by inhibiting the local synthesis of *Limk1*, which promotes actin polymerization and thus growth of spines (Schratt et al., 2006). Both miR-138 and miR-137 have also been implicated in the regulation of dendritic spines (Siegel et al., 2009; Strazisar et al., 2015).

miRNAs are highly expressed in the CNS and show a striking amount subcellular specificity (Schratt, 2009). Several studies have profiled the axonal miRNA population in comparison to that of the cell body and found an abundant population of axonally expressed miRNAs, as well as an enriched set of miRNAs in the axon implying a selective functional role for certain miRNAs within the axon and at the synapse (Natera-Naranjo et al., 2010; Sasaki et al., 2013). For some of these miRNAs, specific roles have been demonstrated in these distal compartments, for example, *mir-9* has been shown to negatively regulate axon length and increase axon branching by locally regulating the expression of its target microtubule-associated protein 1b (*Map1b*), which functions in stabilizing axonal microtubules (Dajas-Bailador et al., 2012). These findings point toward miRNAs having important roles in distinct cells, cellular regions, and cellular processes within the nervous system.

Adenosine-to-inosine editing may have a special role in the brain because ADAR activity is enriched in the brain compared to other tissues. This type of editing has been observed to

occur in pri-miRNAs to block processing by Dicer (Kawahara et al., 2007a) or alter the miRNA seed sequence (Kawahara et al., 2007b), as well as altering the sequence of miRNA target sites (Borchert et al., 2009).

REFERENCES

- Abbott, A.L., Alvarez-Saavedra, E., Miska, E.A., Lau, N.C., Bartel, D.P., Horvitz, H.R., and Ambros, V. (2005). The let-7 MicroRNA family members mir-48, mir-84, and mir-241 function together to regulate developmental timing in *Caenorhabditis elegans*. *Developmental Cell* *9*, 403–414.
- Agarwal, V., Bell, G.W., Nam, J.-W., and Bartel, D.P. (2015). Predicting effective microRNA target sites in mammalian mRNAs. *Elife* *4*, 1–38.
- Arvey, A., Larsson, E., Sander, C., Leslie, C.S., and Marks, D.S. (2010). Target mRNA abundance dilutes microRNA and siRNA activity. *Mol. Syst. Biol.* *6*, 363.
- Auyeung, V.C., Ulitsky, I., McGeary, S.E., and Bartel, D.P. (2013). Beyond secondary structure: primary-sequence determinants license pri-miRNA hairpins for processing. *Cell* *152*, 844–858.
- Baek, D., Villén, J., Shin, C., Camargo, F.D., Gygi, S.P., and Bartel, D.P. (2008). The impact of microRNAs on protein output. *Nature* *455*, 64–71.
- Ballas, N., Grunseich, C., Lu, D.D., Speh, J.C., and Mandel, G. (2005). REST and its corepressors mediate plasticity of neuronal gene chromatin throughout neurogenesis. *Cell* *121*, 645–657.
- Bartel, D.P. (2018). Metazoan MicroRNAs. *Cell* *173*, 20–51.
- Baskerville, S., and Bartel, D.P. (2005). Microarray profiling of microRNAs reveals frequent coexpression with neighboring miRNAs and host genes. *Rna* *11*, 241–247.
- Bazzini, A.A., Lee, M.T., and Giraldez, A.J. (2012). Ribosome profiling shows that miR-430 reduces translation before causing mRNA decay in zebrafish. *Science* *336*, 233–237.
- Béthune, J., Artus-Revel, C.G., and Filipowicz, W. (2012). scientific report. *EMBO Reports* *13*, 716–723.
- Bohnsack, M.T., Czapinski, K., and Gorlich, D. (2004). Exportin 5 is a RanGTP-dependent dsRNA-binding protein that mediates nuclear export of pre-miRNAs. *Rna* *10*, 185–191.
- Borchert, G.M., Gilmore, B.L., Spengler, R.M., Xing, Y., Lanier, W., Bhattacharya, D., and Davidson, B.L. (2009). Adenosine deamination in human transcripts generates novel microRNA binding sites. *Human Molecular Genetics* *18*, 4801–4807.
- Brennecke, J., Stark, A., Russell, R.B., and Cohen, S.M. (2005). Principles of microRNA-target recognition. *Plos Biol* *3*, e85.
- Cai, X., Hagedorn, C.H., and Cullen, B.R. (2004). Human microRNAs are processed from capped, polyadenylated transcripts that can also function as mRNAs. *Rna* *10*, 1957–1966.
- Chang, J., Nicolas, E., Marks, D., Sander, C., Lerro, A., Buendia, M.A., Xu, C., Mason, W.S.,

- Moloshok, T., Bort, R., et al. (2004). miR-122, a mammalian liver-specific microRNA, is processed from hcr mRNA and may downregulate the high affinity cationic amino acid transporter CAT-1. *RNA Biology* 1, 106–113.
- Chen, C.-Y.A., and Shyu, A.-B. (2011). Mechanisms of deadenylation-dependent decay. *WIREs RNA* 2, 167–183.
- Cheng, L.-C., Pastrana, E., Tavazoie, M., and Doetsch, F. (2009). miR-124 regulates adult neurogenesis in the subventricular zone stem cell niche. *Nat Neurosci* 12, 399–408.
- Chi, S.W., Hannon, G.J., and Darnell, R.B. (2012). An alternative mode of microRNA target recognition. *Nat. Struct. Mol. Biol.* 19, 321–327.
- Chi, S.W., Zang, J.B., Mele, A., and Darnell, R.B. (2009). Argonaute HITS-CLIP decodes microRNA-mRNA interaction maps. *Nature* 460, 479–486.
- Chiang, H.R., Schoenfeld, L.W., Ruby, J.G., Auyeung, V.C., Spies, N., Baek, D., Johnston, W.K., Russ, C., Luo, S., Babiarz, J.E., et al. (2010). Mammalian microRNAs: experimental evaluation of novel and previously annotated genes. *Genes & Development* 24, 992–1009.
- Choi, P.S., Zakhary, L., Choi, W.-Y., Caron, S., Alvarez-Saavedra, E., Miska, E.A., McManus, M., Harfe, B., Giraldez, A.J., Horvitz, R.H., et al. (2008). Members of the miRNA-200 Family Regulate Olfactory Neurogenesis. 57, 41–55.
- Chu, C.-Y., and Rana, T.M. (2006). Translation repression in human cells by microRNA-induced gene silencing requires RCK/p54. *Plos Biol* 4, e210.
- Clovis, Y.M., Enard, W., Marinaro, F., Huttner, W.B., and De Pietri Tonelli, D. (2012). Convergent repression of Foxp2 3'UTR by miR-9 and miR-132 in embryonic mouse neocortex: implications for radial migration of neurons. *Development* 139, 3332–3342.
- Cuellar, T.L., Davis, T.H., Nelson, P.T., Loeb, G.B., Harfe, B.D., Ullian, E., and McManus, M.T. (2008). Dicer loss in striatal neurons produces behavioral and neuroanatomical phenotypes in the absence of neurodegeneration. *Proc. Natl. Acad. Sci. U.S.a.* 105, 5614–5619.
- Dajas-Bailador, F., Bonev, B., Garcez, P., Stanley, P., Guillemot, F., and Papalopulu, N. (2012). microRNA-9 regulates axon extension and branching by targeting Map1b in mouse cortical neurons. *Nat Neurosci* 15, 697–699.
- Damiani, D., Alexander, J.J., O'Rourke, J.R., McManus, M., Jadhav, A.P., Cepko, C.L., Hauswirth, W.W., Harfe, B.D., and Strettoi, E. (2008). Dicer inactivation leads to progressive functional and structural degeneration of the mouse retina. *Journal of Neuroscience* 28, 4878–4887.
- Davis, E., Caiment, F., Tordoir, X., Cavaillé, J., Ferguson-Smith, A., Cockett, N., Georges, M., and Charlier, C. (2005). RNAi-mediated allelic trans-interaction at the imprinted Rtl1/Peg1 locus. *Curr. Biol.* 15, 743–749.

- Davis, T.H., Cuellar, T.L., Koch, S.M., Barker, A.J., Harfe, B.D., McManus, M.T., and Ullian, E.M. (2008). Conditional loss of Dicer disrupts cellular and tissue morphogenesis in the cortex and hippocampus. *Journal of Neuroscience* 28, 4322–4330.
- Denzler, R., Agarwal, V., Stefano, J., Bartel, D.P., and Stoffel, M. (2014). Assessing the ceRNA hypothesis with quantitative measurements of miRNA and target abundance. *Mol. Cell* 54, 766–776.
- Denzler, R., McGeary, S.E., Title, A.C., Agarwal, V., Bartel, D.P., and Stoffel, M. (2016). Impact of MicroRNA Levels, Target-Site Complementarity, and Cooperativity on Competing Endogenous RNA-Regulated Gene Expression. *Mol. Cell* 64, 565–579.
- Ding, L., Spencer, A., Morita, K., and Han, M. (2005). The developmental timing regulator AIN-1 interacts with miRISCs and may target the argonaute protein ALG-1 to cytoplasmic P bodies in *C. elegans*. *Mol. Cell* 19, 437–447.
- Djuranovic, S., Nahvi, A., and Green, R. (2012). miRNA-mediated gene silencing by translational repression followed by mRNA deadenylation and decay. *Science* 336, 237–240.
- Doench, J.G., and Sharp, P.A. (2004). Specificity of microRNA target selection in translational repression. *Genes & Development* 18, 504–511.
- Eichhorn, S.W., Guo, H., McGeary, S.E., Rodriguez-Mias, R.A., Shin, C., Baek, D., Hsu, S.-H., Ghoshal, K., Villén, J., and Bartel, D.P. (2014). mRNA destabilization is the dominant effect of mammalian microRNAs by the time substantial repression ensues. *Mol. Cell* 56, 104–115.
- Elkayam, E., Faehnle, C.R., Morales, M., Sun, J., Li, H., and Joshua-Tor, L. (2017). Multivalent Recruitment of Human Argonaute by GW182. *Mol. Cell* 67, 646–658.e3.
- Fang, W., and Bartel, D.P. (2015). The Menu of Features that Define Primary MicroRNAs and Enable De Novo Design of MicroRNA Genes. *Mol. Cell* 60, 131–145.
- Farh, K.K.-H., Grimson, A., Jan, C., Lewis, B.P., Johnston, W.K., Lim, L.P., Burge, C.B., and Bartel, D.P. (2005). The widespread impact of mammalian MicroRNAs on mRNA repression and evolution. *Science* 310, 1817–1821.
- Frank, F., Sonenberg, N., and Nagar, B. (2010). Structural basis for 5'-nucleotide base-specific recognition of guide RNA by human AGO2. *Nature* 465, 818–822.
- Friedman, R.C., Farh, K.K.H., Burge, C.B., and Bartel, D.P. (2008). Most mammalian mRNAs are conserved targets of microRNAs. *Genome Research* 19, 92–105.
- Friedman, R.C., and Burge, C.B. (2013). MicroRNA Target Finding by Comparative Genomics. In *Methods in Molecular Biology*, (Totowa, NJ: Humana Press), pp. 457–476.
- Fromm, B., Billipp, T., Peck, L.E., Johansen, M., Tarver, J.E., King, B.L., Newcomb, J.M., Sempere, L.F., Flatmark, K., Hovig, E., et al. (2015). A Uniform System for the Annotation of Vertebrate microRNA Genes and the Evolution of the Human microRNAome. *Annu. Rev.*

Genet. 49, 213–242.

Gaughwin, P., Ciesla, M., Yang, H., Lim, B., and Brundin, P. (2011). Stage-specific modulation of cortical neuronal development by Mmu-miR-134. *Cereb. Cortex* 21, 1857–1869.

Giraldez, A.J., Cinalli, R.M., Glasner, M.E., Enright, A.J., Thomson, J.M., Baskerville, S., Hammond, S.M., Bartel, D.P., and Schier, A.F. (2005). MicroRNAs regulate brain morphogenesis in zebrafish. *Science* 308, 833–838.

Giraldez, A.J., Mishima, Y., Rihel, J., Grocock, R.J., Van Dongen, S., Inoue, K., Enright, A.J., and Schier, A.F. (2006). Zebrafish MiR-430 promotes deadenylation and clearance of maternal mRNAs. *Science* 312, 75–79.

Grimson, A., Farh, K.K.-H., Johnston, W.K., Garrett-Engele, P., Lim, L.P., and Bartel, D.P. (2007). MicroRNA targeting specificity in mammals: determinants beyond seed pairing. *Mol. Cell* 27, 91–105.

Grosswendt, S., Filipchyk, A., Manzano, M., Klironomos, F., Schilling, M., Herzog, M., Gottwein, E., and Rajewsky, N. (2014). Unambiguous identification of miRNA:target site interactions by different types of ligation reactions. *Mol. Cell* 54, 1042–1054.

Guo, H., Ingolia, N.T., Weissman, J.S., and Bartel, D.P. (2010). Mammalian microRNAs predominantly act to decrease target mRNA levels. *Nature* 466, 835–840.

Hafner, M., Landthaler, M., Burger, L., Khorshid, M., Hausser, J., Berninger, P., Rothballer, A., Ascano, M., Jungkamp, A.-C., Munschauer, M., et al. (2010). Transcriptome-wide identification of RNA-binding protein and microRNA target sites by PAR-CLIP. *Cell* 141, 129–141.

Hansen, T.B., Wiklund, E.D., Bramsen, J.B., Villadsen, S.B., Statham, A.L., Clark, S.J., and Kjems, J. (2011). miRNA-dependent gene silencing involving Ago2-mediated cleavage of a circular antisense RNA. *The EMBO Journal* 30, 4414–4422.

Helwak, A., Kudla, G., Dudnakova, T., and Tollervey, D. (2013). Mapping the human miRNA interactome by CLASH reveals frequent noncanonical binding. *Cell* 153, 654–665.

Hendrickson, D.G., Hogan, D.J., McCullough, H.L., Myers, J.W., Herschlag, D., Ferrell, J.E., and Brown, P.O. (2009). Concordant regulation of translation and mRNA abundance for hundreds of targets of a human microRNA. *Plos Biol* 7, e1000238.

Hon, L.S., and Zhang, Z. (2007). The roles of binding site arrangement and combinatorial targeting in microRNA repression of gene expression. *Genome Biol* 8, R166.

Houbaviy, H.B., Murray, M.F., and Sharp, P.A. (2003). Embryonic stem cell-specific MicroRNAs. *Developmental Cell* 5, 351–358.

Hu, Z., and Li, Z. (2017). miRNAs in synapse development and synaptic plasticity. *Current Opinion in Neurobiology* 45, 24–31.

- Hutvagner, G., and Zamore, P.D. (2002). A microRNA in a multiple-turnover RNAi enzyme complex. *Science* 297, 2056–2060.
- Imayoshi, I., and Kageyama, R. (2011). The role of Notch signaling in adult neurogenesis. *Mol Neurobiol* 44, 7–12.
- Iwasaki, S., Kobayashi, M., Yoda, M., Sakaguchi, Y., Katsuma, S., Suzuki, T., and Tomari, Y. (2010). Hsc70/Hsp90 chaperone machinery mediates ATP-dependent RISC loading of small RNA duplexes. *Mol. Cell* 39, 292–299.
- Jan, C.H., Friedman, R.C., Ruby, J.G., and Bartel, D.P. (2011). Formation, regulation and evolution of *Caenorhabditis elegans* 3'UTRs. *Nature* 469, 97–101.
- Jonas, S., and Izaurralde, E. (2015). Towards a molecular understanding of microRNA-mediated gene silencing. *Nature Publishing Group* 16, 421–433.
- Jones-Rhoades, M.W., Bartel, D.P., and Bartel, B. (2006). MicroRNAs and their regulatory roles in plants. *Annu Rev Plant Biol* 57, 19–53.
- Kamenska, A., Lu, W.-T., Kubacka, D., Broomhead, H., Minshall, N., Bushell, M., and Standart, N. (2014). Human 4E-T represses translation of bound mRNAs and enhances microRNA-mediated silencing. *Nucleic Acids Research* 42, 3298–3313.
- Kamenska, A., Simpson, C., Vindry, C., Broomhead, H., Bénard, M., Ernoult-Lange, M., Lee, B.P., Harries, L.W., Weil, D., and Standart, N. (2016). The DDX6-4E-T interaction mediates translational repression and P-body assembly. *Nucleic Acids Research* 44, 6318–6334.
- Kawahara, Y., Zinshteyn, B., Chendrimada, T.P., Shiekhattar, R., and Nishikura, K. (2007a). RNA editing of the microRNA-151 precursor blocks cleavage by the Dicer-TRBP complex. *EMBO Reports* 8, 763–769.
- Kawahara, Y., Zinshteyn, B., Sethupathy, P., Iizasa, H., Hatzigeorgiou, A.G., and Nishikura, K. (2007b). Redirection of silencing targets by adenosine-to-inosine editing of miRNAs. *Science* 315, 1137–1140.
- Kawamata, T., and Tomari, Y. (2010). Making RISC. *Trends in Biochemical Sciences* 35, 368–376.
- Khvorova, A., Reynolds, A., and Jayasena, S.D. (2003). Functional siRNAs and miRNAs exhibit strand bias. *Cell* 115, 209–216.
- Kim, J., Inoue, K., Ishii, J., Vanti, W.B., Voronov, S.V., Murchison, E., Hannon, G., and Abeliovich, A. (2007). A MicroRNA feedback circuit in midbrain dopamine neurons. *Science* 317, 1220–1224.
- Kozomara, A., and Griffiths-Jones, S. (2014). miRBase: annotating high confidence microRNAs using deep sequencing data. *Nucleic Acids Research* 42, D68–D73.

- Krek, A., Grün, D., Poy, M.N., Wolf, R., Rosenberg, L., Epstein, E.J., MacMenamin, P., da Piedade, I., Gunsalus, K.C., Stoffel, M., et al. (2005). Combinatorial microRNA target predictions. *Nat Genet* 37, 495–500.
- Krichevsky, A.M., King, K.S., Donahue, C.P., Khrapko, K., and Kosik, K.S. (2003). A microRNA array reveals extensive regulation of microRNAs during brain development. *Rna* 9, 1274–1281.
- Krichevsky, A.M., Sonntag, K.-C., Isacson, O., and Kosik, K.S. (2006). Specific microRNAs modulate embryonic stem cell-derived neurogenesis. *Stem Cells* 24, 857–864.
- Krützfeldt, J., Rajewsky, N., Braich, R., Rajeev, K.G., Tuschl, T., Manoharan, M., and Stoffel, M. (2005). Silencing of microRNAs in vivo with 'antagomirs'. *Nature* 438, 685–689.
- Lagos-Quintana, M., Rauhut, R., Lendeckel, W., and Tuschl, T. (2001). Identification of novel genes coding for small expressed RNAs. *Science* 294, 853–858.
- Lagos-Quintana, M., Rauhut, R., Meyer, J., Borkhardt, A., and Tuschl, T. (2003). New microRNAs from mouse and human. *Rna* 9, 175–179.
- Lagos-Quintana, M., Rauhut, R., Yalcin, A., Meyer, J., Lendeckel, W., and Tuschl, T. (2002). Identification of tissue-specific microRNAs from mouse. *Curr. Biol.* 12, 735–739.
- Lai, E.C., Tomancak, P., Williams, R.W., and Rubin, G.M. (2003). Computational identification of *Drosophila* microRNA genes. *Genome Biol* 4, R42.
- Lambert, N., Robertson, A., Jangi, M., McGeary, S., Sharp, P.A., and Burge, C.B. (2014). RNA Bind-n-Seq: quantitative assessment of the sequence and structural binding specificity of RNA binding proteins. *Mol. Cell* 54, 887–900.
- Landgraf, P., Rusu, M., Sheridan, R., Sewer, A., Iovino, N., Aravin, A., Pfeffer, S., Rice, A., Kamphorst, A.O., Landthaler, M., et al. (2007). A mammalian microRNA expression atlas based on small RNA library sequencing. *Cell* 129, 1401–1414.
- Lau, N.C., Lim, L.P., Weinstein, E.G., and Bartel, D.P. (2001). An abundant class of tiny RNAs with probable regulatory roles in *Caenorhabditis elegans*. *Science* 294, 858–862.
- Lazzaretti, D., Tournier, I., and Izaurralde, E. (2009). The C-terminal domains of human TNRC6A, TNRC6B, and TNRC6C silence bound transcripts independently of Argonaute proteins. *Rna* 15, 1059–1066.
- Lee, R.C., and Ambros, V. (2001). An extensive class of small RNAs in *Caenorhabditis elegans*. *Science* 294, 862–864.
- Lee, R.C., Feinbaum, R.L., and Ambros, V. (1993). The *C. elegans* heterochronic gene *lin-4* encodes small RNAs with antisense complementarity to *lin-14*. *Cell* 75, 843–854.
- Lee, Y., Ahn, C., Han, J., Choi, H., Kim, J., Yim, J., Lee, J., Provost, P., Rådmark, O., Kim, S.,

- et al. (2003). The nuclear RNase III Drosha initiates microRNA processing. *Nature* *425*, 415–419.
- Lee, Y., Jeon, K., Lee, J.-T., Kim, S., and Kim, V.N. (2002). MicroRNA maturation: stepwise processing and subcellular localization. *The EMBO Journal* *21*, 4663–4670.
- Lee, Y., Kim, M., Han, J., Yeom, K.-H., Lee, S., Baek, S.H., and Kim, V.N. (2004). MicroRNA genes are transcribed by RNA polymerase II. *The EMBO Journal* *23*, 4051–4060.
- Lewis, B.P., Burge, C.B., and Bartel, D.P. (2005). Conserved Seed Pairing, Often Flanked by Adenosines, Indicates that Thousands of Human Genes are MicroRNA Targets. *Cell* *120*, 15–20.
- Lewis, B.P., Shih, I.-H., Jones-Rhoades, M.W., Bartel, D.P., and Burge, C.B. (2003). Prediction of mammalian microRNA targets. *Cell* *115*, 787–798.
- Lian, S.L., Li, S., Abadal, G.X., Pauley, B.A., Fritzler, M.J., and Chan, E.K.L. (2009). The C-terminal half of human Ago2 binds to multiple GW-rich regions of GW182 and requires GW182 to mediate silencing. *Rna* *15*, 804–813.
- Lim, L.P., Lau, N.C., Garrett-Engele, P., Grimson, A., Schelter, J.M., Castle, J., Bartel, D.P., Linsley, P.S., and Johnson, J.M. (2005). Microarray analysis shows that some microRNAs downregulate large numbers of target mRNAs. *Nature* *433*, 769–773.
- Lim, L.P., Lau, N.C., Weinstein, E.G., Abdelhakim, A., Yekta, S., Rhoades, M.W., Burge, C.B., and Bartel, D.P. (2003). The microRNAs of *Caenorhabditis elegans*. *Genes & Development* *17*, 991–1008.
- Liu, J., Carmell, M.A., Rivas, F.V., Marsden, C.G., Thomson, J.M., Song, J.-J., Hammond, S.M., Joshua-Tor, L., and Hannon, G.J. (2004). Argonaute2 is the catalytic engine of mammalian RNAi. *Science* *305*, 1437–1441.
- Liu, X.S., Chopp, M., Zhang, R.L., Tao, T., Wang, X.L., Kassis, H., Hozeska-Solgot, A., Zhang, L., Chen, C., and Zhang, Z.G. (2011). MicroRNA profiling in subventricular zone after stroke: MiR-124a regulates proliferation of neural progenitor cells through Notch signaling pathway. *PLoS ONE* *6*, e23461.
- Loeb, G.B., Khan, A.A., Canner, D., Hiatt, J.B., Shendure, J., Darnell, R.B., Leslie, C.S., and Rudensky, A.Y. (2012). Transcriptome-wide miR-155 binding map reveals widespread noncanonical microRNA targeting. *Mol. Cell* *48*, 760–770.
- Louvi, A., and Artavanis-Tsakonas, S. (2006). Notch signalling in vertebrate neural development. *Nat Rev Neurosci* *7*, 93–102.
- Lu, C., Tej, S.S., Luo, S., Haudenschild, C.D., Meyers, B.C., and Green, P.J. (2005). Elucidation of the small RNA component of the transcriptome. *Science* *309*, 1567–1569.
- Lund, E., Güttinger, S., Calado, A., Dahlberg, J.E., and Kutay, U. (2004). Nuclear export of microRNA precursors. *Science* *303*, 95–98.

- Makeyev, E.V., Zhang, J., Carrasco, M.A., and Maniatis, T. (2007). The MicroRNA miR-124 promotes neuronal differentiation by triggering brain-specific alternative pre-mRNA splicing. *Mol. Cell* 27, 435–448.
- Mayr, C., and Bartel, D.P. (2009). Widespread shortening of 3'UTRs by alternative cleavage and polyadenylation activates oncogenes in cancer cells. *Cell* 138, 673–684.
- Mayr, C., Hemann, M.T., and Bartel, D.P. (2007). Disrupting the pairing between let-7 and Hmga2 enhances oncogenic transformation. *Science* 315, 1576–1579.
- McGeary, S.E., Lin, K.S., Shi, C.Y., Bisaria, N., and Bartel, D.P. The biochemical basis of microRNA targeting efficacy.
- Meister, G., Landthaler, M., Patkaniowska, A., Dorsett, Y., Teng, G., and Tuschl, T. (2004). Human Argonaute2 mediates RNA cleavage targeted by miRNAs and siRNAs. *Mol. Cell* 15, 185–197.
- Miska, E.A., Alvarez-Saavedra, E., Townsend, M., Yoshii, A., Sestan, N., Rakic, P., Constantine-Paton, M., and Horvitz, H.R. (2004). Microarray analysis of microRNA expression in the developing mammalian brain. *Genome Biol* 5, R68.
- Miura, P., Shenker, S., Andreu-Agullo, C., Westholm, J.O., and Lai, E.C. (2013). Widespread and extensive lengthening of 3' UTRs in the mammalian brain. *Genome Research* 23, 812–825.
- Natera-Naranjo, O., Aschrafi, A., Gioio, A.E., and Kaplan, B.B. (2010). Identification and quantitative analyses of microRNAs located in the distal axons of sympathetic neurons. *Rna* 16, 1516–1529.
- Neilson, J.R., Zheng, G.X.Y., Burge, C.B., and Sharp, P.A. (2007). Dynamic regulation of miRNA expression in ordered stages of cellular development. *Genes & Development* 21, 578–589.
- Nesti, E., Corson, G.M., McCleskey, M., Oyer, J.A., and Mandel, G. (2014). C-terminal domain small phosphatase 1 and MAP kinase reciprocally control REST stability and neuronal differentiation. *Proc. Natl. Acad. Sci. U.S.a.* 111, E3929–E3936.
- Nguyen, T.A., Jo, M.H., Choi, Y.-G., Park, J., Kwon, S.C., Hohng, S., Kim, V.N., and Woo, J.-S. (2015). Functional Anatomy of the Human Microprocessor. *Cell* 161, 1374–1387.
- Nielsen, C.B., Shomron, N., Sandberg, R., Hornstein, E., Kitzman, J., and Burge, C.B. (2007). Determinants of targeting by endogenous and exogenous microRNAs and siRNAs. *Rna* 13, 1894–1910.
- Nishimura, T., Padamsi, Z., Fakim, H., Milette, S., Dunham, W.H., Gingras, A.-C., and Fabian, M.R. (2015). The eIF4E-Binding Protein 4E-T Is a Component of the mRNA Decay Machinery that Bridges the 5' and 3' Termini of Target mRNAs. *CellReports* 11, 1425–1436.
- Obermayer, B., and Levine, E. (2014). Exploring the miRNA regulatory network using

evolutionary correlations. *PLoS Comput Biol* *10*, e1003860.

Ozgur, S., Basquin, J., Kamenska, A., Filipowicz, W., Standart, N., and Conti, E. (2015). Structure of a Human 4E-T/DDX6/CNOT1 Complex Reveals the Different Interplay of DDX6-Binding Proteins with the CCR4-NOT Complex. *CellReports* *13*, 703–711.

Pasquinelli, A.E., Reinhart, B.J., Slack, F., Martindale, M.Q., Kuroda, M.I., Maller, B., Hayward, D.C., Ball, E.E., Degnan, B., Müller, P., et al. (2000). Conservation of the sequence and temporal expression of let-7 heterochronic regulatory RNA. *Nature* *408*, 86–89.

Peng, Z., Cheng, Y., Tan, B.C.-M., Kang, L., Tian, Z., Zhu, Y., Zhang, W., Liang, Y., Hu, X., Tan, X., et al. (2012). Comprehensive analysis of RNA-Seq data reveals extensive RNA editing in a human transcriptome. *Nature Biotechnology* *30*, 253–260.

Rago, L., Beattie, R., Taylor, V., and Winter, J. (2014). miR379-410 cluster miRNAs regulate neurogenesis and neuronal migration by fine-tuning N-cadherin. *The EMBO Journal* *33*, 906–920.

Rajman, M., and Schratt, G. (2017). MicroRNAs in neural development: from master regulators to fine-tuners. *Development* *144*, 2310–2322.

Rehwinkel, J., Behm-Ansmant, I., Gatfield, D., and Izaurralde, E. (2005). A crucial role for GW182 and the DCP1:DCP2 decapping complex in miRNA-mediated gene silencing. *Rna* *11*, 1640–1647.

Reinhart, B.J., Slack, F.J., Basson, M., Pasquinelli, A.E., Bettinger, J.C., Rougvie, A.E., Horvitz, H.R., and Ruvkun, G. (2000). The 21-nucleotide let-7 RNA regulates developmental timing in *Caenorhabditis elegans*. *Nature* *403*, 901–906.

Riley, K.J., Rabinowitz, G.S., Yario, T.A., Luna, J.M., Darnell, R.B., and Steitz, J.A. (2012). EBV and human microRNAs co-target oncogenic and apoptotic viral and human genes during latency. *The EMBO Journal* *31*, 2207–2221.

Robins, H., Li, Y., and Padgett, R.W. (2005). Incorporating structure to predict microRNA targets. *Proc. Natl. Acad. Sci. U.S.A.* *102*, 4006–4009.

Rodriguez, A., Griffiths-Jones, S., Ashurst, J.L., and Bradley, A. (2004). Identification of mammalian microRNA host genes and transcription units. *Genome Research* *14*, 1902–1910.

Rodriguez, A., Vigorito, E., Clare, S., Warren, M.V., Couttet, P., Soond, D.R., Van Dongen, S., Grocock, R.J., Das, P.P., Miska, E.A., et al. (2007). Requirement of bic/microRNA-155 for normal immune function. *Science* *316*, 608–611.

Ruby, J.G., Jan, C., Player, C., Axtell, M.J., Lee, W., Nusbaum, C., Ge, H., and Bartel, D.P. (2006). Large-scale sequencing reveals 21U-RNAs and additional microRNAs and endogenous siRNAs in *C. elegans*. *Cell* *127*, 1193–1207.

Saetrom, P., Heale, B.S.E., Snøve, O., Aagaard, L., Alluin, J., and Rossi, J.J. (2007). Distance

constraints between microRNA target sites dictate efficacy and cooperativity. *Nucleic Acids Research* 35, 2333–2342.

Salmena, L., Poliseno, L., Tay, Y., Kats, L., and Pandolfi, P.P. (2011). A ceRNA hypothesis: the Rosetta Stone of a hidden RNA language? *Cell* 146, 353–358.

Salomon, W.E., Jolly, S.M., Moore, M.J., Zamore, P.D., and Serebrov, V. (2015). Single-Molecule Imaging Reveals that Argonaute Reshapes the Binding Properties of Its Nucleic Acid Guides. *Cell* 162, 84–95.

Sandberg, R., Neilson, J.R., Sarma, A., Sharp, P.A., and Burge, C.B. (2008). Proliferating cells express mRNAs with shortened 3' untranslated regions and fewer microRNA target sites. *Science* 320, 1643–1647.

Santos, M.C.T., Tegge, A.N., Correa, B.R., Mahesula, S., Kohnke, L.Q., Qiao, M., Ferreira, M.A.R., Kokovay, E., and Penalva, L.O.F. (2016). miR-124, -128, and -137 Orchestrate Neural Differentiation by Acting on Overlapping Gene Sets Containing a Highly Connected Transcription Factor Network. *Stem Cells* 34, 220–232.

Sasaki, Y., Gross, C., Xing, L., Goshima, Y., and Bassell, G.J. (2013). Identification of axon-enriched MicroRNAs localized to growth cones of cortical neurons. *Devel Neurobio* 74, 397–406.

Schirle, N.T., Sheu-Gruttadauria, J., and MacRae, I.J. (2014). Structural basis for microRNA targeting. *Science* 346, 608–613.

Schratt, G. (2009). microRNAs at the synapse. *Nat Rev Neurosci* 10, 842–849.

Schratt, G.M., Tuebing, F., Nigh, E.A., Kane, C.G., Sabatini, M.E., Kiebler, M., and Greenberg, M.E. (2006). A brain-specific microRNA regulates dendritic spine development. *Nature* 439, 283–289.

Schwarz, D.S., Hutvagner, G., Du, T., Xu, Z., Aronin, N., and Zamore, P.D. (2003). Asymmetry in the assembly of the RNAi enzyme complex. *Cell* 115, 199–208.

Selbach, M., Schwanhäusser, B., Thierfelder, N., Fang, Z., Khanin, R., and Rajewsky, N. (2008). Widespread changes in protein synthesis induced by microRNAs. *Nature* 455, 58–63.

Sempere, L.F., Freemantle, S., Pitha-Rowe, I., Moss, E., Dmitrovsky, E., and Ambros, V. (2004). Expression profiling of mammalian microRNAs uncovers a subset of brain-expressed microRNAs with possible roles in murine and human neuronal differentiation. *Genome Biol* 5, R13.

Shin, C., Nam, J.-W., Farh, K.K.-H., Chiang, H.R., Shkumatava, A., and Bartel, D.P. (2010). Expanding the microRNA targeting code: functional sites with centered pairing. *Mol. Cell* 38, 789–802.

Siegel, G., Obernosterer, G., Fiore, R., Oehmen, M., Bicker, S., Christensen, M., Khudayberdiev,

- S., Leuschner, P.F., Busch, C.J.L., Kane, C., et al. (2009). A functional screen implicates microRNA-138-dependent regulation of the depalmitoylation enzyme APT1 in dendritic spine morphogenesis. *Nat Cell Biol* *11*, 705–716.
- Silber, J., Lim, D.A., Petritsch, C., Persson, A.I., Maunakea, A.K., Yu, M., Vandenberg, S.R., Ginzinger, D.G., James, C.D., Costello, J.F., et al. (2008). miR-124 and miR-137 inhibit proliferation of glioblastoma multiforme cells and induce differentiation of brain tumor stem cells. *BMC Med* *6*, 14.
- Slack, F.J., Basson, M., Liu, Z., Ambros, V., Horvitz, H.R., and Ruvkun, G. (2000). The lin-41 RBCC gene acts in the *C. elegans* heterochronic pathway between the let-7 regulatory RNA and the LIN-29 transcription factor. *Mol. Cell* *5*, 659–669.
- Stark, A., Brennecke, J., Bushati, N., Russell, R.B., and Cohen, S.M. (2005). Animal MicroRNAs confer robustness to gene expression and have a significant impact on 3'UTR evolution. *Cell* *123*, 1133–1146.
- Strazisar, M., Cammaerts, S., van der Ven, K., Forero, D.A., Lenaerts, A.-S., Nordin, A., Almeida-Souza, L., Genovese, G., Timmerman, V., Liekens, A., et al. (2015). MIR137 variants identified in psychiatric patients affect synaptogenesis and neuronal transmission gene sets. *Mol. Psychiatry* *20*, 472–481.
- Subtelny, A.O., Eichhorn, S.W., Chen, G.R., Sive, H., and Bartel, D.P. (2014). Poly(A)-tail profiling reveals an embryonic switch in translational control. *Nature* *508*, 66–71.
- Suzuki, H.I., Katsura, A., Yasuda, T., Ueno, T., Mano, H., Sugimoto, K., and Miyazono, K. (2015). Small-RNA asymmetry is directly driven by mammalian Argonautes. *Nat. Struct. Mol. Biol.* *22*, 512–521.
- Takimoto, K., Wakiyama, M., and Yokoyama, S. (2009). Mammalian GW182 contains multiple Argonaute-binding sites and functions in microRNA-mediated translational repression. *Rna* *15*, 1078–1089.
- Till, S., Lejeune, E., Thermann, R., Bortfeld, M., Hothorn, M., Enderle, D., Heinrich, C., Hentze, M.W., and Ladurner, A.G. (2007). A conserved motif in Argonaute-interacting proteins mediates functional interactions through the Argonaute PIWI domain. *Nat. Struct. Mol. Biol.* *14*, 897–903.
- Tsang, J.S., Ebert, M.S., and van Oudenaarden, A. (2010). Genome-wide dissection of microRNA functions and cotargeting networks using gene set signatures. *Mol. Cell* *38*, 140–153.
- Visvanathan, J., Lee, S., Lee, B., Lee, J.W., and Lee, S.-K. (2007). The microRNA miR-124 antagonizes the anti-neural REST/SCP1 pathway during embryonic CNS development. *Genes & Development* *21*, 744–749.
- Wee, L.M., Flores-Jasso, C.F., Salomon, W.E., and Zamore, P.D. (2012). Argonaute divides its RNA guide into domains with distinct functions and RNA-binding properties. *Cell* *151*, 1055–1067.

- Wightman, B., Ha, I., and Ruvkun, G. (1993). Posttranscriptional regulation of the heterochronic gene *lin-14* by *lin-4* mediates temporal pattern formation in *C. elegans*. *Cell* 75, 855–862.
- Wu, J.I., Lessard, J., Olave, I.A., Qiu, Z., Ghosh, A., Graef, I.A., and Crabtree, G.R. (2007). Regulation of dendritic development by neuron-specific chromatin remodeling complexes. *Neuron* 56, 94–108.
- Wu, J., and Xie, X. (2006). Comparative sequence analysis reveals an intricate network among REST, CREB and miRNA in mediating neuronal gene expression. *Genome Biol* 7, R85.
- Xia, H., Cheung, W.K.C., Ng, S.S., Jiang, X., Jiang, S., Sze, J., Leung, G.K.K., Lu, G., Chan, D.T.M., Bian, X.-W., et al. (2012). Loss of brain-enriched miR-124 microRNA enhances stem-like traits and invasiveness of glioma cells. *J. Biol. Chem.* 287, 9962–9971.
- Xue, Y., Ouyang, K., Huang, J., Zhou, Y., Ouyang, H., Li, H., Wang, G., Wu, Q., Wei, C., Bi, Y., et al. (2013). Direct conversion of fibroblasts to neurons by reprogramming PTB-regulated microRNA circuits. *Cell* 152, 82–96.
- Yekta, S., Shih, I.-H., and Bartel, D.P. (2004). MicroRNA-directed cleavage of HOXB8 mRNA. *Science* 304, 594–596.
- Yi, R., Qin, Y., Macara, I.G., and Cullen, B.R. (2003). Exportin-5 mediates the nuclear export of pre-microRNAs and short hairpin RNAs. *Genes & Development* 17, 3011–3016.
- Yoo, A.S., Staahl, B.T., Chen, L., and Crabtree, G.R. (2009). MicroRNA-mediated switching of chromatin-remodelling complexes in neural development. *Nature* 460, 642–646.
- Yoo, A.S., Sun, A.X., Li, L., Shcheglovitov, A., Portmann, T., Li, Y., Lee-Messer, C., Dolmetsch, R.E., Tsien, R.W., and Crabtree, G.R. (2011). MicroRNA-mediated conversion of human fibroblasts to neurons. *Nature* 476, 228–231.
- Zhang, H., Kolb, F.A., Jaskiewicz, L., Westhof, E., and Filipowicz, W. (2004). Single processing center models for human Dicer and bacterial RNase III. *Cell* 118, 57–68.

Chapter 2:

Cotargeting among microRNAs is widespread, and is highly enriched in the brain

ABSTRACT

MicroRNAs (miRNAs) play roles in diverse developmental and disease processes. Distinct miRNAs have hundreds to thousands of conserved mRNA binding sites, but typically direct only modest repression via single sites. Cotargeting of individual mRNAs by different miRNAs could potentially achieve stronger and more complex patterns of repression. Comparing target sets of different miRNAs, we identified hundreds of pairs of miRNAs that share more mRNA targets than expected (often by two-fold or more) relative to stringent controls. Genetic perturbations revealed a functional overlap in neuronal differentiation for the cotargeting pair miR-138/miR-137. Clustering of all cotargeting pairs revealed a group of 9 predominantly brain-enriched miRNAs that share many targets. In reporter assays, subsets of these miRNAs together repressed gene expression by 5- to 10-fold, often exhibiting cooperative repression. Together, our results uncover an unexpected pattern in which combinations of miRNAs collaborate to robustly repress cotargets, and suggest important developmental roles for cotargeting.

INTRODUCTION

MicroRNAs (miRNAs) are small, 21-23 nt noncoding RNAs that specify the repression of target mRNAs by the RNA-induced silencing complex (RISC), predominantly via recognition of a short complementary sequence matching the miRNA seed (Bartel, 2018; Lewis et al., 2003). miRNAs regulate a broad set of cellular processes, including differentiation and development, and are mis-regulated in many diseases (Bartel, 2018; Mendell and Olson, 2012). However, genetic studies have found that individual miRNAs are often not essential for viability or development (Miska et al., 2007), and their regulatory roles are often difficult to detect, requiring knockout of multiple family members (Alvarez-Saavedra and Horvitz, 2010) and/or environmental perturbations (van Rooij et al., 2007; Zheng et al., 2011), leaving an incomplete picture of the functional roles of most miRNAs.

Each conserved miRNA often possesses hundreds of target genes or more that are conserved across mammals, together encompassing at least 60% of mammalian mRNAs, as well as additional non-conserved targets (Friedman et al., 2008). However, miRNAs typically elicit modest effects on any given target, often repressing expression by less than 20% (Baek et al., 2008; Selbach et al., 2008). Why miRNAs have so many conserved target sites but typically repress each one only modestly is not well understood. Because some genes contain several conserved miRNA sites, stronger repression may result when these sites are all active.

Theoretically, five target sites that individually repress an mRNA to 80% of its prior level could together repress expression to $(0.8)^5 = \sim 33\%$ of its prior level, since repression by multiple sites appears to be multiplicative (often described as “log-additive”) (Grimson et al., 2007; Nielsen et al., 2007). Cooperativity between closely spaced miRNA sites, characteristically with a distance

of 15-35 nt between seed starts, can further boost the repression exerted by a pair of sites (Doench and Sharp, 2004; Grimson et al., 2007; Saetrom et al., 2007). While a transcript can encode and undergo strong regulation by multiple sites for the same miRNA (Lee et al., 1993; Mayr et al., 2007; Reinhart et al., 2000; Wightman et al., 1993), only 7% of genes containing at least one conserved miRNA site have more than one conserved site for the same miRNA family (Friedman et al., 2008). In contrast, 72% of predicted targets have sites for multiple miRNA families, with an average of more than four highly conserved sites per targeted 3' UTR (Friedman et al., 2008). Thus, there is far more potential for co-regulation of mRNAs by multiple distinct miRNAs than for multiple targeting by the same miRNA.

It has been proposed that individual mRNAs are often regulated by more than one miRNA and that combinations of miRNAs collaborate in repression of specific targets (Friedman and Burge, 2013; Krek et al., 2005), but surprisingly few studies have explored this notion or identified specific examples of coregulation. When predicted target sites across a single 3' UTR have been comprehensively tested in reporter assays, only a subset of these sites were found to be functional (Jiang et al., 2009; Wu et al., 2010). Further, when natural 3' UTR sequences with multiple sites for distinct but co-expressed miRNAs were tested for combinatorial repression, the presence of two or three sites conferred moderate – less than two-fold – repression (Grimson et al., 2007; Krek et al., 2005), or even no observed repression for one trio of sites (Saetrom et al., 2007), although up to four-fold repression for three miRNA sites has been observed in the regulation of viral transcripts by a combination of viral and host miRNAs (Riley et al., 2012). Thus, presence of cognate sites in a 3' UTR and expression of the corresponding miRNAs in the same cell are necessary but not sufficient conditions for effective repression of an mRNA by multiple distinct miRNAs, termed “cotargeting”.

While the genome-wide extent of cotargeting has been explored only rarely, there is some support for coordinated functioning of different miRNAs. Indeed, miRNAs that are expressed from the same polycistronic cluster, and thus generally co-expressed, have predicted target sets that partially overlap and are enriched for components of the same pathways (Tsang et al., 2010). In another study, enrichment for co-conservation of target sites was observed between particular pairs of miRNAs (Obermayer and Levine, 2014). Together, these studies and a few more mentioned below suggest that the functions of different miRNAs may often be coordinated.

We hypothesized that pairs and groups of miRNAs that preferentially share targets may function together in differentiation and development to strongly repress critical targets and reinforce each other's activity. Using a simple but stringent statistical method to identify pairs of miRNAs that share more conserved targets than expected, we identified hundreds of significant cotargeting miRNA pairs and showed that these pairs tend to have related patterns of expression. Genetic analysis of one of these miRNA pairs established a functional relationship between the miRNAs in control of neuronal differentiation. We also observed larger groups of cotargeting miRNAs, including a cluster of mostly brain-enriched miRNAs, and showed that these miRNAs can achieve potent combinatorial repression of shared targets.

RESULTS

Cotargeting by distinct miRNA pairs is prevalent

Because the level of regulation by one miRNA on an individual target is often relatively modest, we sought to understand whether distinct miRNAs commonly function together by regulating the same genes with stronger repression in concert. To explore this idea, we compared the target sets of different miRNA pairs to see if they shared more targets than would be expected to occur by chance. We performed this analysis on a set of 78 conserved miRNAs with distinct seed sequences and at least 300 conserved targets (considering the canonical 8mer, 7mer-m8, and 7mer-A1 target classes) (Agarwal et al., 2015; Lewis et al., 2005), excluding cases where 7mer seed sequences overlapped by 6 or more bases. To control for the biases that may exist within a given miRNA's target set, custom control gene sets were designed for each miRNA, matching the distributions of 3'UTR length, G+C content, and mean sequence conservation of the miRNA's conserved targets. All 78 miRNA target sets were then intersected with each other miRNA target set and its corresponding control set. Significance of the observed overlap was assessed by the chi-square test and corrected for multiple hypothesis testing by computing the false discovery rate (FDR) using the q value method (Storey and Tibshirani, 2003). Because the control set for each miRNA is different, each cotargeting pair is assessed in both directions, comparing miRNA-A to miRNA-B ($A \rightarrow B$) and comparing miRNA-B to miRNA-A ($B \rightarrow A$), so it is possible for two miRNAs to be significant in a unidirectional or bidirectional manner (**Fig. 1A**).

We observed 482 significant cotargeting relationships after applying an FDR-adjusted q-value cutoff of 0.05, with each miRNA having an average of 10 cotargeting relationships (**Fig.**

1B). Of these relationships, 270 (56%) were significant in both directions, $A \rightarrow B$ and $B \rightarrow A$ (**Table S1**). While the bidirectional pairs represent our strongest predictions, the unidirectional cotargeting pairs are still significant statistically and may indicate relevant functional relationships. For example, a miRNA with a small number of targets and a specialized function that shares many of its targets with a multifunctional miRNA that has many targets may achieve unidirectional but not bidirectional significance. Interestingly, particular cotargeting pairs in our analysis have been previously characterized as having coordinated roles in specific biological processes. One notable example is the bidirectional cotargeting pair miR-9 and miR-124, which can together, but not alone, drive the direct conversion of fibroblasts to neurons (Yoo et al., 2011). Another example is a trio of neuronal miRNAs, where miR-124 and miR-128 bidirectionally cotarget with each other and also unidirectionally cotarget with miR-137. This trio has been reported to synergistically regulate Sp1 and other transcription factors to drive neuronal differentiation (Santos et al., 2016). Additionally, we identified miR-200b and miR-182 as a bidirectional cotargeting pair, which have been recently reported to cooperate in driving epithelial-mesenchymal transition (EMT), a process relevant in development and disease (Cursons et al., 2018).

In order for a cotargeting pair to direct coordinated repression, the miRNAs must be expressed in the same time and place. We examined the relationship between the expression patterns of cotargeting pairs across a set of 28 human tissues from a small RNA high-throughput sequencing study (McCall et al., 2017). We observed that bidirectional cotargeting pairs were significantly more correlated in their expression across this set of tissues than the non-significant pairs ($p = 5 \times 10^{-3}$, KS-test) (**Fig. 1C**). For instance, the highly significant cotargeting miRNAs miR-124 and miR-9 had strongly correlated expression patterns ($R_{\text{Spearman}} = 0.82$, $p = 7 \times 10^{-8}$).

This observation suggests that miRNAs that overlap in their expression patterns may more commonly evolve shared targets.

Given that many miRNAs exhibit tissue-specific or tissue-biased expression, we wondered whether the extent of cotargeting varied between different tissues. Considering miRNA expression across the same panel of human tissues (McCall et al., 2017), we converted expression values to z-scores and considered miRNAs with a z-score greater than or equal to 4 in any one tissue as strongly tissue-enriched and all other miRNAs as non-tissue specific. Interestingly, the brain-enriched miRNAs had greater levels of cotargeting than miRNAs enriched in other tissues (**Fig. 1D**), suggesting that cotargeting might have a prominent role in the brain.

The cotargeting miRNAs miR-138 and miR-137 coordinately increase across neuronal differentiation

To explore the functional relevance of the identified cotargeting miRNA pairs, it was important to study one pair in depth. Noting the high levels of cotargeting among brain-enriched miRNAs, we sought to identify a pair of brain-enriched cotargeting miRNAs where both increase in expression across neuronal differentiation. To assess miRNA expression in a relevant system, we performed small RNA sequencing in a murine cell culture model of neuronal differentiation, Cath.-a-differentiated (CAD) cells (Qi et al., 1997). CAD cells were subjected to serum-withdrawal-induced neuronal differentiation, and RNA was collected at 0 days (in serum) and 4 days after serum withdrawal. In all, 57 mammalian-conserved miRNAs increased significantly across the differentiation, including nine that were brain-enriched (z-score > 2 in prefrontal cortex in the tissue data analyzed above) (**Fig. 1E; Table S2**). miR-138 was among the most

Figure 1

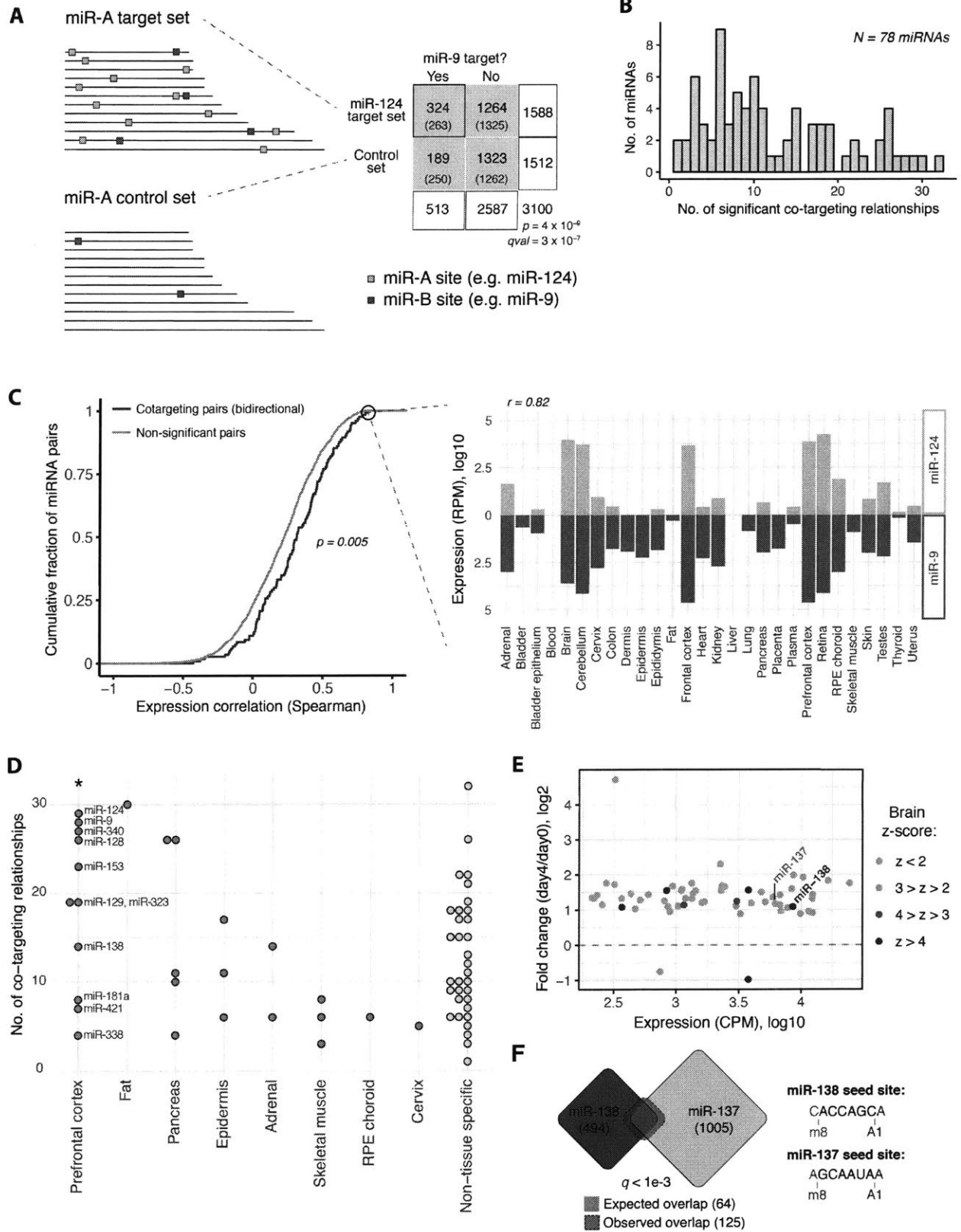


Figure 1. Cotargeting by distinct miRNA pairs is prevalent, particularly among brain-specific miRNAs.

A) Our statistical test for significant cotargeting between a pair of miRNAs is illustrated. Control sets are made for the reference miRNA (e.g., miR-A) that match the distribution of 3' UTR length, C+G content, and sequence conservation of miR-A's TargetScan 7mer and 8mer targets. The number of conserved 7mer and 8mer sites for a second miRNA (e.g., miR-B) (teal boxes) in miR-A targets (miR-A sites marked by light blue boxes) and in miR-A's control set are counted, and significance is determined by chi-square test. Target set overlaps are shown in a contingency table (expected values in parentheses) for miR-9 compared to miR-124 and its control set. **B)** The number of miRNAs with different numbers of significant cotargeting relationships (with $q\text{-val} < 0.05$). **C)** Cumulative distributions of Spearman correlation of miRNA expression across a set of 28 human tissue for bidirectional cotargeting pairs (dark grey) or non-significant pairs (light grey) ($p = 5 \times 10^{-3}$, KS test). Correlation of log expression of miR-124 and miR-9 across human tissues, Spearman $\rho = 0.82$. **D)** Number of cotargeting relationships for tissue-specific miRNAs, defined as having z-score > 4 in any tissue and assigned to the tissue with the highest z-score. Tissues with at least one assigned miRNA are shown. * $p < 0.05$ (Wilcoxon rank-sum test) comparing no. of cotargeting relationships for miRNAs in the designated tissue to non-tissue specific miRNAs or miRNAs in all other tissues. **E)** Fold change (\log_2) and expression (normalized counts per million (CPM), \log_{10}) of significantly changing miRNAs across serum withdrawal-induced CAD cell differentiation (0 to 4 days). Brain-enriched miRNAs were colored by the strength of their brain (prefrontal cortex) z-score. **F)** Overlap of miR-138 (blue) and miR-137 (purple) predicted target sets. Dashed line shows the observed overlap in comparison to the expected overlap (solid line) calculated from the overlap between miR-137 and miR-138 control sets. The q-value shown is the geometric mean of the q-values from miR-138 \rightarrow miR-137 and miR-137 \rightarrow miR-138 comparisons. Seed sites for each miRNA are shown at right. See also Figure S1 and Table S1.

highly expressed miRNAs in this system, increased more than two-fold during differentiation, and had a brain z-score > 4 , making it a strong candidate. miR-137 was one of the most significant cotargeting partners with miR-138, sharing 125 targets, about 1.9 times more than expected by chance ($qval < 1 \times 10^{-3}$) (**Fig. 1F**). miR-137 had an expression level roughly comparable (within 25%) to that of miR-138, was brain-enriched, and increased across CAD differentiation by more than two-fold. We confirmed that expression changes correspondingly in a glutamatergic neuronal differentiation system starting from mESCs by TaqMan miRNA qPCR, and retested CAD cells using this approach. The data confirmed induction of both miR-138 and miR-137 in both systems, revealing a stronger early increase in miR-138 expression (**Fig. S1A,B**). The comparable expression levels, nearly synchronous expression increases during differentiation, and extensive cotargeting potential (despite unrelated seed sequences) together suggested that miR-138 and miR-137 may coordinately regulate a set of targets during CAD cell differentiation.

***mir-138* is required for the differentiation of CAD cells**

Murine miR-138 is encoded by two distinct genomic loci, *mir-138-1* and *mir-138-2*, located on chromosomes 8 and 9, while miR-137 is expressed from a single locus on chromosome 3. To explore the functions of miR-138 and miR-137 in neuronal differentiation, we generated *mir-137* knockout (KO) and *mir-138-1/mir-138-2* double knockout (DKO) CAD cell lines by removing the entire precursor miRNA sequence using CRISPR/Cas9 (Ran et al., 2013). Deletion of the miRNAs was confirmed by genomic PCR around the deletion site (**Fig. 2A**), and absence of expression was confirmed by northern blot and TaqMan qRT-PCR (**Fig. 2B; Fig. S2A,B**).

Wildtype (WT) CAD cells enter the differentiation program within 24 hours after serum withdrawal as indicated by extensive neurite growth (**Fig. 2C,D**) and expression of key neuronal markers like class III beta-tubulin and SNAP-25 (Qi et al., 1997). Strikingly, the *mir-138* DKO cell line no longer projected neurites upon serum withdrawal (**Fig. 2C,D**), suggesting an important role for this miRNA in differentiation. This phenotype was observed in two separately isolated *mir-138* DKO cell lines. Follow-up work was performed with the DKO1 line, which had a cleaner deletion of the *mir-138-1* locus (**Fig. 2A, Methods**). The *mir-137* KO cell line displayed no severe morphological changes (**Fig. S2C**).

To determine whether the block in neuronal differentiation was directly caused by the loss of miR-138, we asked whether re-introducing miR-138 to the cells could rescue the phenotype. *mir-138* DKO cells were transfected with 3 nM miR-138 mimic RNA followed by serum withdrawal two days later (**Fig. 3A**). We observed substantial rescue of the phenotype two days after serum withdrawal, with 51% of cells differentiated compared to only 3% of cells transfected with a negative control mimic (**Fig. 3B,C**), confirming that the phenotype results from loss of miR-138 activity.

To further characterize the *mir-138* DKO cell line, polyA-selected RNA sequencing (RNA-seq) was performed on WT and DKO cells in serum and 24 hours after serum withdrawal. Additional samples were taken at 4 days after serum withdrawal for the WT cells, but this time point was not sampled for the *mir-138* DKO cells because they exhibited extensive cell death after 4 days in serum-free media. RNA-seq analysis indicated that predicted miR-138 target genes were significantly de-repressed in the *mir-138* DKO cell line, as expected (**Fig. S2D**). To better understand how the loss of miR-138 affected the overall differentiation state of these cells, we compared the expression data to available RNA-seq data from an established in vitro system

involving the differentiation of mESCs to mature glutamatergic neurons (Hubbard et al., 2013). Principal component analysis (PCA) of gene expression values from this system was used to define a coordinate system associated with neuronal differentiation (**Fig. 2E**). Cells at different stages distributed along PC1 in chronological order: from mESCs (Day -8) to mature glutamatergic neurons (Day 28). Thus, PC1 reflects neuronal differentiation status. When the CAD RNA-seq data was projected onto this coordinate system, the WT CAD cells moved along PC1 chronologically after serum withdrawal, consistent with literature supporting CAD cells as a model for neuronal differentiation (Qi et al., 1997). The DKO samples projected slightly behind the WT samples on this axis and moved a shorter distance along this axis following serum withdrawal, suggesting that loss of *mir-138* causes cells to partially dedifferentiate and impairs their ability to differentiate upon stimulus (**Fig. 2E**).

Consistent with induction of a dedifferentiated state, many genes that increase across normal differentiation, including many well-established neuronal markers, had reduced expression in DKO cells (**Fig. S2E**). In fact, there was a highly significant overlap ($p = 2 \times 10^{-123}$, hypergeometric test) of 956 genes between genes that increased significantly across WT CAD differentiation (WT Day 0 → WT Day 1) and genes that increased between DKO and WT cells (DKO Day 0 → WT Day 0) (**Fig. 2F**). Gene ontology analysis of the overlapping genes compared to all genes changing in either comparison revealed a significant enrichment for categories related to synapse function and neuron projection (**Fig. 2G**), motivating designation of this set as “miR-138-sensitive differentiation” (MSD) genes. In DKO cell differentiation, 85% of MSD genes (815 genes) failed to increase significantly above expression levels observed in the WT cells in serum, and 52% of MSD genes (498 genes) remained significantly lower than levels observed in WT cells in serum (**Fig. 2H**). MSD genes may therefore represent the core of the

deregulated program in DKO cells. These observations support the interpretation that loss of miR-138 from CAD cells results in a state that is both dedifferentiated and less poised for induction of neuronal differentiation.

In all, 177 predicted miR-138 target genes were de-repressed in the DKO cells in either serum or serum-free conditions, of which 36% (64) significantly decreased across normal CAD differentiation (**Table S3**). Because the expression of miR-138 increases over the differentiation, it is likely that miR-138 contributes to the downregulation of many of these genes following serum withdrawal. Interestingly, this list contained several key neuronal differentiation-associated genes, including *Ctdsp1*, *Sin3a*, and *Ezh2*. CTDSP1 is an important stabilizer of the RE1-Silencing Transcription factor (REST), which is a major repressor of neuronal genes in non-neuronal cells (Nesti et al., 2014). Indeed, we found that *Rest* levels were nearly 2-fold higher in the DKO cells. *Ctdsp1* has 4 conserved miR-124 seed matches in its 3' UTR and is known to be strongly repressed by this neuronally-expressed miRNA (Visvanathan et al., 2007), but we found that miR-124 is not detectably expressed in CAD cells. Thus, miR-138 may play a more prominent role in the repression of *Rest* during CAD cell differentiation than in other neuronal systems, and CAD cells may represent a sensitized system to study miR-138 functions. Interestingly, SIN3A, a corepressor of the REST complex (Huang et al., 1999), contains miR-138 target sites and has elevated levels in the DKO cells. miR-138 target sites are also present in EZH2, the catalytic component of the Polycomb Repressive Complex 2 (PRC2), a well-established repressor of neuronal differentiation (Neo et al., 2014; Pereira et al., 2010). The deregulation of these and perhaps other miR-138 targets may therefore contribute to the block in neuronal differentiation.

Figure 2

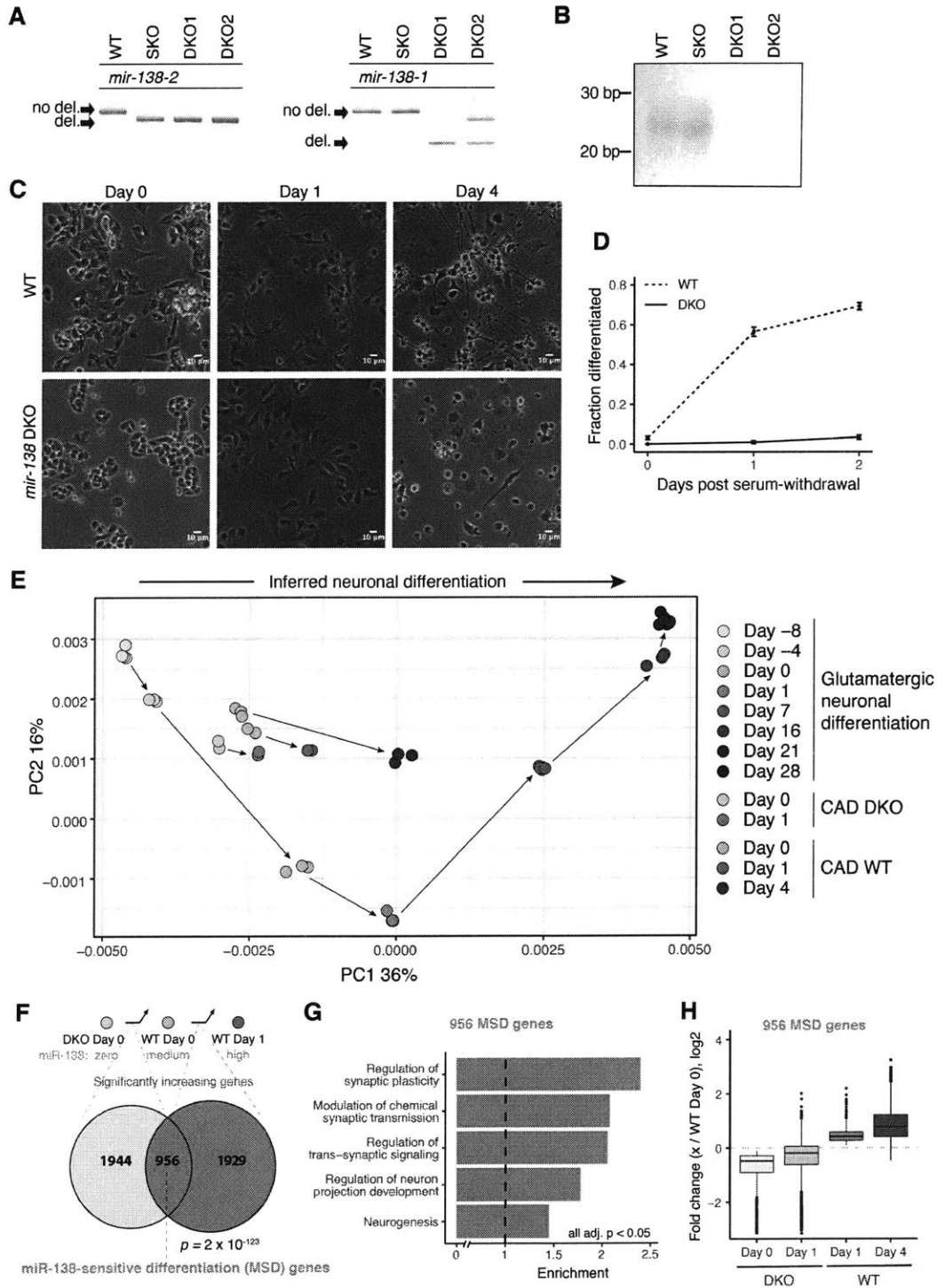


Figure 2. *mir-138* is required for differentiation of CAD cells.

A) PCR of genomic DNA around the CRISPR-targeted sites of the two murine *mir-138* loci, confirming deletion of both loci. Wildtype parental line (WT), single knockout line (SKO), and two double knockout lines (DKO1 and DKO2) are shown. **B)** Northern blot for miR-138 in WT, SKO, DKO1 and DKO2 cell lines. **C)** WT and DKO cells at 0, 1, and 4 d after serum withdrawal (images at 10X magnification; scale bar indicates 10 μ m), and **D)** quantitation of fraction of cells morphologically differentiated (Methods). Mean \pm SD of 3 replicates with at least 100 cell counts each is shown. **E)** Principal component analysis (PCA) of RNA-seq data from 8 time points of murine glutamatergic neuronal differentiation (shades of blue). RNA-seq data from CAD WT (0, 1, and 4 days after serum withdrawal, shades of green) and DKO cells (0 and 1 days after serum withdrawal, pink), projected onto PC1 and PC2 of the glutamatergic differentiation data. Arrows connect consecutive samples in each time series. The two sets of WT Day 0 cells correspond to independent RNA-seq library preps and sequencing runs, as the Day 0 and Day 4 WT cells were sequenced in independent experiments. **F)** Comparison of gene sets significantly increasing between DKO Day 0 and WT Day 0, and between WT Day 0 and WT Day 1. Significance of the 956 gene overlap (defined as MSD genes) was determined by chi-square test. **G)** Gene ontology enrichment of MSD genes against a background of all genes significantly increasing in either DKO Day 0 to WT Day 0 or WT Day 0 to WT Day1, with FDR-corrected $p < 0.05$ for all categories shown. **H)** Fold change (\log_2) of the 956 MSD genes from WT Day 0 to: DKO Day 0, DKO Day 1, WT Day 1, and WT Day 4. *See also Figure S2, Table S1, and Table S3.*

miR-137 can rescue a block in neuronal differentiation caused by loss of *mir-138*

Given the significant potential for cotargeting between miR-137 and miR-138 (**Fig. 1F**), we wondered what effect miR-137 might have on the DKO phenotype. To explore this question, we transfected *mir-138* DKO cells with 3 nM miR-137 mimic. Remarkably, within one day after serum withdrawal, 42% of *mir-138* DKO cells transfected with miR-137 were morphologically differentiated, and by two days after serum withdrawal, 60% of cells had differentiated. In contrast, other miRNA mimics tested, including neuronal miRNAs miR-9, miR-128, miR-7 and muscle miRNA miR-1, failed to produce any detectible increase in morphologically differentiated cells (**Fig. 3B,C; Fig. S3A**). Thus, these rescue experiments confirmed that the differentiation phenotype resulted from loss of miR-138 and established a functional relationship between the studied cotargeting pair, miR-138 and miR-137.

Because the miR-138 and the miR-137 transfections both resulted in a strong morphological rescue of neuronal differentiation, it was of interest to investigate the degree of similarity between their impacts on the transcriptome. We performed polyA-selected RNA-seq on total RNA collected 48 hours after miRNA transfection and 48 hours after serum withdrawal to capture both miRNA-specific effects and the transcriptome profiles of cells that had been morphologically rescued (**Fig. 3A**). Analysis of these data revealed clear repression of predicted targets of each miRNA (**Fig. S3B,C**), demonstrating effective miRNA delivery and specific targeting. In addition, we observed a significant correlation in expression changes ($R_{\text{Spearman}} = 0.28, p = 5 \times 10^{-171}$) between the miR-138 and miR-137 rescues 2 days after serum withdrawal when normalized to control (pUC19 DNA-transfected) cells at the same time point (**Fig. 3D**). Thus, rescue of the phenotype by these miRNAs may result from regulation of the same or related pathways. Genes that were significantly increased above control in each rescue were

enriched for functional categories including cell projection assembly, positive regulation of neuron projection development and microtubule-based movement, all terms associated with differentiation and the development of neurites (**Fig. S3D**). On the other hand, genes that were significantly lower in both rescues compared to controls were enriched for categories associated with cell cycle like DNA-dependent DNA replication and ribosome synthesis (**Fig. S3D**). These observations are consistent with a model in which both miR-138 and miR-137 can trigger a similar neuronal differentiation program that involves slowing of the cell cycle and induction of neuritogenesis.

Overall, 55% (58) of expressed predicted cotargets of miR-137 and miR-138 were significantly repressed in both the miR-137 and miR-138 transfections, supporting a substantial degree of cotargeting in this system (**Table S4**). miR-138 and miR-137 sites in transcripts cotargeted by both miRNAs had higher probability of conserved targeting (P_{CT}) scores (**Fig. 3E**), indicating stronger constraint on function (Friedman et al., 2008).

We sought to assess targeting of two predicted cotargets with regulatory functions, *Nfix* and *Ezh2*, using luciferase assays. *Nfix*, along with paralogs *Nfia* and *Nfib*, regulates both neurite outgrowth and neuronal cell differentiation (Mason et al., 2009). *Nfix* was repressed in both rescues and contains one miR-137 and three miR-138 seed sites. We cloned a portion of the 3' UTR containing one miR-138 site and one miR-137 site downstream of *Renilla* luciferase (rLuc) and generated three mutant versions with either one or both of the seed matches mutated. These plasmids were co-transfected with either: both miR-138 and miR-137, a control miRNA or no miRNA into human HEK293T cells. When normalized to the control miRNA, the miR-137 and miR-138 sites conferred 33% and 40% repression, respectively, and 64% repression in concert (**Fig. 3F**). A slightly longer portion of the 3'UTR containing an additional miR-138 site was

repressed 75% by both miRNAs together, confirming cotargeting of this mRNA. *Ezh2* was significantly repressed in the miR-138 rescue but not in the miR-137 rescue. Because *Ezh2* is a previously validated target of miR-137 (Szulwach et al., 2010) and impacts differentiation, we sought to better understand its regulation by each miRNA. By the same assay, we observed 17% and 33% repression of an *Ezh2* reporter by miR-137 and miR-138, respectively, with 42% combined repression, consistent with the expected log-additive relationship (**Fig. S3E**). Thus, both *Nfix* and *Ezh2* were validated as cotargets of miR-138 and miR-137.

Given their functional relationship, we asked whether miR-138 and miR-137 regulate each other's expression. We observed that the expression of miR-137 is 2.7-fold lower in the *mir-138* DKO cells and fails to increase in DKO cells following serum withdrawal (**Fig. 3G**), suggesting that reduction of miR-137 levels might contribute to the phenotype of these cells. The loss of miR-137 induction in *mir-138* DKO cells could result either from failure to repress a specific negative regulator of *mir-137*, for example, or as a consequence of the impaired differentiation program in DKO cells. Conversely, miR-138 levels were 1.5-fold higher in *mir-137* KO than in WT cells (**Fig. 3G**). Thus, these cotargeting miRNAs regulate each other's expression in opposite directions. We also observed that miR-138 levels increase more rapidly than miR-137 following serum withdrawal, suggesting that miR-138 may regulate earlier stages of differentiation than miR-137 (**Fig. 3G**).

The simplest model to explain the observed differences between the phenotypes of *mir-138* and *mir-137* knockouts is that the strong repression of one or more miR-138/miR-137 cotargets is required for differentiation of CAD cells (**Fig. 3H**). In this model, repression by endogenous miR-137 is insufficient in *mir-138* DKO cells (which have reduced levels of miR-137), but is sufficient in *mir-137* KO cells (which have elevated levels of miR-138), or when

Figure 3

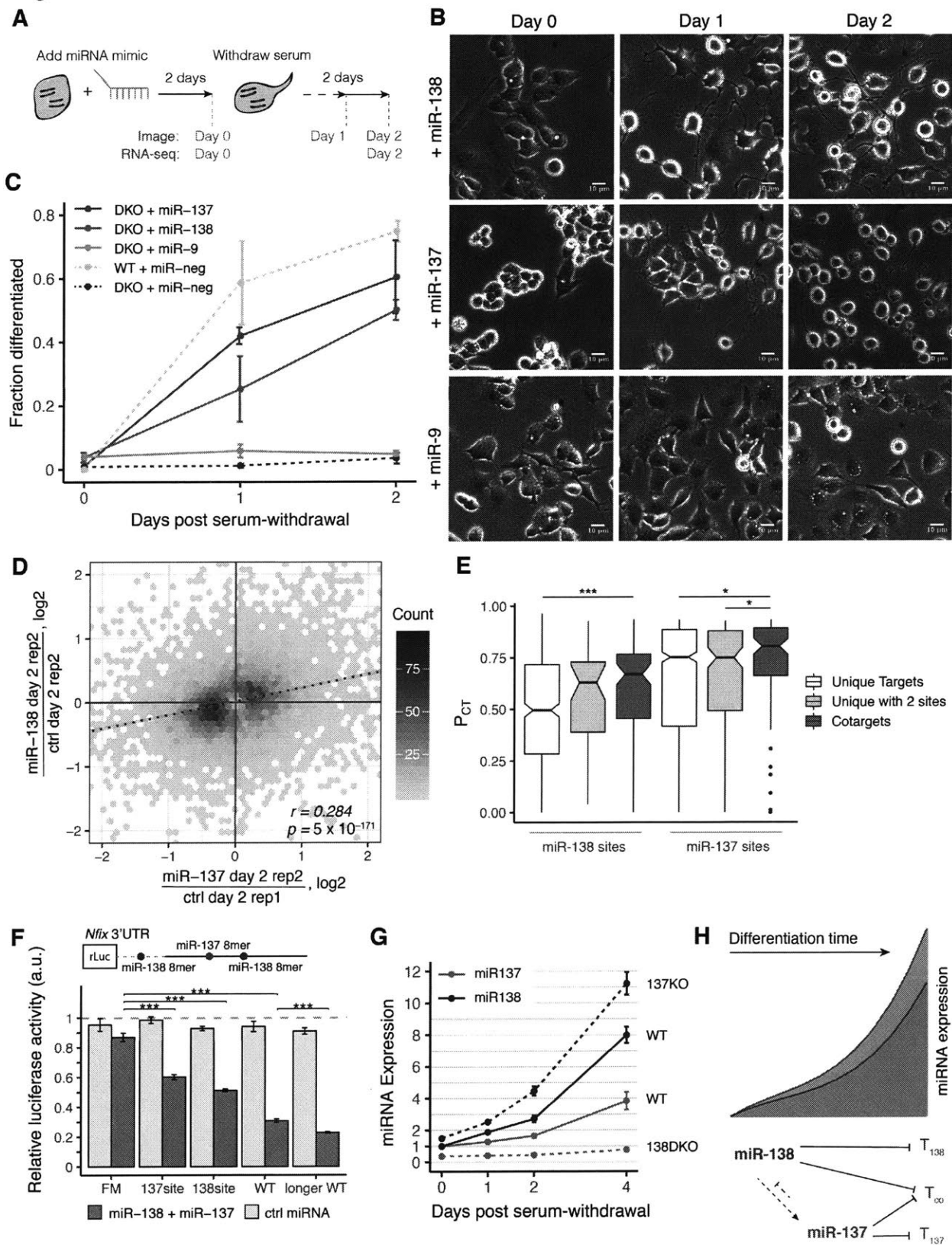


Figure 3. Both miR-138 and its cotargeting partner, miR-137, can rescue the neurite growth phenotype of *mir-138* DKO cells.

A) DKO or WT cells were transfected with a miRNA mimic and serum was withdrawn 2 d later. Images were taken 2 d after the transfection, before serum withdrawal (Day 0), and 1 and 2 d after serum withdrawal (Day 1, 2). RNA-seq libraries were prepared from samples 0 and 2 d after serum withdrawal. **B)** DKO cells transfected with a miRNA mimic (miR-138, miR137, or miR-9) and imaged at 0, 1, and 2 d after serum withdrawal. Images taken at 20X magnification. Scale bar represents 10 μ m. **C)** Quantitation of morphological differentiation at 0, 1, and 2 d after serum withdrawal of WT cells transfected with a negative control miRNA mimic (miR-neg), and DKO cells transfected with miR-137, miR-138, miR-9, or miR-neg mimic. **D)** Hexagonal heat map of significantly changing genes in DKO cells transfected with miR-138 or miR-137 mimic, normalized to different control replicates transfected with pUC19 DNA. The regression line is dotted dark blue ($r = 0.28$, $p = 5 \times 10^{-171}$). **E)** Probability of conserved targeting (P_{CT}) scores of miR-138 and miR-137 sites in targets containing only one target site for that miRNA (white), targets containing two sites for the same miRNA (purple), or cotargets containing one target site for miR-138 and one target site for miR-137 (blue). Significance was determined using the Wilcoxon rank-sum test (* $p < 0.05$, *** $p < 0.001$). **F)** Relative luciferase signal (*Renilla*/firefly) for psiCHECK-2 reporter containing a 500 bp region of the *Nfix* 3' UTR with one miR-138 and one miR-137 site (WT), or with a combination of seed site mutations: both miRNA sites mutated in a full mutant (FM), only the miR-138 site mutated (137 site), or only the miR-137 site mutated (138 site), or an 800 bp region of the 3' UTR containing an additional miR-138 site (longer WT). Co-transfection with miR-138 and miR-137, or a control miRNA (cel-miR-67), were normalized to a transfection with no miRNA mimic added. Significance was assessed by t-test, select comparisons are shown (* $p < 0.05$, ** $p < 0.01$, *** $p < 0.001$). **G)** Relative expression of miR-137 (light blue) or miR-138 (dark blue) measured by TaqMan qPCR (miR/U6) in WT and 138 DKO or 137 KO cells at 0, 1, 2, and 4 d after serum withdrawal, and normalized to the WT Day 0 measurements. **H)** Summary of miR-138 and miR-137 regulation during neuronal differentiation, showing repression of individual and shared (T_{co}) targets, and (indirect) regulatory relationships between the miRNAs. See also Figure S3 and Table S4.

high levels of exogenous miR-137 are provided. (Various more complex models could also explain the observed genotype/phenotype relationships.) The observations above suggest that *mir-138* induction is an early event in CAD cell differentiation, which precedes and promotes induction of *mir-137*, with miR-138 and miR-137 collaborating to drive differentiation, and repression of *mir-138* by miR-137 serving to limit the magnitude and/or duration of the period of robust cotargeting.

Groups of miRNAs preferentially share targets with one another

Given the large number of miRNA pairs identified which have significant cotargeting potential, we asked whether these pairs are organized into larger groups of potentially collaborating miRNAs. To address this possibility, we performed hierarchical clustering of miRNAs based on the degree of similarity between their significant cotargeting relationships to other miRNAs (Methods). This analysis yielded three prominent clusters of six or more miRNAs (labeled A, B and C in **Fig. 4A**). Examining the expression patterns of the clustered miRNAs across human tissues, we noted that most of the nine miRNAs in cluster A were highly enriched in brain tissues (**Fig. 4B**), including the well-known neuronal miRNAs miR-124, miR-128, and miR-137 (Landgraf et al., 2007). Categorizing tissues as brain or non-brain, we found that the miRNAs of cluster A were indeed highly enriched in brain over non-brain tissues ($p = 6.4 \times 10^{-6}$, KS-test), whereas miRNAs of cluster B were enriched in non-brain tissues and those of cluster C showed no trend relative to brain (**Fig. 4C**). Therefore, we designated miRNA cluster A as the “brain cluster”.

The existence of clusters of miRNAs that preferentially share cotargeting partners with one another suggests that “cliques” of three or more miRNAs may often team up together in

target regulation. To explore this idea, we focused on the brain cluster because of its large size and strong tissue-specific bias. Strikingly, some transcripts were targeted by as many as 8 of the 9 miRNAs in the brain cluster, and some 1804 transcripts were brain cluster “multi-targets”, in that they were targeted by three or more brain cluster miRNAs (**Fig. 4D**). A number of these mRNAs encode known regulators of neuronal differentiation, such as *Jag1*, *Neurod1*, *Ptbp1*, *Rock1*, and *Rcor1* (Åkerblom and Jakobsson, 2014), or have precise dosage requirements for proper synaptic function, such as *Fmr1* (Oostra and Willemsen, 2003). Genes with multiple target sites to brain cluster miRNAs also preferentially conserved these sites (**Fig. 4E**), as assessed by their relative P_{CT} scores, a measure which controls for miRNA-specific differences in seed match conservation (as observed in **Fig. 3E**). This observation suggests the possibility that multi-targeting may be more functionally important overall than single targeting, and is consistent with seed match conservation patterns observed previously (Friedman et al., 2008).

Groups of brain cluster miRNAs can collaborate to exert strong repression

We next sought to explore the potential for collaborative repression of targets by miRNAs from the brain cluster. Not every seed match confers detectable repression, even when considering those that are conserved across mammals. In addition, while site type (e.g., 8mer, 7mer-m8, 7mer-A1) and context scores correlate with site efficacy, it remains difficult to accurately predict the magnitude of repression (Agarwal et al., 2015; Grimson et al., 2007). Therefore, we designed sets of luciferase reporters to measure the level of repression associated with each miRNA seed match and cognate miRNA, singly and in combination, for several genes multiply targeted by miRNAs from the brain cluster.

Figure 4

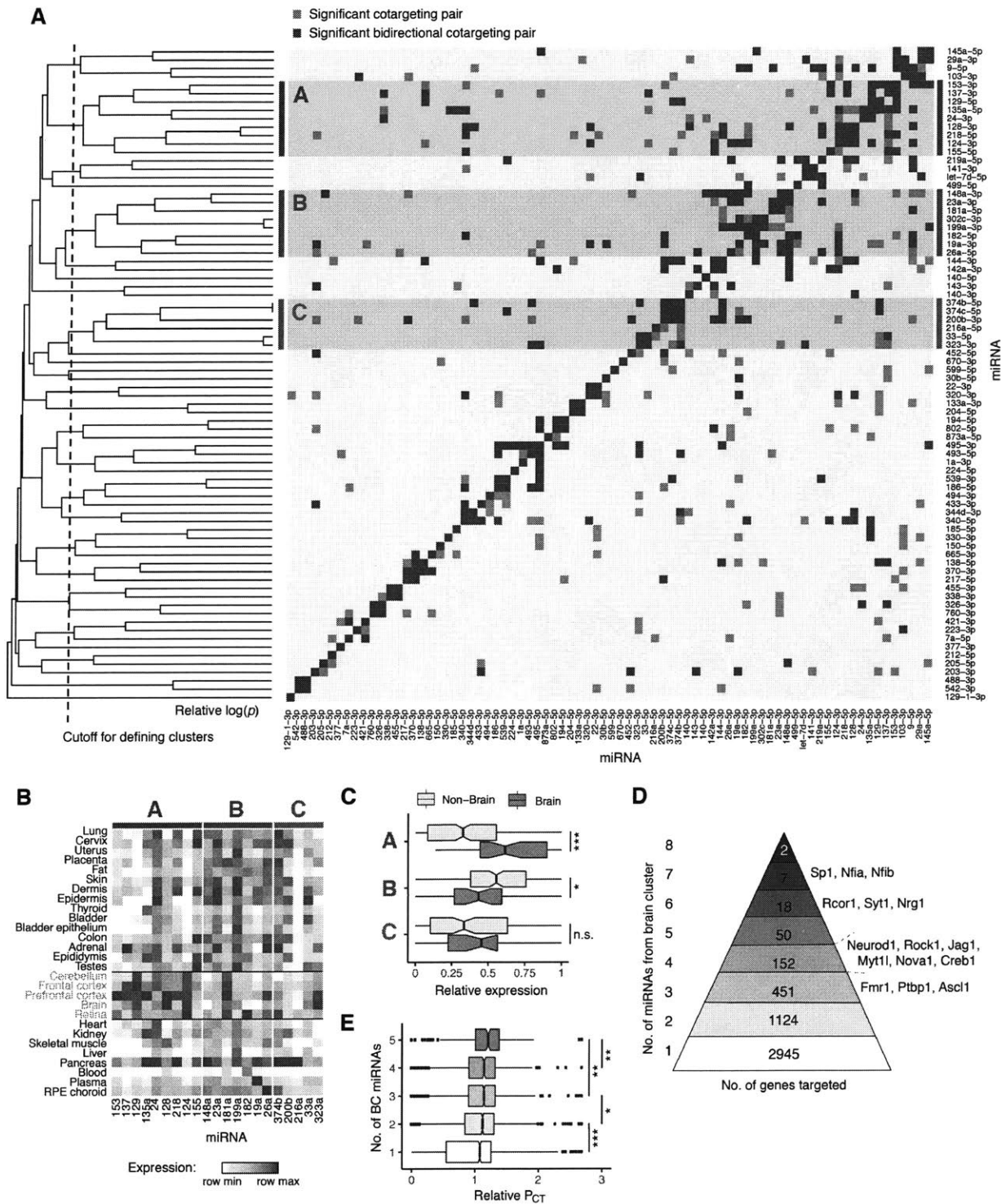


Figure 4. Patterns of cotargeting among pairs and groups of miRNAs.

A) Pairwise cotargeting relationships for 78 conserved miRNA families, showing unidirectional significant cotargeting relationships with the reference miRNA on the y-axis (light blue) and bidirectional significant cotargeting relationships (dark blue) (both with $q\text{-val} < 0.05$), and non-significant relationships (light grey). Rows were clustered using average linkage hierarchical clustering with distances defined as $M - \text{avg}(-\log_{10}(p\text{val}))$ from a binomial test of the extent of overlap of significant cotargeting relationships between rows, where M is the maximum $-\log(p\text{val})$ observed. Vertical dotted line indicates cutoff distance ($= 2.8$) at which clusters of 5 or more miRNAs were defined. Clusters are highlighted with red (Cluster A), blue (Cluster B), or green (Cluster C). **B)** Heatmap of miRNA expression clustering across human tissues (brain tissues labeled in pink). Samples are normalized to the max and min values in each row, and relative expression is expressed as $(\text{sample} - \text{min}) / (\text{max} - \text{min})$. **C)** Tissues were designated as brain or non-brain (as indicated in B). Box plots are shown of the relative expression of each miRNA in each cluster in brain tissues versus non-brain tissues. Significance was assessed by KS-test. **D)** The number of genes predicted as targets of different numbers of miRNAs from the brain cluster are shown, with selected genes listed at right. **E)** Relative P_{CT} scores (normalized to the mean P_{CT} of sites for each miRNA) for miRNA sites in genes targeted by different numbers of brain cluster miRNAs. Significance was calculated by Wilcoxon rank-sum test (* $p < 0.05$, ** $p < 0.01$, *** $p < 0.001$).

The assay was designed and controlled so as to determine the total amount of regulation resulting from the combination of miRNAs and the relative contribution of each miRNA to that total, thus also enabling us to assess potential cooperativity between sites. We selected four candidate genes (*Neurod1*, *Fmr1*, *Rock1*, and *Rcor1*) which have important functions in neurobiology and whose 3' UTRs contained conserved seed matches to three or more miRNAs from the brain cluster. Their full-length 3' UTRs were cloned downstream of the rLuc gene in the psiCHECK-2 expression vector, which also expresses fLuc as an internal normalization control. Reporter clones containing disrupted seed matches were generated by mutating two bases in the center of the seed match. For each gene, we also generated a full mutant (FM) clone in which all seed matches to brain cluster miRNAs were mutated, as well as clones for combinations of individual seed match mutations (**Fig. 5A**).

A unique miRNA expression plasmid was constructed for use with each reporter, containing hairpins expressing each of the brain cluster miRNAs targeting that gene's 3' UTR, inserted into an intron of GFP under doxycycline control. miRNA expression following transfection into human HEK293T cells was confirmed using miRNA TaqMan assays (**Fig. S4**). We also generated two control miRNA expression plasmids: one expressing miR-103, a broadly expressed miRNA with no seed match in any of the selected 3' UTRs, and an empty vector with no miRNA inserted. Luciferase reporter plasmids were co-transfected with either their cognate miRNA expression plasmid (+miR-ALL), or the miR-103 control plasmid (+miR-103), or the empty vector control (+empty), and *Renilla* and firefly luciferase levels were assayed 48 hours later (**Fig. 5A**). Each renilla/firefly (R/F) ratio from the +miR-ALL treatment was normalized to the R/F ratio from the +miR-103 control, or to that from the +empty control. Comparison of

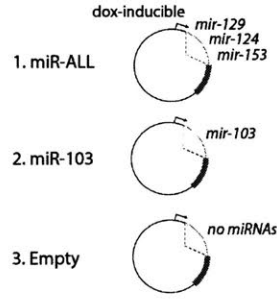
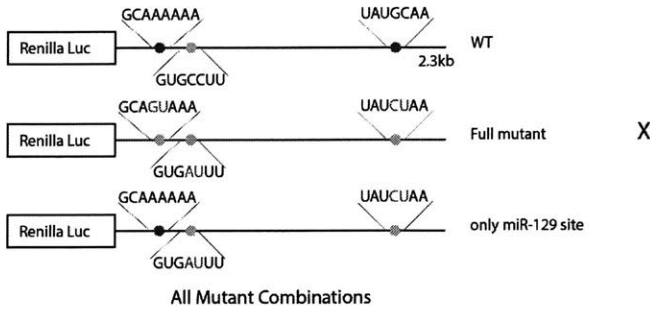
these two controls can provide information about the extent to which displacement of endogenous miRNAs from RISC by exogenous small RNAs may influence reporter expression.

Neurogenic differentiation factor 1 (*Neurod1*), a basic helix-loop-helix transcription factor, is a potent pro-neural factor that drives neurogenesis by directly binding to and activating transcription of key neuronal development genes (Pataskar et al., 2016). The *Neurod1* 3' UTR contains conserved seed matches to three brain cluster miRNAs: miR-137, miR-153, and miR-124. The WT reporter was repressed ~75% when transfected with the miR-ALL plasmid compared to either control plasmid, but the FM was not repressed at all, confirming that the observed repression results from miRNAs acting on the three miRNA sites (**Fig. 5B**). We measured the amount of repression conferred by each individual site by comparing mutant versions in which the other two sites were mutated to the FM reporter. This approach revealed that the miR-137, miR-153, and miR-124 seed matches confer 12%, 56%, and 22% repression, respectively.

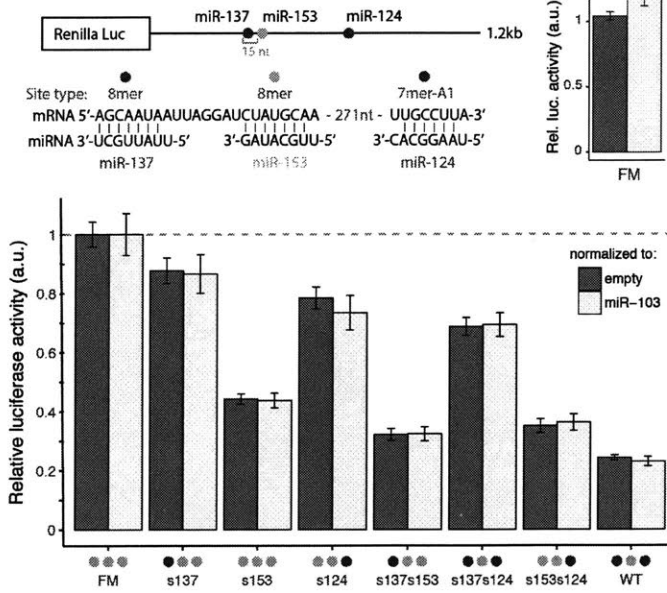
Fragile X mental retardation 1 (*Fmr1*) mRNA is also targeted by three miRNAs in the brain cluster: miR-129, miR-124, and miR-153 (**Fig. 5C**). The encoded RNA-binding protein FMRP acts as a translational regulator at synapses and affects dendritic spine morphology (Oostra and Willemsen, 2003). Repression of *Fmr1* in fragile X syndrome (FXS) results in a range of developmental disabilities including cognitive impairment, and elevated levels of *Fmr1* mRNA have been observed in premature ovarian failure (POF) and fragile X-associated tremor/ataxia syndrome (FXTAS), indicating that the gene is highly dosage-sensitive (Oostra and Willemsen, 2003). We found that the three targeting miRNAs together repressed the *Fmr1* reporter by about 60%, with individual seed matches to miR-129, miR-124, and miR-153 conferring 10%, 30% and 15% repression, respectively.

Figure 5

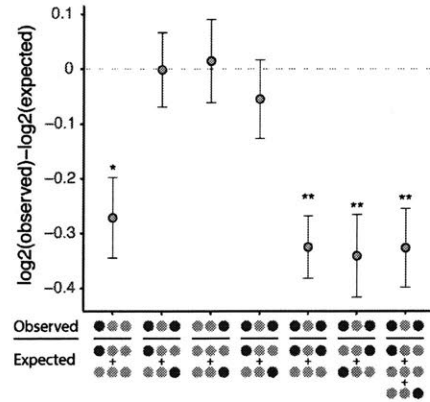
A Example scheme with *Fmr1* 3'UTR:



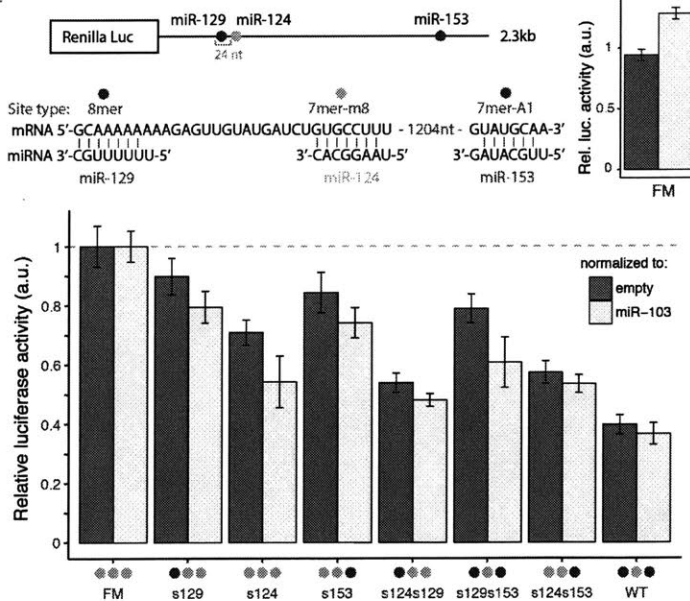
B *Neurod1* 3'UTR



D



C *Fmr1* 3'UTR



E

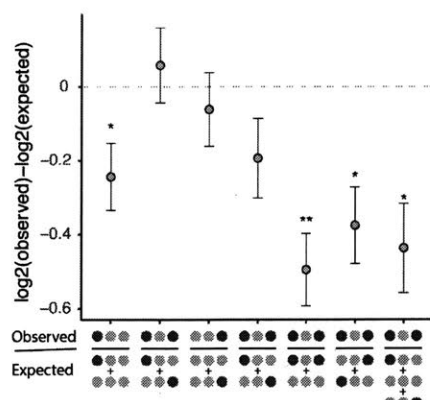


Figure 5. Brain cluster miRNAs collaborate to strongly repress *Neurod1* and *Fmr1*.

A) Luciferase reporter designs (*Fmr1* 3' UTR used in example): two bases in the center of the 7mer seed were changed to produce mutant versions. Reporter plasmids were co-transfected with dox-inducible miRNA expression plasmid (+ miR-ALL), miRNA control plasmid (+ miR-103), or empty plasmid (+ empty). Locations of seed matches to four brain cluster miRNAs are shown by colored dots, with seed and seed match sequences shown at right, using same color scheme.

B) *Neurod1* and **C)** *Fmr1* full length 3' UTRs were cloned downstream of the *Renilla* luciferase gene. Relative luciferase = $(R_{\text{miR-ALL}}/F_{\text{miR-ALL}}) / (R_{\text{norm}}/F_{\text{norm}})/\text{FM}$, where $R_X = \text{rLuc}$ in condition X , $F_X = \text{fLuc}$ in condition X , and samples were normalized to the FM from the corresponding control to assess the repression exerted by a miRNA/site pair. Samples were normalized to the empty plasmid (dark teal) and to the miR-103 control (light teal). Site combinations present are marked with a colored dot corresponding to the 3' UTR schematic. MEAN \pm SD of biological triplicates is shown.

D) *Neurod1* and **E)** *Fmr1* observed versus expected repression from combinations of individual sites or combinations of an individual site and a pair of sites, as indicated under the x-axis. $\log_2(\text{observed relative luciferase}) - \log_2(\text{expected relative luciferase})$ is plotted. Error bars show standard error propagated from biological triplicate measurements. Significance was calculated by Student's t-test: * $p < 0.05$, ** $p < 0.01$. See also Figure S4.

Together, these experiments confirm the ability of different sets of miRNAs from the brain cluster to act together to strongly repress shared targets. To our knowledge, these magnitudes of repression are the highest that have been observed for three different miRNAs targeting a natural, full length 3' UTR (Grimson et al., 2007; Krek et al., 2005).

Cotargeting miRNA sites with close spacing act cooperatively

Our experimental design enabled us to assess the extent of cooperativity between different pairs of seed matches and miRNAs. Previous studies have found that repression from multiple seed matches to the same miRNA in the same 3' UTR is typically multiplicative (equivalently, log-additive), so that two sites which independently repress an mRNA level to 80% of control levels will together repress the mRNA to about $(0.8) \times (0.8) = 64\%$ of control levels, i.e. 36% repression (Grimson et al., 2007; Nielsen et al., 2007). This rule is thought to hold unless the sites are located within a cooperative distance from one another, canonically 13-35 nt between seed starts. Therefore, we used log-additivity to calculate expected levels of reporter expression using measurements from single sites (or from two sites) and compared these values to the observed levels of reporters containing two or three sites to assess potential cooperativity (**Fig. 5D,E**).

The *Neurod1* and *Fmr1* reporters each contained a pair of sites with cooperative spacing: the miR-137 and miR-153 seed starts are 15 nt apart, and miR-129 and miR-124 are 24 nt apart. In both reporters, we found that pair of sites with distant spacing generally yielded log-additive repression, as expected, while the closely spaced pair of sites in each reporter exhibited significantly stronger repression, suggesting cooperative activity. Defining the cooperative effect (CE) as the difference between the base 2 logs of the observed and expected repression levels for the pair of seed matches, we observed CE of -0.27 ($p < 0.025$, student's t-test) for miR-137/miR-

153 *Neurod1*, and -0.24 ($p < 0.05$, student's t-test) for miR-129/miR-124 in *Fmr1*, confirming cooperativity. We obtained similar CE values when computing repression from pairs of sites relative to single sites, or from trios compared to either three single sites or a pair of sites and a single site. Interestingly, in both of these UTRs, the weakest site occurs at a cooperative distance from a much stronger site, thus conferring greater repressive potential to the weak site than if it occurred in isolation.

Cotargeting miRNAs direct potent and complex patterns of repression

To ask whether the patterns of activity observed above for multi-targeting combinations hold for larger numbers of sites in the same 3' UTR, we constructed similar mutant reporter series for two additional genes, with 4 and 7 seed matches to brain cluster miRNAs in their 3' UTRs. Rho-associated protein kinase 1 (ROCK1) is a downstream effector of RhoA GTPase, controlling actin filament bundling and F-actin accumulation (Julian and Olson, 2014). While ROCK1 mediates chemorepulsion of the growth cone for axonal pathfinding, mis-expression in developing neurons can inhibit neuritogenesis or cause neurite retraction in differentiated neurons (Gu et al., 2014; Mueller et al., 2005). Thus, *Rock1* levels must be strongly repressed in mature neurons. The 3' UTR of *Rock1* contains conserved target sites to four miRNAs from the brain cluster: miR-218, miR-153, miR-135, and miR-124. When the WT reporter was transfected with the miR-ALL plasmid containing the four miRNAs, expression was repressed a remarkable 93% (**Fig. 6A, S5**). The FM reporter was repressed 27-37% depending on the control used for normalization, suggesting the presence of some additional repressive element activated by transfection of these miRNAs. However, even after normalizing to the FM reporter, ROCK1 levels were still directly repressed 90% by the miRNAs. This magnitude of repression is beyond

the range typically attributed to miRNAs and may be the strongest yet observed for a natural non-cleaved 3' UTR. Each miRNA site contributed to this repression: miR-218, miR-153, miR-135, and miR-124 repressed *Rock1* by 14%, 34%, 40%, and 68%, respectively. The 68% repression conferred by the miR-124 site is among the strongest known for a single non-cleavage site in an endogenous 3' UTR.

The *Rock1* 3'UTR also contains sites for miR-153 and miR-135 within a cooperative spacing of 15 nt apart. We observed a significant CE of -0.36 ($p < 0.0025$, student's t-test) between these sites (**Fig. 6B**). We also observed a significant CE of -0.17 ($p < 0.05$, student's t-test) between miR-218 and miR-153, which was surprising because these sites are spaced 561 nt apart, far beyond the canonical range for cooperativity. The trio of the miR-218, miR-153, and miR-135 sites together had an even greater CE of -0.45 ($p < 0.0025$, student's t-test). However, reporters that also contained the miR-124 site, including the WT reporter, failed to exhibit significant cooperativity (**Fig. 6B**). This observation suggests that either the presence of the miR-124 seed match somehow interferes with cooperativity between the other sites, or possibly that the limits of repression detectable by our luciferase assay have been reached (Methods).

We also tested the 3' UTR of REST Corepressor 1 (*Rcor1*), which contains 7 sites to 5 distinct miRNAs from the brain cluster. RCOR1 functions to help recruit histone deacetylases to the REST complex, but also functions independently in the differentiation of early neuronal progenitor cells and in control of neuronal migration (Qureshi et al., 2010). *Rcor1* mRNA levels peak in early neuronal progenitors and decrease sharply across differentiation ((Qureshi et al., 2010), and data from (Hubbard et al., 2013)). Each tested site in the *Rcor1* reporter exerted only a modest level of repression (no more than 30%), yet together they conferred 80% repression (**Fig. 6C**). A small amount of cooperativity between all of the sites was observed, which may be

related to the 48 nt spacing between the miR-218 site and the second miR-153 site, miR-153.2 (Methods). The regulation of *Rcor1* provides an example in which moderate repression by individual miRNAs can combine to achieve more pronounced levels when several miRNAs act together in concert. Together, the data in Figures 5 and 6 validate four multi-targets of brain cluster miRNAs, establish typical patterns of log-additive and cooperative activity, and demonstrate the potential for combinations of miRNAs to repress expression by 60-90% or more.

Figure 6

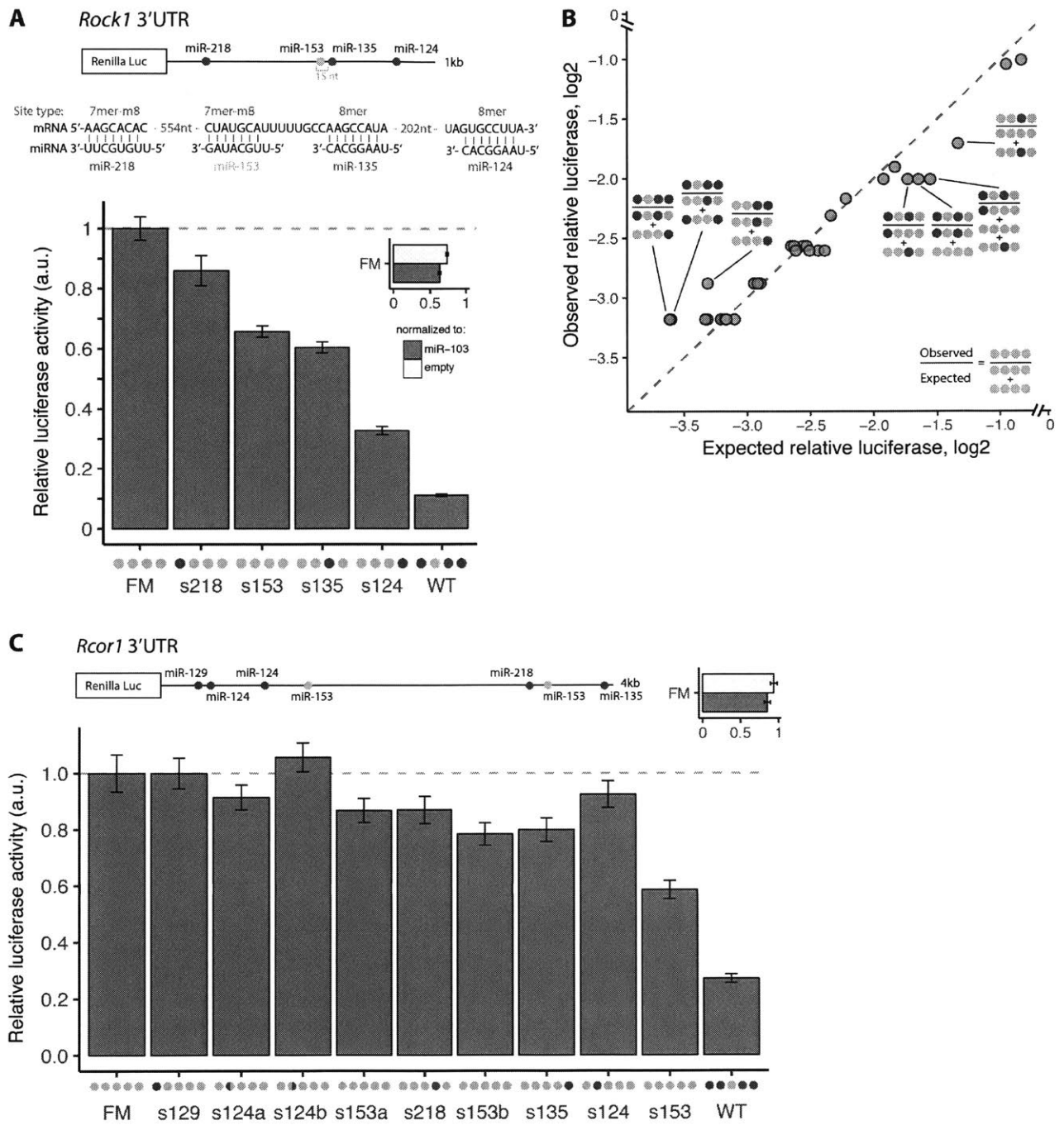


Figure 6. Strong and complex patterns of repression of *Rock1* and *Rcor1* 3' UTRs by brain cluster miRNAs.

A) *Rock1* 3' UTR cloned downstream of *Renilla* luciferase, as in Fig. 5. Samples normalized to miR-103 transfection are shown. **B)** observed relative luciferase (\log_2) over expected relative luciferase (\log_2) for all combinations of sites are shown. Seed match combinations used in normalization are shown adjacent to values that were significant relative to empty vector or miR-103 controls. **C)** *Rcor1* 3' UTR cloned downstream of *Renilla* luciferase. Relative luciferase activity normalized to miR-103 transfection are shown for FM and WT 3' UTRs, and for 3' UTRs containing each individual site. Colored semi-circles are used to indicate first (left semicircle) or second (right semicircle) sites in UTR for miR-124 and miR-153, which each have two sites in the WT 3' UTR. *See also Figure S5.*

DISCUSSION

The regulatory logic underlying miRNA regulation remains incompletely understood. When two-fold changes in the expression of most genes appear to be phenotypically neutral (Nanjundiah, 1993), it is unclear why miRNAs and so many individual miRNA target sites – which typically exert only modest ~10-30% repression – should be so highly conserved through evolution (Spies et al., 2013). While it is possible, even likely, that many genes have greater dosage sensitivity under real world conditions than can be detected in the lab, our findings suggest another explanation. The magnitudes of target repression observed here for combinations of miRNAs, between ~2.5- and 10-fold, are in a range where phenotypic consequences are more common. Correlated expression of the involved miRNAs – as observed for the brain cluster – may enable fold changes in this range to be exerted by groups of miRNAs on individual targets, likely contributing a major component of the developmental or condition-specific regulation of multi-targeted genes.

Multi-targeted genes appear to be quite numerous in mammalian genomes (e.g., **Fig. 4D**), leading us to consider how this regulatory pattern may evolve. In a cell type or condition where post-transcriptional repression of a specific gene would provide a fitness advantage, the emergence and maintenance of seed matches to expressed miRNAs should be evolutionarily favored. Given that all miRNAs are thought to enter similar or identical RISC complexes and to have similar activity when paired to a seed match, selection is likely to favor gain of sites for any miRNA with appropriate expression indiscriminately, until the optimal level of repression is achieved. If two seed matches worth of repression are needed, and ten different miRNAs are expressed at appropriate levels in the relevant cell type(s), then the second site to emerge has a

9/10 chance to match a different miRNA than the first, making two sites to different miRNAs nine times more likely to evolve than two sites to the same miRNA. Once two sites to different miRNAs are present, if there is selection for additional repression then eight times out of ten the third site will be to an miRNA distinct from the first two, and so forth. Thus, multi-targeting is likely to evolve fairly readily in comparison to repeated targeting by the same miRNA, consistent with its much more frequent incidence in mammalian genomes (Friedman et al., 2008).

Cotargeting by distinct miRNAs might also offer regulatory advantages over acquisition of multiple sites to a single miRNA. Regulation by different miRNAs can produce more complex temporal patterns of repression during cellular differentiation, stress response or other dynamic processes, while multiple sites to a single miRNA will necessarily have correlated activity, deriving from their dependence on the concentration of the same miRNA species. Multi-targeting may provide robustness advantages even in non-dynamic situations. Regulation by miRNAs can reduce noise from bursts of transcription, by enabling higher burst frequency at a given protein expression level by reducing the number of proteins produced per mRNA. Cotargeting should further reduce noise in target expression resulting from stochastic fluctuations in miRNA expression, as the uncorrelated fluctuations in each miRNA's expression will tend to cancel each other out (Schmiedel et al., 2015).

Shared targets tend to be more evolutionarily conserved than other targets (e.g., **Figs. 3E, 4E**), suggesting functional importance. The evolutionary signature of shared targeting between miR-138 and miR-137 led us to test and confirm the hypothesis that excess miR-137 could compensate for absence of miR-138 in CAD cell differentiation. This example suggests that cotargeting relationships may often reflect overlapping or related functions of pairs of miRNAs.

Genetic perturbation of specific cotargeting pairs or groups of miRNAs may be a generally useful strategy to reveal phenotypes, identify functional relationships and to help narrow down the list of targets relevant to a given phenotype (Alvarez-Saavedra and Horvitz, 2010).

Our results reveal a particularly strong signature of co- and multi-targeting among miRNAs with prominent expression in the brain. Neurons may require levels of key proteins to remain within a particular range for proper function, as in the case of *FMRI* (Oostra and Willemsen, 2003), so the noise reduction benefits of cotargeting might be of special importance in the brain. The brain may represent particularly fertile ground for the evolution of these regulatory relationships because the 3' UTRs of mRNAs expressed in the brain are much longer than in other tissues (Ramsköld et al., 2009), 3' UTR length increases across neuronal differentiation (Miura et al., 2013), and many miRNAs are brain-enriched (Bartel, 2018). The brain also has an extremely complex architecture of functionally distinct cell types, with more than 40 distinct neuronal types in the cortex alone (Tasic et al., 2016), so multi-targeting by miRNAs with overlapping but distinct expression patterns in different neuronal subtypes might be used to tune cell type-specific expression. Perturbation of the expression of multiple miRNAs belonging to the brain cluster occurs in several diseases of the brain, including glioblastoma, Huntington's Disease and dementia with Lewy bodies (Nelson et al., 2018; Shea et al., 2016; Skalsky and Cullen, 2011; Soldati et al., 2013). Our results imply that concerted changes in the levels of pairs or groups of miRNAs that cotarget together can exert large magnitude effects on the expression levels of multiply targeted mRNAs and may contribute to pathology.

AUTHOR CONTRIBUTIONS

J.M.C. performed experiments, analyses, and drafted the manuscript. V.J. performed experiments. C.B.B. supervised the project and revised the manuscript. All authors reviewed and approved the final manuscript.

ACKNOWLEDGEMENTS

We thank Myriam Heiman, Phil Sharp, David Sabatini, Michael McManus, D’Juan Farmer, Malin Akerblom and members of the Burge Lab for helpful discussions and comments.

SUPPLEMENTARY FIGURES

Figure S1

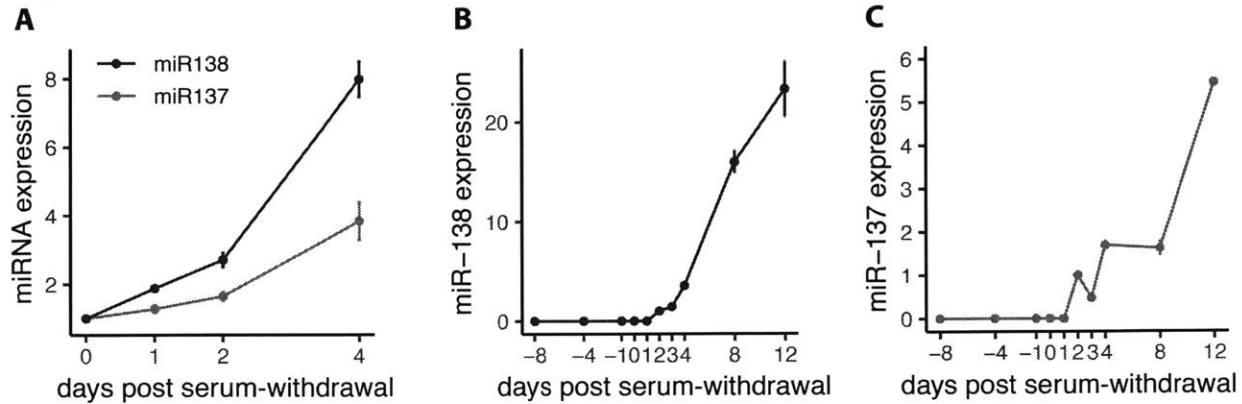


Figure S1. miR-138 and miR-137 are expressed across neuronal differentiation, Related to Figure 1.

A) Expression of miR-138 (dark blue) and miR-137 (light blue) in CAD cells 0, 1, 2, and 4 days after serum withdrawal. Expression of **B)** miR-138 and **C)** miR-137 across differentiation of glutamatergic neurons from mESCs. All expression measurements performed by TaqMan qPCR normalized to U6 snRNA.

Figure S2

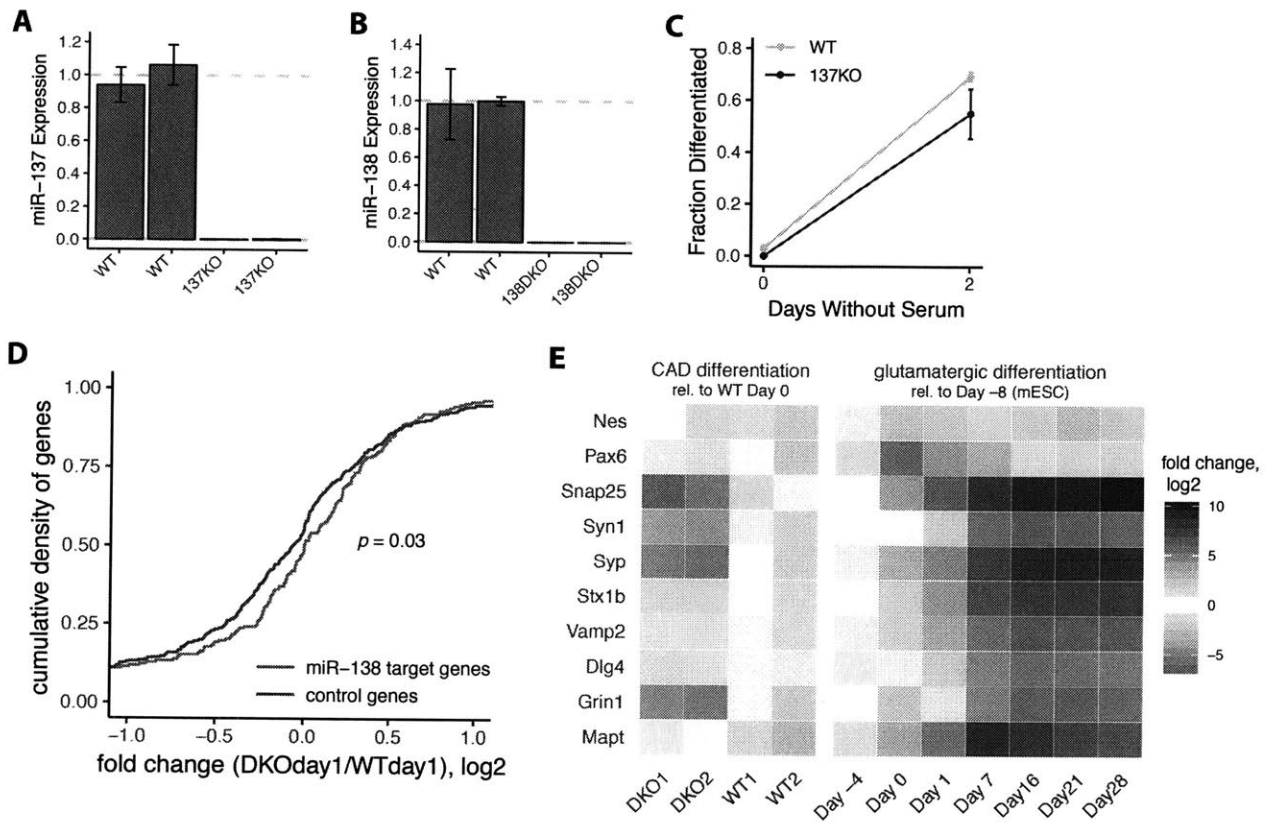


Figure S2. mRNA and miRNA expression changes in *mir-138* knockout cells, Related to Figure 2.

A) Expression of miR-137 in WT and 137KO cells measured by TaqMan qPCR normalized to U6 snRNA. Expression in KO cells normalized to the average of the WT samples. Duplicate bars show data for biological duplicates. **B)** Expression of miR-138 in WT and 138DKO cells, with conventions as in A). **C)** Quantitation of *mir-137* KO (137KO) and WT cell line differentiation at 0 and 2 days after serum withdrawal. **D)** Empirical cumulative distribution function (ecdf) of the fold change of miR-138 targets (blue) or shuffled seed control genes (red). $p = 0.03$ (Wilcoxon rank-sum test). **E)** Fold change (\log_2) in expression from CAD WT Day 0 of neuronal differentiation markers in CAD WT and 138DKO cells, and in a glutamatergic neuronal differentiation relative to Day -8 (representing mESCs). All measurements based on RNA-seq TPM values.

Figure S3

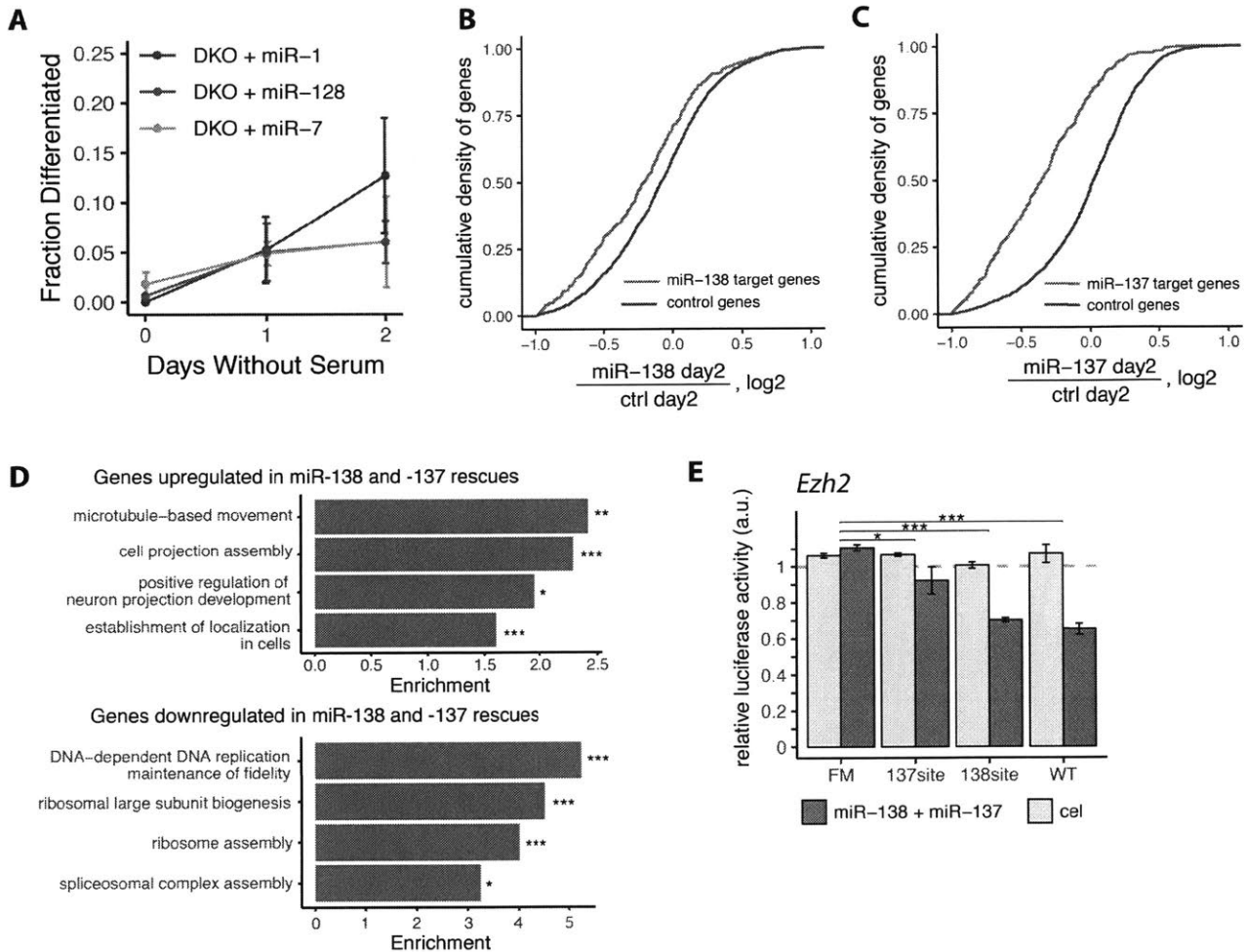


Figure S3. Gene expression changes in miR-138 and miR-137 rescue experiments, Related to Figure 3.

A) Quantitation of differentiation of DKO cells transfected with miR-1, miR-128, or miR-7 at 0, 1, and 2 days after serum withdrawal. **B)** Cumulative distributions of the fold change of miR-138 or **C)** miR-137 targets (blue) and shuffled seed control genes (red) in the corresponding miRNA mimic transfection at Day 0 compared to the pUC19 DNA control transfection. **D)** Gene ontology of genes significantly up-regulated or down-regulated in both miR-138 and miR-137 mimic transfections 2 days after serum withdrawal, normalized to the pUC19 DNA transfection control. FDR-corrected significance levels are marked with asterisks. **E)** *Renilla* over firefly luciferase signal for psiCHECK-2 reporter containing the *Ezh2* 3' UTR with one miR-138 and one miR-137 site (WT), or with both seed site mutations (FM). Treatment with miR-138 and miR-137 or control (cel-miR-67) were normalized to transfection with no miRNA mimic added. Significance was assessed by t-test, and select comparisons are shown. * $p < 0.05$, ** $p < 0.01$, *** $p < 0.001$.

Figure S4

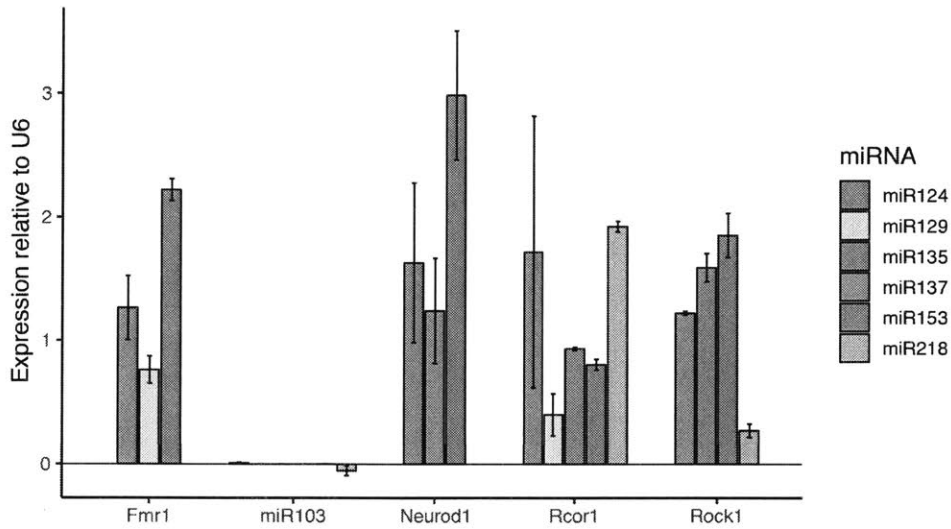


Figure S4. miRNAs are efficiently expressed from engineered cassette plasmids, Related to Figure 5.

miRNA expression measured by TaqMan qPCR, normalized to U6 snRNA. Background expression levels (measured in samples transfected with the empty plasmid) were subtracted. miRNAs were expressed from plasmids designed for *Neurod1*, *Fmr1*, *Rock1*, *Rcor1*, and miR-103 miRNA expression plasmids.

Figure S5

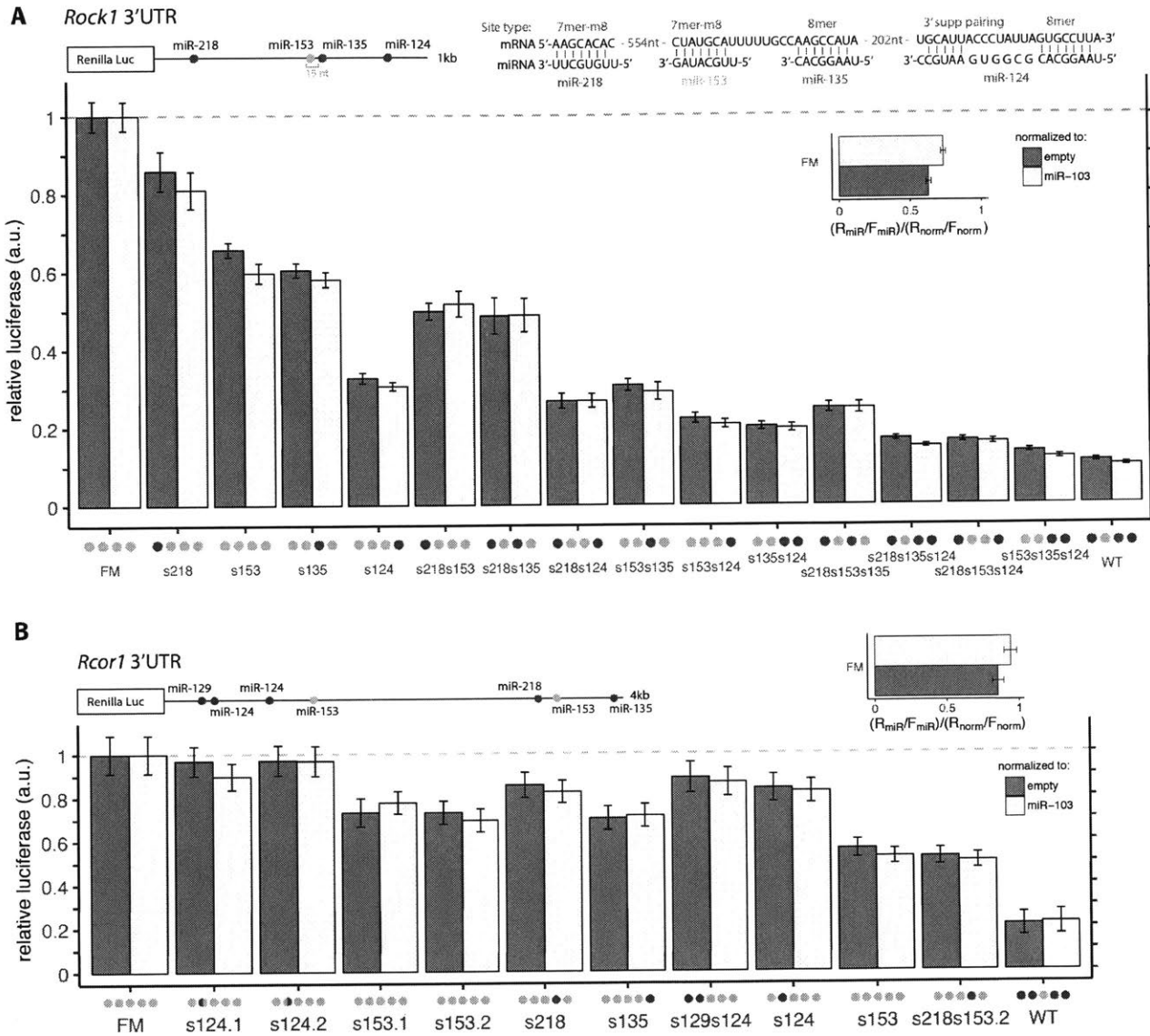


Figure S5. *Rock1* and *Rcor1* reporters reveal dynamic regulation, Related to Figure 6.

A) Relative luciferase activity (Renilla/firefly) for *Rock1* 3' UTR cloned downstream of Renilla luciferase, with different combinations of seed site mutations. Organized as in Figure 5B,C. **B)** Relative luciferase activity (Renilla/firefly) for *Rcor1* 3'UTR cloned downstream of Renilla luciferase. Organized as in Figure 5B,C.

METHODS

Cell Culture

All CAD cells (WT and knockout lines) were grown in DMEM/F12 (Gibco) supplemented with 10% fetal bovine serum (FBS) and differentiated in DMEM/F12 with no FBS added. HEK293 cells were grown in DMEM (Gibco) supplemented with 10% FBS. Cells were plated on poly-l-lysine coated plates before transfections to increase survival.

RNA-seq

For the WT and *mir-138* DKO CAD cells in serum or 24-96 h without serum, strand-specific, polyA-selected libraries were constructed using the dUTP incorporation method and sequenced on an Illumina NextSeq sequencer with paired-end 75-bp reads. Samples were prepared and sequenced in duplicate or triplicate (WT 0 and 96 h without serum), yielding approximately 30-45 million read pairs per replicate. For the *mir-138* DKO CAD cells transfected with either a miR-138 mimic, miR-137 mimic, or pUC19 DNA, strand-specific, polyA-selected libraries were constructed in duplicate with the Illumina's TruSeq Stranded mRNA Library Prep Kit for Neoprep and sequenced on an Illumina NextSeq sequencer with 50 bp single-end reads, yielding 18-36 M reads per replicate.

RNA-seq Analysis

For sequencing WT and *miR-138* DKO cell lines before and after serum withdrawal, cells were plated in a 6-well plate. For wells intended to differentiate, the media was replaced with serum-free media after 24 h. The serum-free samples were incubated at 37° C for an additional 24 or 96

h. RNA was collected with a Qiagen RNeasy Mini kit. Strand-specific libraries were made, and the samples were sequenced on an Illumina NextSeq sequencer in triplicate, yielding 30-45 million read pairs per replicate. Reads were aligned to the mm9 genome using STAR (Dobin et al., 2013), expression levels were quantified, and differentially expressed genes were assessed using DESeq2 (Love et al., 2014). Gene ontology enrichments were performed using the Gene Ontology Consortium powered by the Panther Classification System (Ashburner et al., 2000).

Small RNA sequencing

For sequencing of mature miRNA species, total RNA was harvested from CAD cells in serum or 4 days after serum withdrawal using the miRVana kit (Thermo Fisher). 1000 ng of total RNA was used with the Bioo Scientific NEXTFlex Small RNA Sequencing Kit v2 and libraries were sequenced on an Illumina HighSeq Sequencer in triplicate, yielding 9-18 M reads per replicate. Adapter sequences were trimmed from reads using cutadapt, and then reads with identical 4 bp barcodes on the 5' and 3' ends (8 bp total with a constrained distance in between) were collapsed to single reads, yielding 4-7 M unique reads remaining per replicate. Barcode sequences were trimmed from each end using cutadapt, and reads were mapped to the miRBase genome annotations using bwa with the following options: -n 1 -o 0 -e 0 -k 1, resulting in 50-66% of reads mapped per replicate. The miRNAs were filtered, requiring a minimum of 5 counts in at least one of the samples. Differential expression was assessed using DESeq (Anders and Huber, 2010). Size factors used for normalization were calculated from two spike-in miRNAs from different species: dme-miR-14-5p (*Drosophila*) and xtr-miR-427 (*Xenopus*). An expression cutoff of at least 500 normalized counts in at least one sample was used to further filter down candidate miRNAs for future study.

Northern blot analysis

15 ug of total RNA was loaded in a 15% Criterion TBE-Urea gel with a ³³P-ATP 5'-labeled Decade Marker RNA ladder (Ambion), transferred to a Amersham Hybond-NX membrane (GE Healthcare), crosslinked with EDC solution for 1 hour at 60 °C, and incubated in prehybridization solution (5X SSC, 20 mM Na₂HPO₄ pH 7.2, 7% SDS, 2X Denhardt's Solution) with 1 mg of denatured sheared salmon sperm DNA at 50 °C for 2 hours. 20 pmoles of miR-138 probe, sequence: 5'-cggcctgattcacaacaccagct-3', was end-labeled with 2 ul ³²P -ATP, >7000Ci/mmole (~150 µCi/µl) in a 20 ul reaction with 1 ul T4 PNK for 1 hour at 37 °C, and purified on a G-25 MicroSpin Column (GE). 10 ul of labeled probe was denatured at 85 °C for 5 minutes, added to the blot pre-hybridization solution and incubated overnight. The blot was washed for 30 min three times, with non-stringent wash buffer (3X SSC, 5% SDS), and once for 15 minutes with stringent wash buffer (1X SSC, 1% SDS). Blots were exposed 1 h to overnight and measured on a Typhoon FLA biomolecular imager.

miRNA expression quantitation

Total RNA was extracted using the mirVana miRNA Isolation Kit. miRNAs were amplified with the Taqman MicroRNA Assay (Applied Biosystems), in which each miRNA has a specific set of RT primers and qPCR primer/probe set. RT was performed with the TaqMan miRNA Reverse Transcription Kit, and qPCRs were run with the Taqman Universal Master Mix II (Thermo Fisher), no UNG on a Light Cycler 480 II Real-time PCR Machine (Roche). All miRNA measurements were normalized to measurements of U6 snRNA in the same sample.

Generation of miRNA KO cell lines and genotyping

miRNA KO cell lines were made by designing one gRNA to cut on either side of the precursor miRNA sequence to delete the entire hairpin region, generally following the protocol described by (Ran et al., 2013). *mir-138* DKO cell lines were made sequentially by first removing the *mir-138-2* locus and isolating a clonal population by FACS, and then removing the *mir-138-1* locus from the isolated *mir-138-2* SKO cell line. DNA was isolated from clonal populations with QuickExtract DNA Extraction Solution (Lucigen/EpicentreBio) and PCRed with (1) cell_mir138-1_way3'_F and cell_mir138-1_5'_R primers for the *mir-138-1* locus, and (2) cell_mir138-2_F and cell_mir138-2_R primers for the *mir-138-2* locus. Sizes of PCR products from around the intended deletion sites were assessed to identify KO lines. The deletion products were cloned with the TOPO TA Cloning Kit for Sequencing (Thermo Fisher), and several colonies were prepped and Sanger-sequenced to verify the exact sequence deletion.

gRNA sequences:

mir138-1_5'_1F	CACCgcatggtgttgggacagc
mir138-1_5'_1R	AAACgctgtcccacaacaccatgc
mir138-1_way3'F	CACCGCCTCAGTTACACCATAGGGC
mir138-1_way3'R	AAACGCCCTATGGTGTAAGTACTGAGGC
mir138-2_5'F	CACCgtctggtatggtgctgcagc
mir138-2_5'R	AAACgctgcagcaaccataaccagac
mir138-2_3'_2F	CACCGGATGGGTAGGGTGCAACCC
mir138-2_3'_2R	AAACGGGTTGCACCCTACCCATCC
mir137_3'F	CACCgCTTAAGAATACGCGTAGTCG

mir137_3'R	AAACCGACTACGCGTATTCTTAAGc
mir137_5'F	CACCgCCGTCACCGAAGAGAGTCAG
mir137_5'R	AAACCTGACTCTCTTCGGTGACGGc

PCR primers for Cell1 assay and deletion assay:

Cell_mir137_F	cacagctttggagccttctt
Cell_mir137_R	CTTTCAGATCCGCACTTTGC
mir137_del_R2	CTAAAAGCGGTCTGGGTCAC
cell_mir138-1_5_F	CAGAGCCACCTTTGGATCAT
cell_mir138-1_R	CAGCAGCCTCAGTTACACCA
cell_mir138-1_3_F	TGATGCACGTAGAGCAGAGG
cell_mir138-1_way3'_F	GCCAATCAGAGAACGGCTAC
cell_mir138-1_way3'_R	TTCCAGACCCTCTGAGGAGA
cell_mir138-2_F	TGGCAATCCTAGACCTCTGC
cell_mir138-2_R	GGGGAGCAGTTCAACTCTGA

Quantitation of neuronal differentiation

CAD WT and *mir-138* DKO cells were plated at 0.6e5 cells/well in a 12-well dish and media was changed to serum free media 24 hours later. Images were taken with a 10X and 20X aperture. The fraction of differentiated cells was quantified by counting any cell with a neurite at least twice the length of the cell body as differentiated, and all others as undifferentiated. Images were counted until a minimum of 100 cells was counted per replicate, and performed in triplicate. All counting was performed blinded.

miRNA target expression analysis

To assess global miR-138 and miR137 target expression changes (**Fig. S2D, S3B,C**), miRNA target sets were compared to background gene sets controlled for base composition and sequence conservation. Background gene sets were generated by randomly permuting the miRNA seed sequence to preserve base composition and CpG dinucleotide composition, and selecting genes that contained conserved instances of the shuffled seeds.

miRNA mimic rescues

mir-138 DKO cells were plated at 0.6×10^5 cells/well in a poly-l-lysine coated 12-well dish. mirVana miRNA mimics were transfected at 1 nM, 3 nM, and 9 nM with the Lipofectamine RNAiMAX reagent. miRNA mimics tested include: miR-138, miR-137, miR-1, miR-9, miR-7, miR-128, and negative control. Media was changed to serum-free media 48 h later, images were taken 0, 1, and 2 days after this media change, and differentiation was quantified based on cell morphology as described above. For RNA-seq of these rescues, total RNA was collected at 0 and 2 days after serum withdrawal using the Qiagen RNeasy kit.

Generating miRNA control sets

Control gene sets were generated for each miRNA target set that matched the distribution of 3' UTR length, C+G content, and sequence conservation (PhyloP scores) of the targets of the given miRNA. For example, miR-A target genes were binned into x quantile bins of 3' UTR length, which were further binned into y quantile bins of GC content, which were further divided into z quantile bins of PhyloP scores. All other genes (not targeted by miR-A) were divided into these

miR-A-defined bins and controls were sampled across these bins in the same proportions as miR-A target genes. The values of x , y , and z were chosen from the range 3 to 7 for each miRNA to meet the competing demands of matching the three properties as closely as possible while retaining sufficient control genes to ensure statistical power for the cotargeting analysis. Genes were sampled to generate the largest control set possible. All control sets were evaluated to verify that the distributions did not differ significantly from the control sets.

miRNA target set enrichment test

We limited this analysis to broadly conserved miRNAs with at least 300 broadly conserved targets, as defined by TargetScan v7.0 (Agarwal et al., 2015). Additionally, to eliminate miRNA pairs that might have an excess of shared targets due to related seeds, we collapsed miRNAs with identical 7mer seed sequences or 7mer seed sequences shifted by one nucleotide, keeping the miRNA with the larger number of conserved targets, or – in cases where both miRNAs had more than 1000 conserved targets – we kept the miRNA with broader evolutionary conservation.

Cotargeting pair expression analysis

Using small RNA sequencing data from a set of human tissues (compiled by (McCall et al., 2017)), we selected a set of 28 distinct tissues, keeping the samples with the highest read counts. We calculated the Spearman correlation of miRNA expression across these tissues for all miRNA pairs, and compared these correlations between significant cotargeting miRNA pairs and all other pairs.

miRNA cotargeting relationship clustering

Each cotargeting relationship was simplified to a binary code: 1 if significant (q-value < 0.05) and 0 if not significant. Because the zeroes represent uninteresting information (i.e. absence of a significant relationship between two miRNAs), we could not use standard clustering techniques on with these values. To properly weight the importance of the significant pairs, we performed a binomial test of overlap between the sets of significant cotargeting relationships for all miRNA pairs and used the $-\log$ of the p-values subtracted from the maximum value (excluding self comparisons) as distances, with average linkage clustering. To determine clusters we cut the tree at a height of 2.8, as shown in **Figure 4A**.

Luciferase reporter assays

3' UTRs were cloned into the psiCHECK-2 vector downstream of the *Renilla* luciferase gene using In-Fusion Cloning (Clontech). miRNA sites were mutated using QuikChange (Agilent Genomics) following manufacturer's instructions and mutant clones were confirmed by Sanger sequencing. miRNA hairpins plus ~100bp upstream and downstream were cloned into the pRD-RIPE vector in sequence next to one another. For each well of a 24-well plate, 100 ng psiCHECK-2 reporter plasmid and 300 ng miRNA expression plasmid were cotransfected into HEK293 cells using 1 ul lipofectamine 2000 and incubated with 1.5ug/mL doxycycline. *Renilla* and firefly luciferase levels were assayed 48 h later using the Dual Luciferase Reporter Assay System (Promega) and measured on a Varioskan Flash (Thermo Fisher). We normalized each *Renilla*/firefly ratio (R/F) from the plasmid +miR-ALL to the R/F ratio from the +miR-103 control, or to the ratio from the +empty control. Use of these two controls can provide information about the extent to which displacement of endogenous miRNAs from RISC by exogenous small RNAs may influence reporter expression. It is possible that for extreme levels

of repression (e.g., 10-fold or more), the sensitivity of the assay could be reduced due to varying levels of miRNA expression to luciferase reporter expression across cells.

Because we observed repression of the *Rock1* reporter by the miRNA specifically by expressing plasmid, we looked for additional non-conserved sites to the four miRNAs. Other than one 6mer site for miR-124, the 3' UTR lacks additional non-conserved target sites for these miRNAs. To further confirm that our mutated sites lacked residual activity, we mutated an additional two bp in the seed sequence yielding a total of 4 out of 7 bp in the seed mutated. We observed the same level of repression of this doubly mutated FM reporter as with our original FM plasmid, demonstrating that the repression is nonspecific and is not caused by direct binding of any of the expressed miRNAs.

For the *Rcor1* reporter plasmid, we found an alternative polyadenylation site downstream of the second miR-124 site and hypothesized that these upstream sites might be more active in the shorter isoform. While we did not observe stronger repression when we made a reporter with the shorter 3' UTR, it is possible that stronger repression may occur in different contexts.

REFERENCES

- Agarwal, V., Bell, G.W., Nam, J.-W., and Bartel, D.P. (2015). Predicting effective microRNA target sites in mammalian mRNAs. *Elife* 4, 1–38.
- Alvarez-Saavedra, E., and Horvitz, H.R. (2010). Many families of *C. elegans* microRNAs are not essential for development or viability. *Curr. Biol.* 20, 367–373.
- Anders, S., and Huber, W. (2010). Differential expression analysis for sequence count data. *Genome Biol* 11, R106.
- Ashburner, M., Ball, C.A., Blake, J.A., Botstein, D., Butler, H., Cherry, J.M., Davis, A.P., Dolinski, K., Dwight, S.S., Eppig, J.T., et al. (2000). Gene ontology: tool for the unification of biology. The Gene Ontology Consortium. *Nat Genet* 25, 25–29.
- Åkerblom, M., and Jakobsson, J. (2014). MicroRNAs as Neuronal Fate Determinants. *Neuroscientist* 20, 235–242.
- Baek, D., Villén, J., Shin, C., Camargo, F.D., Gygi, S.P., and Bartel, D.P. (2008). The impact of microRNAs on protein output. *Nature* 455, 64–71.
- Bartel, D.P. (2018). Metazoan MicroRNAs. *Cell* 173, 20–51.
- Cursons, J., Pillman, K.A., Scheer, K.G., Gregory, P.A., Foroutan, M., Hediye-Zadeh, S., Toubia, J., Crampin, E.J., Goodall, G.J., Bracken, C.P., et al. (2018). Combinatorial Targeting by MicroRNAs Co-ordinates Post-transcriptional Control of EMT. *Cell Syst* 7, 77–91.e77.
- Dobin, A., Davis, C.A., Schlesinger, F., Drenkow, J., Zaleski, C., Jha, S., Batut, P., Chaisson, M., and Gingeras, T.R. (2013). STAR: ultrafast universal RNA-seq aligner. *Bioinformatics* 29, 15–21.
- Doench, J.G., and Sharp, P.A. (2004). Specificity of microRNA target selection in translational repression. *Genes & Development* 18, 504–511.
- Friedman, R.C., Farh, K.K.H., Burge, C.B., and Bartel, D.P. (2008). Most mammalian mRNAs are conserved targets of microRNAs. *Genome Research* 19, 92–105.
- Friedman, R.C., and Burge, C.B. (2013). MicroRNA Target Finding by Comparative Genomics. In *Methods in Molecular Biology*, (Totowa, NJ: Humana Press), pp. 457–476.
- Grimson, A., Farh, K.K.-H., Johnston, W.K., Garrett-Engle, P., Lim, L.P., and Bartel, D.P. (2007). MicroRNA targeting specificity in mammals: determinants beyond seed pairing. *Mol. Cell* 27, 91–105.
- Gu, X., Meng, S., Liu, S., Jia, C., Fang, Y., Li, S., Fu, C., Song, Q., Lin, L., and Wang, X. (2014). miR-124 represses ROCK1 expression to promote neurite elongation through activation of the PI3K/Akt signal pathway. *J. Mol. Neurosci.* 52, 156–165.

- Huang, Y., Myers, S.J., and Dingleline, R. (1999). Transcriptional repression by REST: recruitment of Sin3A and histone deacetylase to neuronal genes. *Nat Neurosci* 2, 867–872.
- Hubbard, K.S., Gut, I.M., Lyman, M.E., and McNutt, P.M. (2013). Longitudinal RNA sequencing of the deep transcriptome during neurogenesis of cortical glutamatergic neurons from murine ESCs. *F1000Res* 2, 35.
- Jiang, Q., Feng, M.-G., and Mo, Y.-Y. (2009). Systematic validation of predicted microRNAs for cyclin D1. *BMC Cancer* 9, 194.
- Julian, L., and Olson, M.F. (2014). Rho-associated coiled-coil containing kinases (ROCK): structure, regulation, and functions. *Small GTPases* 5, e29846.
- Krek, A., Grün, D., Poy, M.N., Wolf, R., Rosenberg, L., Epstein, E.J., MacMenamin, P., da Piedade, I., Gunsalus, K.C., Stoffel, M., et al. (2005). Combinatorial microRNA target predictions. *Nat Genet* 37, 495–500.
- Landgraf, P., Rusu, M., Sheridan, R., Sewer, A., Iovino, N., Aravin, A., Pfeffer, S., Rice, A., Kamphorst, A.O., Landthaler, M., et al. (2007). A mammalian microRNA expression atlas based on small RNA library sequencing. *Cell* 129, 1401–1414.
- Lee, R.C., Feinbaum, R.L., and Ambros, V. (1993). The *C. elegans* heterochronic gene *lin-4* encodes small RNAs with antisense complementarity to *lin-14*. *Cell* 75, 843–854.
- Lewis, B.P., Burge, C.B., and Bartel, D.P. (2005). Conserved Seed Pairing, Often Flanked by Adenosines, Indicates that Thousands of Human Genes are MicroRNA Targets. *Cell* 120, 15–20.
- Lewis, B.P., Shih, I.-H., Jones-Rhoades, M.W., Bartel, D.P., and Burge, C.B. (2003). Prediction of mammalian microRNA targets. *Cell* 115, 787–798.
- Love, M.I., Huber, W., and Anders, S. (2014). Moderated estimation of fold change and dispersion for RNA-seq data with DESeq2. *Genome Biol* 15, 550.
- Mason, S., Piper, M., Gronostajski, R.M., and Richards, L.J. (2009). Nuclear factor one transcription factors in CNS development. *Mol Neurobiol* 39, 10–23.
- Mayr, C., Hemann, M.T., and Bartel, D.P. (2007). Disrupting the pairing between *let-7* and *Hmga2* enhances oncogenic transformation. *Science* 315, 1576–1579.
- McCall, M.N., Kim, M.-S., Adil, M., Patil, A.H., Lu, Y., Mitchell, C.J., Leal-Rojas, P., Xu, J., Kumar, M., Dawson, V.L., et al. (2017). Toward the human cellular microRNAome. *Genome Research* 27, 1769–1781.
- Mendell, J.T., and Olson, E.N. (2012). MicroRNAs in stress signaling and human disease. *Cell* 148, 1172–1187.
- Miska, E.A., Alvarez-Saavedra, E., Abbott, A.L., Lau, N.C., Hellman, A.B., McGonagle, S.M.,

Bartel, D.P., Ambros, V.R., and Horvitz, H.R. (2007). Most *Caenorhabditis elegans* microRNAs are individually not essential for development or viability. *PLoS Genet* 3, e215.

Miura, P., Shenker, S., Andreu-Agullo, C., Westholm, J.O., and Lai, E.C. (2013). Widespread and extensive lengthening of 3' UTRs in the mammalian brain. *Genome Research* 23, 812–825.

Mueller, B.K., Mack, H., and Teusch, N. (2005). Rho kinase, a promising drug target for neurological disorders. *Nat Rev Drug Discov* 4, 387–398.

Nanjundiah, V. (1993). Why are most mutations recessive? *Journal of Genetics* 72, 85–97.

Nelson, P.T., Wang, W.-X., Janse, S.A., and Thompson, K.L. (2018). MicroRNA expression patterns in human anterior cingulate and motor cortex: A study of dementia with Lewy bodies cases and controls. *Brain Research* 1678, 374–383.

Neo, W.H., Yap, K., Lee, S.H., Looi, L.S., Khandelia, P., Neo, S.X., Makeyev, E.V., and Su, I.-H. (2014). MicroRNA miR-124 Controls the Choice between Neuronal and Astrocyte Differentiation by Fine-tuning Ezh2 Expression. *J. Biol. Chem.* 289, 20788–20801.

Nesti, E., Corson, G.M., McCleskey, M., Oyer, J.A., and Mandel, G. (2014). C-terminal domain small phosphatase 1 and MAP kinase reciprocally control REST stability and neuronal differentiation. *Proc. Natl. Acad. Sci. U.S.A.* 111, E3929–E3936.

Nielsen, C.B., Shomron, N., Sandberg, R., Hornstein, E., Kitzman, J., and Burge, C.B. (2007). Determinants of targeting by endogenous and exogenous microRNAs and siRNAs. *Rna* 13, 1894–1910.

Obermayer, B., and Levine, E. (2014). Exploring the miRNA regulatory network using evolutionary correlations. *PLoS Comput Biol* 10, e1003860.

Oostra, B.A., and Willemsen, R. (2003). A fragile balance: FMR1 expression levels. *Human Molecular Genetics* 12 *Spec No 2*, R249–R257.

Pataskar, A., Jung, J., Smialowski, P., Noack, F., Calegari, F., Straub, T., and Tiwari, V.K. (2016). NeuroD1 reprograms chromatin and transcription factor landscapes to induce the neuronal program. *The EMBO Journal* 35, 24–45.

Pereira, J.D., Sansom, S.N., Smith, J., Dobenecker, M.-W., Tarakhovskiy, A., and Livesey, F.J. (2010). Ezh2, the histone methyltransferase of PRC2, regulates the balance between self-renewal and differentiation in the cerebral cortex. *Proc. Natl. Acad. Sci. U.S.A.* 107, 15957–15962.

Qi, Y., Wang, J.K., McMillian, M., and Chikaraishi, D.M. (1997). Characterization of a CNS cell line, CAD, in which morphological differentiation is initiated by serum deprivation. *J. Neurosci.* 17, 1217–1225.

Qureshi, I.A., Gokhan, S., and Mehler, M.F. (2010). REST and CoREST are transcriptional and epigenetic regulators of seminal neural fate decisions. *Cell Cycle* 9, 4477–4486.

Ramsköld, D., Wang, E.T., Burge, C.B., and Sandberg, R. (2009). An abundance of ubiquitously expressed genes revealed by tissue transcriptome sequence data. *PLoS Comput Biol* 5, e1000598.

Ran, F.A., Hsu, P.D., Wright, J., Agarwala, V., Scott, D.A., and Zhang, F. (2013). Genome engineering using the CRISPR-Cas9 system. *Nat Protoc* 8, 2281–2308.

Reinhart, B.J., Slack, F.J., Basson, M., Pasquinelli, A.E., Bettinger, J.C., Rougvie, A.E., Horvitz, H.R., and Ruvkun, G. (2000). The 21-nucleotide let-7 RNA regulates developmental timing in *Caenorhabditis elegans*. *Nature* 403, 901–906.

Riley, K.J., Rabinowitz, G.S., Yario, T.A., Luna, J.M., Darnell, R.B., and Steitz, J.A. (2012). EBV and human microRNAs co-target oncogenic and apoptotic viral and human genes during latency. *The EMBO Journal* 31, 2207–2221.

Saetrom, P., Heale, B.S.E., Snøve, O., Aagaard, L., Alluin, J., and Rossi, J.J. (2007). Distance constraints between microRNA target sites dictate efficacy and cooperativity. *Nucleic Acids Research* 35, 2333–2342.

Santos, M.C.T., Tegge, A.N., Correa, B.R., Mahesula, S., Kohnke, L.Q., Qiao, M., Ferreira, M.A.R., Kokovay, E., and Penalva, L.O.F. (2016). miR-124, -128, and -137 Orchestrate Neural Differentiation by Acting on Overlapping Gene Sets Containing a Highly Connected Transcription Factor Network. *Stem Cells* 34, 220–232.

Schmiedel, J.M., Klemm, S.L., Zheng, Y., Sahay, A., Blüthgen, N., Marks, D.S., and van Oudenaarden, A. (2015). Gene expression. MicroRNA control of protein expression noise. *Science* 348, 128–132.

Selbach, M., Schwanhäusser, B., Thierfelder, N., Fang, Z., Khanin, R., and Rajewsky, N. (2008). Widespread changes in protein synthesis induced by microRNAs. *Nature* 455, 58–63.

Shea, A., Harish, V., Afzal, Z., Chijioke, J., Kedir, H., Dusmatova, S., Roy, A., Ramalinga, M., Harris, B., Blancato, J., et al. (2016). MicroRNAs in glioblastoma multiforme pathogenesis and therapeutics. *Cancer Med* 5, 1917–1946.

Skalsky, R.L., and Cullen, B.R. (2011). Reduced expression of brain-enriched microRNAs in glioblastomas permits targeted regulation of a cell death gene. *PLoS ONE* 6, e24248.

Soldati, C., Bithell, A., Johnston, C., Wong, K.-Y., Stanton, L.W., and Buckley, N.J. (2013). Dysregulation of REST-regulated coding and non-coding RNAs in a cellular model of Huntington's disease. *J. Neurochem.* 124, 418–430.

Spies, N., Burge, C.B., and Bartel, D.P. (2013). 3' UTR-isoform choice has limited influence on

the stability and translational efficiency of most mRNAs in mouse fibroblasts. *Genome Research* 23, 2078–2090.

Storey, J.D., and Tibshirani, R. (2003). Statistical significance for genomewide studies. *Proc. Natl. Acad. Sci. U.S.A.* 100, 9440–9445.

Szulwach, K.E., Li, X., Smrt, R.D., Li, Y., Luo, Y., Lin, L., Santistevan, N.J., Li, W., Zhao, X., and Jin, P. (2010). Cross talk between microRNA and epigenetic regulation in adult neurogenesis. *The Journal of Cell Biology* 189, 127–141.

Tasic, B., Menon, V., Nguyen, T.N., Kim, T.-K., Jarsky, T., Yao, Z., Levi, B., Gray, L.T., Sorensen, S.A., Dolbeare, T., et al. (2016). Adult mouse cortical cell taxonomy revealed by single cell transcriptomics. *Nat Neurosci* 19, 335–346.

Tsang, J.S., Ebert, M.S., and van Oudenaarden, A. (2010). Genome-wide dissection of microRNA functions and cotargeting networks using gene set signatures. *Mol. Cell* 38, 140–153.

van Rooij, E., Sutherland, L.B., Qi, X., Richardson, J.A., Hill, J., and Olson, E.N. (2007). Control of stress-dependent cardiac growth and gene expression by a microRNA. *Science* 316, 575–579.

Visvanathan, J., Lee, S., Lee, B., Lee, J.W., and Lee, S.-K. (2007). The microRNA miR-124 antagonizes the anti-neural REST/SCP1 pathway during embryonic CNS development. *Genes & Development* 21, 744–749.

Wightman, B., Ha, I., and Ruvkun, G. (1993). Posttranscriptional regulation of the heterochronic gene *lin-14* by *lin-4* mediates temporal pattern formation in *C. elegans*. *Cell* 75, 855–862.

Wu, S., Huang, S., Ding, J., Zhao, Y., Liang, L., Liu, T., Zhan, R., and He, X. (2010). Multiple microRNAs modulate p21Cip1/Waf1 expression by directly targeting its 3' untranslated region. *Oncogene* 29, 2302–2308.

Yoo, A.S., Sun, A.X., Li, L., Shcheglovitov, A., Portmann, T., Li, Y., Lee-Messer, C., Dolmetsch, R.E., Tsien, R.W., and Crabtree, G.R. (2011). MicroRNA-mediated conversion of human fibroblasts to neurons. *Nature* 476, 228–231.

Zheng, G.X.Y., Ravi, A., Calabrese, J.M., Medeiros, L.A., Kirak, O., Dennis, L.M., Jaenisch, R., Burge, C.B., and Sharp, P.A. (2011). A latent pro-survival function for the mir-290-295 cluster in mouse embryonic stem cells. *PLoS Genet* 7, e1002054.

Chapter 3:

Conclusions

Implications

Twenty-five years after the initial discovery of miRNAs, we have learned so much – we have identified an entire new class of regulatory molecules encompassing hundreds to thousands of miRNA genes in more than 200 species and characterized how those miRNA genes are expressed, processed, and orchestrate repression on an mRNA target. We have learned how miRNAs meaningfully integrate into gene regulatory networks to impact nearly every level of development, and how they can contribute to the pathology of disease (Bartel, 2018). And yet, it feels as though we are at the next front of miRNA discovery – still learning new ways in which miRNAs target genes through non-canonical interactions in modes that are miRNA-specific (McGeary et al.), still discovering new phenotypes and processes miRNAs are involved in to integrate them into larger gene regulatory networks (Bartel, 2018), and better defining the ways in which miRNAs work together to co-target large sets of genes and drive much greater levels of repression than was once thought possible. With better estimates of cell-type-specific miRNA expression (for the most part, we are currently limited by tissue level data or *in vitro* cell cultures), we may be able to integrate biochemical binding models, co-targeting relationships, and expression data to predict the impact of miRNAs within different gene regulatory networks. And importantly, we can begin to understand how these regulatory networks are disrupted in disease where large sets of miRNAs are often dysregulated.

We have identified several neurological diseases in which a majority of the miRNAs from our co-targeting brain cluster is improperly expressed. Glioblastoma is among the most aggressive malignant tumors manifest from glial cells in the brain and has one of the poorest prognoses with a median survival time of 14 months (Ohgaki and Kleihues, 2005). miRNA profiling in glioblastomas has identified sets of miRNAs which are up- or down-regulated in the

disease state, of which many of the down-regulated miRNAs were brain-enriched (Shea et al., 2016; Skalsky and Cullen, 2011). These significantly down-regulated miRNAs include miR-128, miR-124, miR-137, miR-218, miR-153, and in some experiments but not others miR-135 (Shea et al., 2016), which is 6 out of the 9 miRNAs in our co-targeting brain cluster in Chapter 2. Our results would indicate that special attention should be paid to the genes multiply-targeted by these miRNAs as they are likely more significantly impacted than genes targeted by only one of these miRNAs. We made similar observations when looking at miRNA expression data in Huntington's Disease (Soldati et al., 2013), as well as dementia with Lewy bodies (Nelson et al., 2018).

We focused our attention on the brain cluster because it had the most striking tissue-specific expression, but there is more to be learned about the non-neuronal co-targeting relationships as well. Our second largest cluster of co-targeting miRNAs contains multiple miRNAs involved in cholesterol metabolism (Aryal et al., 2017), ESC versus somatic cell state and cancer phenotypes (Razak et al., 2013). Thus, the exploration of these miRNAs warrants further investigation both in normal and pathological processes. In addition, individual relationship pairs could also be interesting and meaningful, for example, the co-targeting pair miR-148 and miR-155 are two immune-regulatory miRNAs enriched in the hematopoietic system (Ramkissoon et al., 2006) and often found deregulated with one another in diseases including multiple sclerosis (Ma et al., 2014).

Our results also have implications for how we think about the contribution of miRNAs in defining cell identity and driving developmental transitions to reach those final states. Elegant studies in *C. Elegans* have demonstrated the temporal regulation miRNAs orchestrate to time key developmental transitions (Abbott et al., 2005; Reinhart et al., 2000; Slack et al., 2000). It is

likely that miRNAs exert similar temporal controls in mammalian systems but it is harder to detect the time and space of expression due to the increased tissue and organism complexity. Particularly interesting is the regulation of neurogenesis, from transition out of the early neuronal progenitor populations, to migration and formation of synaptic connections, these are all highly time-dependent processes which when deregulated could lead to microcephaly or many other forms of neurologic disease. We have a rough picture of the miRNAs that are expressed at these different periods and how they might contribute to transitioning between differentiation states, but we have a lot to do in this area, and considering co-targeting relationships in these transitions may add substantial value to our understanding. For example, when two miRNAs lie within a cooperative distance and yield more repression than the sum of their parts, this can drive stronger and cleaner transitions. Analogously, cell type specificity, such as the vast number of neuronal subtypes (Tasic et al., 2016), may be sculpted by the specific profiles of miRNA expression in each of these cell types. Again, cooperativity between miRNAs can deliver stronger effects on target gene expression between the different cell types. Lastly, miRNAs also have specific patterns of subcellular localization, which is particularly exaggerated and key in neurons (Schratt, 2009). The implications of co-targeting within these distinct cellular compartments should be given additional consideration.

We presented a model at the end of Chapter 2 for how and why these co-targeting relationships between miRNAs might exist. As miRNA target sites drift in and out of locations throughout the transcriptome, some are selected for when they improve fitness and conversely, some are selected against when they reduce fitness (Farh et al., 2005). Because the selective avoidance is so strong, it demonstrates at least on some level that the majority of sites that appear, if they are in genes that are co-expressed with the miRNA, they will confer some level of

repression – otherwise, they would not be selected against. This supports our model that the creation of a target site for any expressed miRNA can be efficient to achieve repression of an intended target, rather than the need to develop sites to the same miRNA repeatedly. Not all non-conserved sites are 100% avoided when in genes that are co-expressed with the miRNA. While some of these could represent non-functional sites or newly evolved, species-specific sites, it is also possible that the organism can sustain a certain amount of spurious targeting because repression only becomes biologically meaningful on the level co-targeting. So the ability to evolve new sites freely without detrimental phenotypic effects to the organism could be part of the regulatory logic of miRNAs and how they are able to evolve complex regulation that can define subtypes of cells.

Future directions

Fairly new knowledge about the magnitude of repression possible from particular non-canonical miRNA site types (McGeary et al.), demonstrates a new need to incorporate these sites into future analyses. *In vivo* data suggests that 25% of all Ago-miR-miRNA interactions in the brain are mediated through binding to bulge sites, of which 75% contain G bulges (the bulge site with the strongest predicted binding (McGeary et al.)), so incorporating these sites may uncover even greater levels of co-targeting in the brain (Chi et al., 2012; 2009).

For reasons discussed in the implications section, it would be useful to attain cell type-specific small RNA sequencing data. One group developed a miRNA tagging and affinity-purification (miRAP) method to isolate miRNAs from specific neuronal subtypes in the mouse brain (He et al., 2012). Perhaps this technique could be expanded on to include a larger diversity of cell types or to isolate different time points over the course of embryonic and postnatal

development. It is possible that the material needed may be a limitation for the second application, but I think there is a lot of value in performing these assays in a developing mouse brain over a cell culture system where the miRNA repertoire can usually be quite different.

Lastly, we are at a place in the current status of genome editing technology where high throughput KO of miRNA target sites is not out of the question – both editing by TALENs and the CRISPR-Cas9 system are capable of being scaled up. I think the possible importance of co-targeting warrants a new form of investigating the functions of miRNAs. Instead of adding or removing a miRNA, I propose to remove sets of target sites shared among co-targeting miRNAs and looking for effects or phenotypes. One can imagine starting with a disease where many co-targeting miRNAs have already been observed to increase or decrease in expression together. The highly co-targeted transcripts of these miRNAs can then be investigated for their potential contribution to the disease phenotype.

REFERENCES

- Abbott, A.L., Alvarez-Saavedra, E., Miska, E.A., Lau, N.C., Bartel, D.P., Horvitz, H.R., and Ambros, V. (2005). The let-7 MicroRNA family members mir-48, mir-84, and mir-241 function together to regulate developmental timing in *Caenorhabditis elegans*. *Developmental Cell* 9, 403–414.
- Aryal, B., Singh, A.K., Rotllan, N., Price, N., and Fernández-Hernando, C. (2017). MicroRNAs and lipid metabolism. *Current Opinion in Lipidology* 28, 273–280.
- Bartel, D.P. (2018). Metazoan MicroRNAs. *Cell* 173, 20–51.
- Chi, S.W., Hannon, G.J., and Darnell, R.B. (2012). An alternative mode of microRNA target recognition. *Nat. Struct. Mol. Biol.* 19, 321–327.
- Chi, S.W., Zang, J.B., Mele, A., and Darnell, R.B. (2009). Argonaute HITS-CLIP decodes microRNA-mRNA interaction maps. *Nature* 460, 479–486.
- Farh, K.K.-H., Grimson, A., Jan, C., Lewis, B.P., Johnston, W.K., Lim, L.P., Burge, C.B., and Bartel, D.P. (2005). The widespread impact of mammalian MicroRNAs on mRNA repression and evolution. *Science* 310, 1817–1821.
- He, M., Liu, Y., Wang, X., Zhang, M.Q., Hannon, G.J., and Huang, Z.J. (2012). NeuroResource. *Neuron* 73, 35–48.
- Ma, X., Zhou, J., Zhong, Y., Jiang, L., Mu, P., Li, Y., Singh, N., Nagarkatti, M., and Nagarkatti, P. (2014). Expression, regulation and function of microRNAs in multiple sclerosis. *Int J Med Sci* 11, 810–818.
- McGeary, S.E., Lin, K.S., Shi, C.Y., Bisaria, N., and Bartel, D.P. The biochemical basis of microRNA targeting efficacy.
- Nelson, P.T., Wang, W.-X., Janse, S.A., and Thompson, K.L. (2018). MicroRNA expression patterns in human anterior cingulate and motor cortex: A study of dementia with Lewy bodies cases and controls. *Brain Research* 1678, 374–383.
- Ohgaki, H., and Kleihues, P. (2005). Population-based studies on incidence, survival rates, and genetic alterations in astrocytic and oligodendroglial gliomas. *J. Neuropathol. Exp. Neurol.* 64, 479–489.
- Ramkissoon, S.H., Mainwaring, L.A., Ogasawara, Y., Keyvanfar, K., McCoy, J.P., Sloand, E.M., Kajigaya, S., and Young, N.S. (2006). Hematopoietic-specific microRNA expression in human cells. *Leuk. Res.* 30, 643–647.
- Razak, S.R.A., Ueno, K., Takayama, N., Nariyai, N., Nagasaki, M., Saito, R., Koso, H., Lai, C.-Y., Murakami, M., Tsuji, K., et al. (2013). Profiling of microRNA in human and mouse ES and iPS cells reveals overlapping but distinct microRNA expression patterns. *PLoS ONE* 8, e73532.

Reinhart, B.J., Slack, F.J., Basson, M., Pasquinelli, A.E., Bettinger, J.C., Rougvie, A.E., Horvitz, H.R., and Ruvkun, G. (2000). The 21-nucleotide let-7 RNA regulates developmental timing in *Caenorhabditis elegans*. *Nature* *403*, 901–906.

Schratt, G. (2009). microRNAs at the synapse. *Nat Rev Neurosci* *10*, 842–849.

Shea, A., Harish, V., Afzal, Z., Chijioke, J., Kedir, H., Dusmatova, S., Roy, A., Ramalinga, M., Harris, B., Blancato, J., et al. (2016). MicroRNAs in glioblastoma multiforme pathogenesis and therapeutics. *Cancer Med* *5*, 1917–1946.

Skalsky, R.L., and Cullen, B.R. (2011). Reduced expression of brain-enriched microRNAs in glioblastomas permits targeted regulation of a cell death gene. *PLoS ONE* *6*, e24248.

Slack, F.J., Basson, M., Liu, Z., Ambros, V., Horvitz, H.R., and Ruvkun, G. (2000). The lin-41 RBCC gene acts in the *C. elegans* heterochronic pathway between the let-7 regulatory RNA and the LIN-29 transcription factor. *Mol. Cell* *5*, 659–669.

Soldati, C., Bithell, A., Johnston, C., Wong, K.-Y., Stanton, L.W., and Buckley, N.J. (2013). Dysregulation of REST-regulated coding and non-coding RNAs in a cellular model of Huntington's disease. *J. Neurochem.* *124*, 418–430.

Tasic, B., Menon, V., Nguyen, T.N., Kim, T.-K., Jarsky, T., Yao, Z., Levi, B., Gray, L.T., Sorensen, S.A., Dolbeare, T., et al. (2016). Adult mouse cortical cell taxonomy revealed by single cell transcriptomics. *Nat Neurosci* *19*, 335–346.

Appendix I:

Supplemental Tables to Chapter 2

Table II-S1.

miRNA1	miRNA2	qval1	qval2	OR1	OR2	geomean(qval)
miR-374b-5p_miR-374c-5p	miR-374c-5p_miR-374b-5p	2.57E-13	3.09E-11	3.03	2.96	2.82E-12
miR-148a-3p_miR-19a-3p	miR-19a-3p_miR-148a-3p	1.32E-09	1.48E-12	2.57	2.69	4.41E-11
miR-128-3p_miR-144-3p	miR-144-3p_miR-128-3p	7.97E-12	1.14E-07	2.72	2.07	9.53E-10
miR-344d-3p_miR-374b-5p	miR-374b-5p_miR-344d-3p	3.24E-06	2.83E-09	3.04	3.13	9.57E-08
miR-128-3p_miR-218-5p	miR-218-5p_miR-128-3p	4.62E-08	3.11E-07	2.15	2.03	1.20E-07
miR-200b-3p_miR-374c-5p	miR-374c-5p_miR-200b-3p	1.87E-07	5.36E-07	2.13	2.09	3.17E-07
miR-323-3p_miR-493-5p	miR-493-5p_miR-323-3p	2.42E-09	9.69E-05	3.15	2.09	4.85E-07
miR-182-5p_miR-9-5p	miR-9-5p_miR-182-5p	1.41E-05	5.54E-08	1.75	1.94	8.84E-07
miR-124-3p.1_miR-9-5p	miR-9-5p_miR-124-3p.1	1.41E-05	2.90E-07	1.66	1.79	2.02E-06
miR-128-3p_miR-148a-3p	miR-148a-3p_miR-128-3p	3.09E-06	6.73E-06	2.07	2.28	4.56E-06
miR-137-3p_miR-218-5p	miR-218-5p_miR-137-3p	4.35E-06	7.68E-05	1.94	1.85	1.83E-05
miR-182-5p_miR-200b-3p	miR-200b-3p_miR-182-5p	5.74E-07	1.37E-03	2.01	1.61	2.81E-05
miR-186-5p_miR-340-5p	miR-340-5p_miR-186-5p	2.20E-05	5.43E-05	1.97	1.78	3.46E-05
miR-135a-5p_miR-153-3p	miR-153-3p_miR-135a-5p	1.25E-05	1.15E-04	2.66	1.88	3.80E-05
miR-137-3p_miR-33-5p	miR-33-5p_miR-137-3p	6.60E-04	2.76E-06	2.03	2.80	4.27E-05
miR-138-5p_miR-370-3p	miR-370-3p_miR-138-5p	1.41E-05	1.50E-04	2.45	2.64	4.60E-05
miR-23a-3p_miR-26a-5p	miR-26a-5p_miR-23a-3p	6.15E-05	8.40E-05	1.78	1.90	7.19E-05
miR-124-3p.1_miR-19a-3p	miR-19a-3p_miR-124-3p.1	6.15E-05	9.21E-05	1.65	1.67	7.53E-05
miR-137-3p_miR-153-3p	miR-153-3p_miR-137-3p	1.18E-04	1.76E-04	1.91	1.87	1.44E-04
miR-200b-3p_miR-452-5p	miR-452-5p_miR-200b-3p	9.84E-06	2.31E-03	2.19	2.05	1.51E-04
miR-320-3p_miR-340-5p	miR-340-5p_miR-320-3p	6.26E-05	1.34E-03	2.05	1.74	2.90E-04
miR-129-5p_miR-	miR-374c-5p_miR-	2.54E-05	5.22E-03	2.31	1.89	3.64E-04

374c-5p	129-5p					
miR-124-3p.1_miR-182-5p	miR-182-5p_miR-124-3p.1	2.32E-04	7.49E-04	1.59	1.56	4.17E-04
miR-135a-5p_miR-137-3p	miR-137-3p_miR-135a-5p	1.28E-02	1.75E-05	1.69	1.84	4.74E-04
miR-144-3p_miR-199a-3p	miR-199a-3p_miR-144-3p	1.85E-04	1.29E-03	2.09	2.12	4.88E-04
miR-326-3p_miR-760-3p	miR-760-3p_miR-326-3p	7.22E-05	4.30E-03	2.65	2.30	5.58E-04
miR-370-3p_miR-665-3p	miR-665-3p_miR-370-3p	7.96E-04	6.05E-04	2.44	2.45	6.94E-04
miR-137-3p_miR-138-5p	miR-138-5p_miR-137-3p	5.67E-05	1.39E-02	1.95	1.74	8.88E-04
miR-200b-3p_miR-374b-5p	miR-374b-5p_miR-200b-3p	1.90E-02	5.12E-05	1.59	1.98	9.87E-04
miR-135a-5p_miR-9-5p	miR-9-5p_miR-135a-5p	5.98E-03	1.93E-04	1.71	1.74	1.07E-03
miR-144-3p_miR-374b-5p	miR-374b-5p_miR-144-3p	1.96E-03	6.39E-04	1.79	1.93	1.12E-03
miR-219a-5p_miR-9-5p	miR-9-5p_miR-219a-5p	2.87E-02	5.22E-05	1.69	2.16	1.22E-03
miR-145a-5p_miR-199a-3p	miR-199a-3p_miR-145a-5p	7.11E-04	2.49E-03	2.41	2.23	1.33E-03
let-7d-5p_miR-29a-3p	miR-29a-3p_let-7d-5p	1.09E-02	2.08E-04	1.67	2.10	1.51E-03
miR-124-3p.1_miR-128-3p	miR-128-3p_miR-124-3p.1	3.47E-03	6.83E-04	1.50	1.58	1.54E-03
miR-124-3p.1_miR-320-3p	miR-320-3p_miR-124-3p.1	1.93E-04	1.38E-02	1.80	1.54	1.63E-03
miR-133a-3p.1_miR-204-5p	miR-204-5p_miR-133a-3p.1	7.18E-03	3.74E-04	2.08	2.31	1.64E-03
miR-103-3p_miR-29a-3p	miR-29a-3p_miR-103-3p	7.96E-03	3.74E-04	1.67	2.06	1.73E-03
miR-323-3p_miR-495-3p	miR-495-3p_miR-323-3p	4.49E-03	7.49E-04	2.02	2.02	1.83E-03
miR-153-3p_miR-218-5p	miR-218-5p_miR-153-3p	1.36E-04	2.50E-02	1.93	1.58	1.84E-03
miR-19a-3p_miR-9-5p	miR-9-5p_miR-19a-3p	5.98E-03	6.87E-04	1.53	1.62	2.03E-03
miR-143-3p_miR-203-3p.1	miR-203-3p.1_miR-143-3p	8.87E-05	4.92E-02	2.34	1.65	2.09E-03
miR-128-3p_miR-9-5p	miR-9-5p_miR-128-3p	2.87E-02	2.19E-04	1.42	1.70	2.50E-03
miR-199a-3p_miR-26a-5p	miR-26a-5p_miR-199a-3p	8.26E-04	7.72E-03	2.02	1.99	2.52E-03
miR-153-3p_miR-155-5p	miR-155-5p_miR-153-3p	1.31E-03	4.97E-03	2.04	2.22	2.55E-03

miR-219a-5p_miR-26a-5p	miR-26a-5p_miR-219a-5p	6.39E-04	1.19E-02	2.06	1.88	2.76E-03
miR-186-5p_miR-495-3p	miR-495-3p_miR-186-5p	2.04E-02	3.79E-04	1.62	1.85	2.78E-03
miR-194-5p_miR-802-5p	miR-802-5p_miR-194-5p	2.10E-03	3.71E-03	2.24	2.19	2.79E-03
miR-144-3p_miR-148a-3p	miR-148a-3p_miR-144-3p	2.12E-03	4.19E-03	1.76	1.92	2.98E-03
miR-181a-5p_miR-9-5p	miR-9-5p_miR-181a-5p	1.31E-03	9.73E-03	1.80	1.57	3.57E-03
miR-148a-3p_miR-23a-3p	miR-23a-3p_miR-148a-3p	2.68E-04	4.94E-02	2.08	1.52	3.64E-03
miR-144-3p_miR-200b-3p	miR-200b-3p_miR-144-3p	6.83E-04	2.19E-02	1.71	1.54	3.87E-03
miR-124-3p.1_miR-135a-5p	miR-135a-5p_miR-124-3p.1	1.12E-03	1.77E-02	1.60	1.56	4.45E-03
miR-374c-5p_miR-539-3p	miR-539-3p_miR-374c-5p	1.43E-03	1.78E-02	1.88	1.76	5.05E-03
miR-219a-5p_miR-23a-3p	miR-23a-3p_miR-219a-5p	1.39E-02	2.14E-03	1.84	2.01	5.46E-03
miR-124-3p.1_miR-26a-5p	miR-26a-5p_miR-124-3p.1	2.09E-03	1.58E-02	1.53	1.52	5.75E-03
miR-323-3p_miR-374b-5p	miR-374b-5p_miR-323-3p	4.11E-03	9.03E-03	2.13	1.85	6.09E-03
miR-19a-3p_miR-23a-3p	miR-23a-3p_miR-19a-3p	1.43E-03	2.63E-02	1.65	1.47	6.13E-03
miR-194-5p_miR-495-3p	miR-495-3p_miR-194-5p	2.83E-02	1.37E-03	1.78	1.77	6.22E-03
miR-495-3p_miR-539-3p	miR-539-3p_miR-495-3p	9.38E-04	4.37E-02	1.98	1.74	6.40E-03
miR-19a-3p_miR-302c-3p	miR-302c-3p_miR-19a-3p	2.01E-03	2.10E-02	1.81	1.60	6.50E-03
miR-128-3p_miR-140-3p.1	miR-140-3p.1_miR-128-3p	2.43E-03	1.87E-02	1.69	1.71	6.75E-03
miR-135a-5p_miR-24-3p	miR-24-3p_miR-135a-5p	2.61E-03	1.86E-02	1.96	1.68	6.97E-03
miR-142a-3p.2_miR-148a-3p	miR-148a-3p_miR-142a-3p.2	2.26E-02	2.31E-03	1.78	2.20	7.23E-03
miR-148a-3p_miR-182-5p	miR-182-5p_miR-148a-3p	4.49E-02	1.19E-03	1.54	1.79	7.30E-03
miR-186-5p_miR-539-3p	miR-539-3p_miR-186-5p	2.70E-03	2.30E-02	1.83	1.69	7.89E-03
miR-19a-3p_miR-320-3p	miR-320-3p_miR-19a-3p	8.41E-03	7.96E-03	1.68	1.67	8.18E-03
miR-493-5p_miR-495-3p	miR-495-3p_miR-493-5p	2.44E-02	2.81E-03	1.62	1.75	8.29E-03
miR-182-5p_miR-	miR-340-5p_miR-	5.66E-03	1.37E-02	1.55	1.45	8.81E-03

340-5p	182-5p					
miR-19a-3p_miR-30b-5p	miR-30b-5p_miR-19a-3p	1.51E-02	5.45E-03	1.75	1.97	9.08E-03
miR-218-5p_miR-219a-5p	miR-219a-5p_miR-218-5p	6.36E-03	1.39E-02	1.82	1.88	9.41E-03
miR-128-3p_miR-344d-3p	miR-344d-3p_miR-128-3p	2.13E-03	4.29E-02	2.05	1.79	9.56E-03
miR-218-5p_miR-340-5p	miR-340-5p_miR-218-5p	4.43E-03	2.09E-02	1.63	1.49	9.63E-03
miR-24-3p_miR-326-3p	miR-326-3p_miR-24-3p	5.45E-03	2.39E-02	2.35	2.21	1.14E-02
miR-340-5p_miR-433-3p	miR-433-3p_miR-340-5p	6.60E-03	1.99E-02	1.77	1.93	1.15E-02
miR-145a-5p_miR-153-3p	miR-153-3p_miR-145a-5p	6.36E-03	2.21E-02	1.99	1.65	1.19E-02
miR-181a-5p_miR-23a-3p	miR-23a-3p_miR-181a-5p	9.82E-03	1.47E-02	1.64	1.59	1.20E-02
miR-199a-3p_miR-302c-3p	miR-302c-3p_miR-199a-3p	1.43E-02	1.03E-02	2.06	2.09	1.22E-02
miR-142a-3p.2_miR-155-5p	miR-155-5p_miR-142a-3p.2	3.46E-02	4.43E-03	1.80	2.22	1.24E-02
miR-203-3p.1_miR-452-5p	miR-452-5p_miR-203-3p.1	8.77E-03	1.77E-02	1.81	1.87	1.24E-02
miR-323-3p_miR-33-5p	miR-33-5p_miR-323-3p	4.19E-02	3.76E-03	1.99	2.33	1.26E-02
miR-148a-3p_miR-26a-5p	miR-26a-5p_miR-148a-3p	9.51E-03	1.69E-02	1.73	1.74	1.27E-02
let-7d-5p_miR-323-3p	miR-323-3p_let-7d-5p	7.59E-03	2.12E-02	2.00	1.82	1.27E-02
miR-155-5p_miR-340-5p	miR-340-5p_miR-155-5p	6.87E-03	2.40E-02	1.95	1.62	1.28E-02
miR-144-3p_miR-374c-5p	miR-374c-5p_miR-144-3p	1.08E-02	1.57E-02	1.59	1.63	1.30E-02
miR-200b-3p_miR-217-5p	miR-217-5p_miR-200b-3p	6.87E-03	2.63E-02	1.83	1.68	1.34E-02
miR-142a-3p.2_miR-143-3p	miR-143-3p_miR-142a-3p.2	3.02E-02	6.32E-03	2.05	2.38	1.38E-02
miR-144-3p_miR-495-3p	miR-495-3p_miR-144-3p	4.81E-02	4.01E-03	1.51	1.80	1.39E-02
miR-22-3p_miR-320-3p	miR-320-3p_miR-22-3p	1.43E-02	1.35E-02	2.00	1.82	1.39E-02
miR-142a-3p.2_miR-200b-3p	miR-200b-3p_miR-142a-3p.2	2.27E-02	8.80E-03	1.68	1.74	1.41E-02
miR-103-3p_miR-9-5p	miR-9-5p_miR-103-3p	2.44E-02	8.22E-03	1.57	1.62	1.42E-02
miR-124-3p.1_miR-142a-3p.2	miR-142a-3p.2_miR-124-3p.1	6.30E-03	3.95E-02	1.65	1.52	1.58E-02

3p.2	3p.1					
miR-19a-3p_miR-203-3p.1	miR-203-3p.1_miR-19a-3p	1.69E-02	1.48E-02	1.50	1.54	1.58E-02
miR-135a-5p_miR-340-5p	miR-340-5p_miR-135a-5p	1.35E-02	1.90E-02	1.70	1.49	1.61E-02
miR-129-5p_miR-374b-5p	miR-374b-5p_miR-129-5p	1.46E-02	1.78E-02	1.83	1.79	1.61E-02
miR-421-3p_miR-7a-5p	miR-7a-5p_miR-421-3p	6.72E-03	3.94E-02	2.31	1.85	1.63E-02
miR-182-5p_miR-199a-3p	miR-199a-3p_miR-182-5p	1.32E-02	2.15E-02	1.79	1.77	1.69E-02
miR-219a-5p_miR-539-3p	miR-539-3p_miR-219a-5p	3.61E-02	8.08E-03	1.86	2.20	1.71E-02
miR-224-5p_miR-495-3p	miR-495-3p_miR-224-5p	4.16E-02	7.64E-03	1.95	1.87	1.78E-02
miR-199a-3p_miR-19a-3p	miR-19a-3p_miR-199a-3p	7.96E-03	4.07E-02	1.84	1.62	1.80E-02
miR-138-5p_miR-144-3p	miR-144-3p_miR-138-5p	8.29E-03	4.14E-02	1.92	1.54	1.85E-02
miR-495-3p_miR-802-5p	miR-802-5p_miR-495-3p	4.45E-02	8.22E-03	1.65	2.23	1.91E-02
miR-19a-3p_miR-200b-3p	miR-200b-3p_miR-19a-3p	1.47E-02	2.51E-02	1.52	1.47	1.92E-02
miR-135a-5p_miR-185-5p	miR-185-5p_miR-135a-5p	2.15E-02	1.75E-02	2.06	1.97	1.94E-02
miR-142a-3p.2_miR-802-5p	miR-802-5p_miR-142a-3p.2	1.76E-02	2.35E-02	2.01	2.17	2.03E-02
miR-203-3p.1_miR-433-3p	miR-433-3p_miR-203-3p.1	1.31E-02	3.57E-02	1.85	1.82	2.16E-02
miR-338-3p_miR-455-3p.1	miR-455-3p.1_miR-338-3p	3.57E-02	1.37E-02	2.05	2.60	2.21E-02
miR-124-3p.1_miR-218-5p	miR-218-5p_miR-124-3p.1	3.07E-02	1.68E-02	1.41	1.44	2.27E-02
miR-186-5p_miR-493-5p	miR-493-5p_miR-186-5p	4.84E-02	1.12E-02	1.51	1.65	2.33E-02
miR-137-3p_miR-155-5p	miR-155-5p_miR-137-3p	2.68E-02	2.04E-02	1.62	1.84	2.34E-02
miR-128-3p_miR-320-3p	miR-320-3p_miR-128-3p	1.34E-02	4.30E-02	1.62	1.51	2.40E-02
miR-128-3p_miR-340-5p	miR-340-5p_miR-128-3p	2.05E-02	2.87E-02	1.51	1.45	2.43E-02
miR-103-3p_miR-223-3p	miR-223-3p_miR-103-3p	1.64E-02	3.64E-02	2.09	1.92	2.44E-02
miR-219a-5p_miR-499-5p	miR-499-5p_miR-219a-5p	1.37E-02	4.47E-02	2.45	2.02	2.47E-02
miR-128-3p_miR-219a-5p	miR-219a-5p_miR-128-3p	2.60E-02	2.53E-02	1.67	1.78	2.57E-02

miR-340-5p_miR-344d-3p	miR-344d-3p_miR-340-5p	2.21E-02	3.07E-02	1.68	1.78	2.61E-02
miR-374b-5p_miR-493-5p	miR-493-5p_miR-374b-5p	1.62E-02	4.49E-02	1.67	1.60	2.70E-02
miR-217-5p_miR-370-3p	miR-370-3p_miR-217-5p	1.47E-02	4.97E-02	2.14	2.24	2.71E-02
miR-144-3p_miR-218-5p	miR-218-5p_miR-144-3p	2.83E-02	2.68E-02	1.53	1.56	2.76E-02
miR-1a-3p_miR-495-3p	miR-495-3p_miR-1a-3p	2.19E-02	3.79E-02	1.83	1.60	2.88E-02
miR-143-3p_miR-26a-5p	miR-26a-5p_miR-143-3p	1.86E-02	4.49E-02	1.78	1.80	2.89E-02
miR-129-5p_miR-138-5p	miR-138-5p_miR-129-5p	2.39E-02	3.59E-02	1.72	1.80	2.93E-02
miR-182-5p_miR-499-5p	miR-499-5p_miR-182-5p	3.87E-02	2.30E-02	1.68	1.80	2.99E-02
miR-141-3p_miR-9-5p	miR-9-5p_miR-141-3p	4.46E-02	2.02E-02	1.48	1.58	3.00E-02
miR-137-3p_miR-326-3p	miR-326-3p_miR-137-3p	2.84E-02	3.21E-02	1.78	2.24	3.02E-02
let-7d-5p_miR-141-3p	miR-141-3p_let-7d-5p	3.47E-02	2.73E-02	1.73	1.66	3.08E-02
miR-148a-3p_miR-205-5p	miR-205-5p_miR-148a-3p	4.07E-02	2.39E-02	1.77	1.87	3.12E-02
miR-153-3p_miR-29a-3p	miR-29a-3p_miR-153-3p	4.77E-02	2.15E-02	1.46	1.75	3.21E-02
miR-129-5p_miR-135a-5p	miR-135a-5p_miR-129-5p	2.39E-02	4.85E-02	1.61	1.69	3.41E-02
miR-142a-3p.2_miR-144-3p	miR-144-3p_miR-142a-3p.2	3.91E-02	3.00E-02	1.68	1.61	3.43E-02
miR-129-5p_miR-153-3p	miR-153-3p_miR-129-5p	4.85E-02	2.60E-02	1.62	1.67	3.55E-02
miR-153-3p_miR-9-5p	miR-9-5p_miR-153-3p	4.38E-02	2.90E-02	1.46	1.55	3.57E-02
miR-488-3p_miR-542-3p	miR-542-3p_miR-488-3p	3.84E-02	3.46E-02	2.07	2.12	3.64E-02
let-7d-5p_miR-219a-5p	miR-219a-5p_let-7d-5p	3.40E-02	4.45E-02	1.77	1.73	3.89E-02
miR-135a-5p_miR-330-3p.1	miR-330-3p.1_miR-135a-5p	3.82E-02	4.18E-02	1.61	1.50	4.00E-02
miR-140-5p_miR-148a-3p	miR-148a-3p_miR-140-5p	4.37E-02	3.93E-02	1.99	1.94	4.14E-02
miR-145a-5p_miR-495-3p	miR-495-3p_miR-145a-5p	4.81E-02	3.82E-02	1.70	1.64	4.29E-02
miR-145a-5p_miR-29a-3p	miR-29a-3p_miR-145a-5p	4.85E-02	4.16E-02	1.54	1.64	4.49E-02

Table II-S2.

id	baseMeanA	baseMeanB	log2FoldChange	padj	CPM	neuronal
mmu-miR-301a-3p	4098	2078	-0.98	1.20E-02	3.6	z4
mmu-miR-212-3p	811	479	-0.76	8.98E-02	2.9	no
mmu-miR-322-5p	10732	19811	0.88	9.54E-02	4.0	no
mmu-miR-151-3p	3546	6556	0.89	8.29E-02	3.5	z2
mmu-miR-24-3p	13435	25286	0.91	8.29E-02	4.1	no
mmu-miR-140-5p	972	1879	0.95	6.93E-02	3.0	no
mmu-miR-30a-5p	12537	24288	0.95	5.96E-02	4.1	no
mmu-miR-30e-5p	7487	14625	0.97	5.96E-02	3.8	no
mmu-miR-497a-5p	515	1053	1.03	4.80E-02	2.7	no
mmu-let-7e-5p	8478	17678	1.06	2.97E-02	3.9	no
mmu-miR-98-5p	401	847	1.08	2.53E-02	2.6	z4
mmu-miR-138-5p	9315	19790	1.09	2.57E-02	3.9	z4
mmu-miR-542-3p	937	2001	1.09	8.29E-02	2.9	no
mmu-miR-151-5p	3265	7021	1.10	2.22E-02	3.5	z2
mmu-miR-301b-3p	1129	2433	1.11	2.75E-02	3.0	no
mmu-miR-125b-5p	7358	16137	1.13	1.65E-02	3.8	no
mmu-miR-328-3p	1255	2768	1.14	1.56E-02	3.1	z3
mmu-miR-194-5p	278	619	1.15	2.39E-02	2.4	no
mmu-miR-137-3p	6766	15263	1.17	1.39E-02	3.8	z2
mmu-let-7g-5p	4330	9886	1.19	8.86E-03	3.6	no
mmu-miR-744-5p	1755	4060	1.21	8.86E-03	3.2	no
mmu-miR-26b-5p	5606	13057	1.22	8.12E-03	3.7	no
mmu-miR-183-5p	1821	4272	1.23	1.71E-02	3.2	no
mmu-miR-181d-5p	3307	7815	1.24	6.59E-03	3.5	z3
mmu-let-7d-5p	878	2101	1.26	6.12E-03	2.9	no
mmu-miR-145a-5p	564	1368	1.28	7.08E-03	2.7	no
mmu-miR-103-3p	13336	33171	1.31	4.10E-03	4.1	no
mmu-miR-190a-5p	1457	3650	1.32	2.76E-03	3.1	no
mmu-miR-344d-3p	1297	3263	1.33	5.74E-03	3.1	no
mmu-miR-1249-3p	398	1003	1.33	4.64E-03	2.6	no
mmu-miR-6540-5p	240	608	1.34	4.88E-03	2.3	no
mmu-miR-28a-3p	230	585	1.35	6.03E-03	2.3	no
mmu-miR-10a-5p	6472	16601	1.36	3.18E-03	3.8	no
mmu-let-7a-5p	7395	19814	1.42	1.19E-03	3.8	no
mmu-miR-196b-5p	252	676	1.42	2.69E-03	2.4	no
mmu-miR-30d-5p	13468	36354	1.43	1.50E-03	4.1	no
mmu-miR-100-5p	653	1766	1.44	1.65E-03	2.8	no
mmu-miR-196a-5p	475	1307	1.46	6.84E-04	2.6	no
mmu-miR-107-3p	1480	4091	1.47	1.19E-03	3.1	no
mmu-let-7f-5p	5212	14774	1.50	6.04E-04	3.7	no
mmu-miR-361-5p	1554	4541	1.55	5.33E-04	3.2	no
mmu-miR-488-3p	1198	3501	1.55	6.84E-04	3.0	no
mmu-miR-708-5p	2486	7282	1.55	4.14E-04	3.4	no
mmu-miR-181c-5p	915	2685	1.55	6.56E-04	2.9	z4
mmu-miR-181a-5p	4108	12118	1.56	4.35E-04	3.6	z4
mmu-miR-146b-5p	1213	3627	1.58	5.08E-03	3.0	no
mmu-let-7b-5p	9135	27666	1.60	2.39E-04	3.9	no

mmu-miR-320-3p	2652	8398	1.66	2.54E-04	3.4	no
mmu-miR-195a-5p	1019	3258	1.68	1.53E-03	3.0	no
mmu-let-7i-5p	2523	8109	1.68	9.20E-05	3.4	no
mmu-miR-185-5p	348	1151	1.73	4.18E-04	2.5	no
mmu-miR-182-5p	26607	89835	1.76	3.82E-04	4.4	no
mmu-miR-652-3p	1449	4902	1.76	7.29E-05	3.1	no
mmu-miR-28a-5p	300	1021	1.77	1.06E-04	2.4	no
mmu-miR-143-3p	17948	63837	1.83	1.53E-03	4.2	no
mmu-miR-7b-5p	11240	42600	1.92	1.06E-04	4.0	no
mmu-miR-26a-5p	9436	37423	1.99	3.04E-05	3.9	no
mmu-miR-152-3p	2444	12097	2.31	2.17E-05	3.4	no
mmu-miR-210-3p	352	9196	4.71	1.16E-25	2.5	no

Table II-S3.

genes	baseMean	log2FoldChange(DKOserum/WTserum)	padj.DKOsWTs	log2FoldChange(DKOs24/WT24)	padj.DKO24WT24	log2FoldChange(WT24/WTserum)	padj.DKO24WTs	SYMBOL	down across WTdiff
ENSMUSG00000000751	4282	0.36	7.50E-06	0.48	1.58E-09	-0.75	1.36E-21	Rpa1	yes
ENSMUSG00000000827	2880	0.26	8.70E-03	-0.05	6.94E-01	0.13	2.36E-01	Tpd52l2	no
ENSMUSG00000001911	2688	2.61	7.53E-94	2.58	3.58E-90	-0.05	8.14E-01	Nfix	no
ENSMUSG00000002068	458	0.67	3.85E-04	0.21	3.73E-01	-0.11	6.81E-01	Ccne1	no
ENSMUSG00000002222	2476	0.34	3.42E-03	0.09	5.55E-01	0.74	2.50E-12	Rmnd5a	no
ENSMUSG00000002227	1916	0.50	1.86E-05	0.18	1.91E-01	0.65	1.69E-08	Mov10	no
ENSMUSG00000002233	1659	1.27	3.07E-31	0.29	2.33E-02	0.39	1.39E-03	Rhoc	no
ENSMUSG00000002250	1222	0.65	1.39E-07	0.85	2.54E-12	0.14	3.79E-01	Ppard	no
ENSMUSG00000002948	3281	0.14	1.86E-01	0.20	4.00E-02	0.03	8.41E-01	Map2k7	no
ENSMUSG00000005481	4455	0.13	2.10E-01	0.18	6.56E-02	-0.83	1.71E-22	Ddx39	yes
ENSMUSG00000006010	1771	0.00	9.87E-01	0.25	7.20E-02	0.29	3.29E-02	BC003331	no
ENSMUSG00000008575	10332	1.06	7.64E-23	1.06	5.53E-23	0.27	3.09E-02	Nfib	no
ENSMUSG00000008730	4607	0.39	8.61E-05	0.39	7.36E-05	-0.06	6.28E-01	Hipk1	no
ENSMUSG00000010048	1492	0.45	8.31E-03	0.97	7.48E-10	-0.97	1.09E-09	lfrd2	yes
ENSMUSG00000010205	2888	0.11	4.54E-01	0.28	2.18E-02	-0.30	1.17E-02	Raver1	yes
ENSMUSG00000012117	2232	0.33	2.06E-03	0.25	2.89E-02	0.01	9.53E-01	Dhdds	no
ENSMUSG00000015837	17452	0.45	2.94E-04	0.53	1.01E-05	0.42	7.15E-04	Sqstm1	no
ENSMUSG00000016239	390	0.47	5.28E-02	1.28	2.56E-09	-0.72	1.87E-03	Lonrf3	yes
ENSMUSG00000016757	3647	-0.02	8.71E-01	0.22	1.87E-02	-0.57	2.42E-11	Ttll12	yes
ENSMUSG00000016921	8819	0.04	7.77E-01	0.18	8.53E-02	-0.36	1.42E-04	Srsf6	yes
ENSMUSG00000017774	2455	0.28	4.69E-02	-0.07	6.92E-01	-0.14	3.69E-01	Myo1c	no
ENSMUSG00000017802	2189	0.23	4.38E-02	0.05	7.49E-01	0.21	6.26E-02	Fam134c	no
ENSMUSG00000018415	1499	0.51	6.75E-05	0.85	3.24E-12	-0.01	9.44E-01	Gid4	no
ENSMUSG00000018648	54	0.36	5.48E-01	1.43	1.98E-03	-0.49	3.83E-01	Dusp14	no
ENSMUSG00000020167	3376	0.27	5.87E-02	0.27	5.63E-02	-0.28	4.42E-02	Tcf3	yes
ENSMUSG00000020515	2462	0.51	1.21E-07	0.32	1.66E-03	0.06	6.69E-01	Cnot8	no
ENSMUSG00000020580	5044	0.20	5.98E-02	0.23	2.70E-02	-0.16	1.46E-01	Rock2	no
ENSMUSG00000020888	1662	0.09	5.40E-01	0.21	8.45E-02	0.28	1.81E-02	Dvl2	no
ENSMUSG00000021109	6055	0.47	6.89E-07	0.67	1.94E-13	-0.14	2.03E-01	Hif1a	no
ENSMUSG00000021156	3682	0.23	5.56E-03	-0.02	9.01E-01	0.09	3.39E-01	Zmynd11	no
ENSMUSG00000021186	73	1.82	3.70E-03	2.00	9.53E-04	0.54	4.83E-01	Fbln5	no
ENSMUSG00000021254	665	0.46	5.54E-03	-0.05	8.37E-01	0.15	4.64E-01	Gpatch2l	no
ENSMUSG00000021377	3746	0.43	4.87E-03	0.80	1.83E-08	-0.82	1.00E-08	Dek	yes
ENSMUSG00000021725	2430	0.38	1.04E-05	-0.12	2.12E-01	0.54	8.54E-11	Parp8	no
ENSMUSG00000021767	1237	0.39	5.59E-02	0.13	6.11E-01	0.93	2.59E-07	Kat6b	no
ENSMUSG00000022051	1892	-0.36	1.69E-02	0.46	8.97E-04	0.87	1.05E-10	Bnip3l	no
ENSMUSG00000022426	2212	0.13	3.02E-01	0.27	1.13E-02	0.07	6.00E-01	Josd1	no
ENSMUSG00000022708	1478	0.64	1.14E-03	1.21	3.52E-11	0.07	7.96E-01	Zbtb20	no
ENSMUSG00000023845	1594	0.59	1.09E-03	0.47	1.18E-02	-0.27	1.84E-01	Lnpep	no
ENSMUSG00000023991	2881	0.28	5.49E-02	0.34	1.41E-02	-0.37	7.46E-03	Foxp4	yes
ENSMUSG00000024251	1431	0.26	6.99E-02	0.48	2.09E-04	-0.57	7.92E-06	Thada	yes
ENSMUSG00000024927	1062	0.48	5.33E-04	0.32	2.60E-02	0.33	2.43E-02	Rela	no
ENSMUSG00000025332	6139	0.25	4.99E-02	0.21	9.61E-02	0.11	4.64E-01	Kdm5c	no
ENSMUSG00000025878	675	0.26	1.96E-01	0.33	9.42E-02	-0.38	4.78E-02	Uimc1	yes
ENSMUSG00000025935	3140	0.21	1.22E-01	0.38	2.51E-03	-0.53	1.42E-05	Tram1	yes
ENSMUSG00000025958	1541	0.42	1.22E-02	0.42	9.97E-03	-0.03	8.98E-01	Creb1	no

ENSMUSG00000026142	494	0.25	2.97E-01	0.87	6.13E-06	0.04	8.93E-01	Rhbdd1	no
ENSMUSG00000026174	2644	0.42	1.35E-04	0.46	3.07E-05	-0.34	3.03E-03	Rqcd1	yes
ENSMUSG00000026176	1426	0.58	1.26E-07	0.80	1.36E-13	-0.26	3.75E-02	Ctdsp1	yes
ENSMUSG00000026313	901	0.25	1.75E-01	0.57	2.19E-04	0.38	2.28E-02	Hdac4	no
ENSMUSG00000026478	13748	1.19	5.79E-22	1.31	1.14E-26	-0.30	3.87E-02	Lamc1	yes
ENSMUSG00000026499	3573	0.19	4.20E-02	0.20	3.19E-02	-0.09	3.96E-01	Acbd3	no
ENSMUSG00000026502	1316	-0.06	7.83E-01	0.41	9.35E-03	-0.49	1.84E-03	Desi2	yes
ENSMUSG00000026510	7316	0.33	6.55E-06	0.00	9.96E-01	-0.01	9.10E-01	Trp53bp 2	no
ENSMUSG00000026622	4268	0.42	3.61E-01	0.71	7.98E-02	-1.13	2.82E-03	Nek2	yes
ENSMUSG00000026657	5367	0.29	6.88E-03	0.58	3.11E-09	-0.39	1.83E-04	Frmd4a	yes
ENSMUSG00000026728	41011	0.95	3.72E-65	0.62	1.02E-27	-0.06	4.56E-01	Vim	no
ENSMUSG00000026872	2537	0.33	2.46E-02	0.43	2.52E-03	0.01	9.56E-01	Zeb2	no
ENSMUSG00000027236	1595	0.08	5.86E-01	0.31	1.11E-02	-0.50	1.30E-05	Eif3j1	yes
ENSMUSG00000027454	728	0.09	7.10E-01	0.31	9.96E-02	-0.89	4.28E-08	Gins1	yes
ENSMUSG00000027519	2184	0.32	3.53E-03	0.33	2.59E-03	0.29	8.97E-03	Rab22a	no
ENSMUSG00000027677	978	0.24	2.73E-01	0.42	3.25E-02	-0.38	6.03E-02	Ttc14	yes
ENSMUSG00000027737	538	-0.65	1.57E-02	2.35	9.56E-25	0.35	2.35E-01	Slc7a11	no
ENSMUSG00000027864	3701	2.27	6.74E-77	2.11	3.08E-65	-0.35	1.52E-02	Ptgfrn	yes
ENSMUSG00000028059	4512	-0.04	8.20E-01	0.55	1.04E-05	0.23	1.10E-01	Arhgef2	no
ENSMUSG00000028108	172	1.14	4.94E-03	1.26	1.18E-03	0.63	1.63E-01	Ecm1	no
ENSMUSG00000028284	2435	0.43	4.54E-07	0.37	1.71E-05	-0.35	9.73E-05	Map3k7	yes
ENSMUSG00000028430	2739	0.28	2.39E-02	0.48	2.76E-05	-0.66	3.95E-09	Nol6	yes
ENSMUSG00000028565	108	0.44	3.95E-01	1.02	1.42E-02	0.86	5.17E-02	Nfia	no
ENSMUSG00000028649	4748	0.39	2.00E-02	0.18	3.57E-01	0.11	5.82E-01	Macf1	no
ENSMUSG00000028772	1004	0.37	2.83E-03	0.05	7.80E-01	0.07	6.88E-01	Zcchc17	no
ENSMUSG00000028788	7437	0.26	2.10E-03	0.26	2.15E-03	-0.15	1.14E-01	Ptp4a2	no
ENSMUSG00000029135	1838	0.22	1.61E-01	0.39	5.22E-03	0.66	8.05E-07	Fosl2	no
ENSMUSG00000029439	2830	0.15	1.71E-01	0.37	1.16E-04	-0.27	8.62E-03	Sfswap	yes
ENSMUSG00000029516	789	0.13	5.36E-01	0.67	9.87E-06	-0.59	1.32E-04	Cit	yes
ENSMUSG00000029687	2893	0.57	4.40E-02	0.95	2.03E-04	-1.03	6.05E-05	Ezh2	yes
ENSMUSG00000030103	1539	-1.00	8.58E-09	1.08	6.24E-11	0.55	2.23E-03	Bhlhe40	no
ENSMUSG00000030180	2105	0.37	1.27E-02	0.37	1.15E-02	0.32	3.51E-02	Kdm5a	no
ENSMUSG00000030232	3078	0.29	9.26E-04	0.49	8.74E-09	-0.26	3.76E-03	Aebp2	yes
ENSMUSG00000030254	1071	-0.09	6.18E-01	0.68	5.15E-08	-0.81	6.99E-11	Rad18	yes
ENSMUSG00000030314	682	0.54	1.49E-03	0.10	6.55E-01	0.09	6.93E-01	Atg7	no
ENSMUSG00000030516	3498	0.35	9.39E-03	0.59	2.36E-06	-0.12	4.69E-01	Tjp1	no
ENSMUSG00000030655	2926	-0.15	5.47E-01	0.41	4.01E-02	-0.25	2.62E-01	Smg1	no
ENSMUSG00000031389	176	0.32	3.31E-01	0.51	8.74E-02	-0.32	3.30E-01	Arhgap4	no
ENSMUSG00000031490	2300	-0.36	6.84E-03	0.94	3.04E-15	-0.50	8.78E-05	Eif4ebp1	yes
ENSMUSG00000031527	3652	0.53	9.01E-07	0.66	3.29E-10	-0.40	2.97E-04	Eri1	yes
ENSMUSG00000031628	2132	0.39	3.78E-04	0.40	2.29E-04	0.35	1.74E-03	Casp3	no
ENSMUSG00000031774	1886	0.23	3.64E-02	0.03	8.29E-01	0.12	3.28E-01	Fam192a	no
ENSMUSG00000031783	2447	0.47	6.58E-07	0.44	6.19E-06	-0.47	1.30E-06	Polr2c	yes
ENSMUSG00000031821	1207	0.30	9.14E-02	0.32	6.81E-02	-0.89	1.10E-08	Gins2	yes
ENSMUSG00000031826	6943	-0.04	7.12E-01	0.16	5.31E-02	-0.48	6.80E-12	Usp10	yes
ENSMUSG00000031910	12	1.80	1.96E-02	0.65	4.83E-01	1.33	9.77E-02	Has3	no
ENSMUSG00000031922	685	0.39	4.10E-02	0.84	1.68E-06	-0.52	5.26E-03	Cep57	yes
ENSMUSG00000032077	538	0.34	8.71E-02	0.44	2.28E-02	-0.43	2.73E-02	Bud13	yes
ENSMUSG00000032228	2460	0.27	1.23E-02	0.27	1.26E-02	-0.11	3.96E-01	Tcf12	no
ENSMUSG00000032449	677	0.12	6.66E-01	0.40	5.22E-02	0.78	4.71E-05	Slc25a36	no
ENSMUSG00000032562	4884	0.35	5.06E-04	-0.21	4.27E-02	0.41	3.23E-05	Gnai2	no
ENSMUSG00000032727	1297	0.10	6.48E-01	0.30	9.64E-02	-0.13	5.28E-01	Mier3	no
ENSMUSG00000033055	1203	0.45	1.29E-02	0.12	6.02E-01	0.43	1.93E-02	Ankrd54	no
ENSMUSG00000033075	1602	0.30	3.58E-02	0.63	1.54E-06	-0.64	1.23E-06	Senp1	yes
ENSMUSG00000033411	1140	0.09	6.77E-01	0.59	6.48E-05	-0.31	5.52E-02	Ctdspl2	yes

ENSMUSG00000033684	2120	0.41	5.16E-05	0.48	1.27E-06	-0.13	3.01E-01	Qsox1	no
ENSMUSG00000034154	1475	0.05	8.14E-01	0.36	9.96E-03	-0.23	1.30E-01	Ino80	no
ENSMUSG00000034165	2637	1.71	2.82E-39	1.74	3.75E-40	-0.04	8.51E-01	Ccnd3	no
ENSMUSG00000034518	1163	0.30	6.12E-02	0.50	5.94E-04	-0.38	1.13E-02	Hmgxb4	yes
ENSMUSG00000034612	3029	0.46	1.34E-04	0.35	4.27E-03	0.44	3.06E-04	Chst11	no
ENSMUSG00000034640	980	-0.10	6.80E-01	0.57	1.34E-03	-0.14	5.28E-01	Tiparp	no
ENSMUSG00000035107	9591	0.39	2.74E-05	0.19	6.56E-02	0.50	2.83E-08	Dcbld2	no
ENSMUSG00000035199	1301	0.34	9.66E-03	0.14	3.66E-01	0.10	5.53E-01	Arl6ip5	no
ENSMUSG00000035696	1537	0.42	1.91E-03	0.26	7.68E-02	0.41	2.74E-03	Rnf38	no
ENSMUSG00000036104	1483	0.69	5.06E-07	0.43	2.43E-03	0.22	1.86E-01	Rab3gap 1	no
ENSMUSG00000036180	6434	0.36	3.04E-04	0.27	8.18E-03	-0.37	2.04E-04	Gatad2a	yes
ENSMUSG00000036241	3364	0.18	3.78E-02	-0.10	2.89E-01	0.14	1.17E-01	Ube2r2	no
ENSMUSG00000037235	1989	0.52	1.76E-03	-0.48	2.33E-03	2.20	1.38E-50	Mxd4	no
ENSMUSG00000037286	1536	0.21	1.77E-01	0.58	1.87E-05	-0.73	5.93E-08	Stag1	yes
ENSMUSG00000037486	1256	-0.14	5.31E-01	0.46	8.41E-03	-0.37	4.26E-02	Asxl2	yes
ENSMUSG00000037736	2215	1.38	1.14E-61	1.20	1.50E-46	0.14	1.80E-01	Limch1	no
ENSMUSG00000037876	1914	0.42	2.28E-02	0.75	9.09E-06	-0.04	8.74E-01	Jmjd1c	no
ENSMUSG00000037992	2166	-0.29	5.57E-02	0.32	3.20E-02	-0.51	3.20E-04	Rara	yes
ENSMUSG00000038481	1056	0.64	1.15E-04	0.53	1.62E-03	0.64	1.33E-04	Cdk19	no
ENSMUSG00000038544	616	0.15	4.55E-01	0.49	2.51E-03	-0.55	6.04E-04	Inip	yes
ENSMUSG00000038679	4146	0.21	1.90E-01	0.35	1.42E-02	0.31	3.45E-02	Trps1	no
ENSMUSG00000038780	2407	0.17	1.74E-01	0.24	3.83E-02	0.10	4.54E-01	Smurf1	no
ENSMUSG00000039298	4524	0.17	1.02E-01	0.27	5.13E-03	-0.05	7.01E-01	Cdk5rap 2	no
ENSMUSG00000039738	1203	-0.04	8.73E-01	0.34	7.37E-02	-0.20	3.50E-01	Slx4	no
ENSMUSG00000040260	6837	1.50	7.64E-12	2.20	1.27E-24	-1.19	1.36E-07	Daam2	yes
ENSMUSG00000040612	88	0.85	3.98E-02	1.58	1.33E-04	-1.75	2.23E-05	Ildr2	yes
ENSMUSG00000040688	3011	0.42	3.53E-04	0.19	1.44E-01	-0.44	1.55E-04	Tbl3	yes
ENSMUSG00000040842	5599	0.52	2.64E-11	0.47	3.38E-09	-0.39	1.34E-06	Szrd1	yes
ENSMUSG00000040943	1061	-0.08	7.90E-01	0.69	6.04E-04	0.05	8.71E-01	Tet2	no
ENSMUSG00000041272	495	0.41	5.72E-02	0.08	8.00E-01	0.31	1.69E-01	Tox	no
ENSMUSG00000041440	378	0.09	8.28E-01	0.79	2.83E-03	-0.61	2.64E-02	Gk5	yes
ENSMUSG00000041498	1195	0.12	5.68E-01	0.83	2.20E-08	-1.29	6.53E-19	Kif14	yes
ENSMUSG00000041594	288	0.09	8.03E-01	0.53	3.76E-02	-0.20	5.11E-01	Tmtc4	no
ENSMUSG00000041741	592	1.25	8.06E-08	1.07	3.91E-06	0.90	2.41E-04	Pde3a	no
ENSMUSG00000041779	397	0.92	3.33E-05	1.15	9.05E-08	-0.16	5.98E-01	Tram2	no
ENSMUSG00000041836	389	1.00	1.08E-04	-0.03	9.45E-01	1.02	7.35E-05	Ptpre	no
ENSMUSG00000041974	844	0.36	1.54E-02	1.06	5.91E-15	-0.82	6.29E-09	Spidr	yes
ENSMUSG00000042042	368	0.93	1.16E-04	1.44	5.29E-10	-0.28	3.51E-01	Csgalnac t2	no
ENSMUSG00000042225	505	0.30	9.90E-02	0.79	8.37E-07	-0.67	4.38E-05	Ammecr 1	yes
ENSMUSG00000042557	2928	0.17	1.40E-01	0.29	3.93E-03	-0.25	1.58E-02	Sin3a	yes
ENSMUSG00000042694	690	0.21	3.42E-01	0.36	6.35E-02	0.06	8.25E-01	Obfc1	no
ENSMUSG00000043154	1764	0.31	2.01E-02	0.37	3.05E-03	0.13	3.79E-01	Ppp2r3a	no
ENSMUSG00000043241	1384	-0.01	9.86E-01	0.26	8.72E-02	-0.31	3.74E-02	Upf2	yes
ENSMUSG00000043962	5543	0.26	3.42E-04	0.26	3.38E-04	-0.27	2.00E-04	Thrap3	yes
ENSMUSG00000045098	1109	0.02	9.56E-01	0.33	4.22E-02	0.22	2.19E-01	Suv420h 1	no
ENSMUSG00000045817	4082	0.87	4.35E-15	1.20	8.22E-28	-0.28	3.03E-02	Zfp36l2	yes
ENSMUSG00000045969	3224	0.89	2.65E-31	1.04	4.22E-42	0.00	9.75E-01	Ing1	no
ENSMUSG00000046707	2465	0.03	8.67E-01	0.28	1.16E-02	-0.50	1.07E-06	Csnk2a2	yes
ENSMUSG00000046807	1199	0.55	5.40E-04	-0.32	7.03E-02	-0.15	4.35E-01	Lrrc75b	no
ENSMUSG00000047412	815	0.28	2.66E-01	0.43	6.58E-02	0.08	7.80E-01	Zbtb44	no
ENSMUSG00000047454	1923	0.31	2.03E-02	0.35	6.27E-03	-0.18	2.15E-01	Gphn	no

ENSMUSG00000048232	1190	0.49	4.58E-05	0.76	1.98E-11	0.30	1.94E-02	Fbxo10	no
ENSMUSG00000049932	1665	-0.01	9.40E-01	0.36	4.24E-04	-0.59	2.94E-09	H2afx	yes
ENSMUSG00000050174	211	0.15	6.65E-01	0.53	3.36E-02	0.41	1.26E-01	Nudt6	no
ENSMUSG00000050295	311	1.45	3.45E-05	1.30	1.84E-04	0.81	3.28E-02	Foxc1	no
ENSMUSG00000050890	555	0.39	1.25E-01	0.57	1.47E-02	0.12	6.96E-01	Pdik1l	no
ENSMUSG00000051579	246	0.72	2.37E-02	0.70	2.79E-02	-0.25	5.26E-01	Tceal8	no
ENSMUSG00000052752	3198	0.46	5.17E-07	0.41	1.06E-05	-0.06	6.17E-01	Traf7	no
ENSMUSG00000053460	622	0.45	1.80E-02	0.88	4.00E-07	-0.24	2.49E-01	Ggcx	no
ENSMUSG00000058729	1238	0.25	1.79E-01	0.94	1.06E-09	-0.65	5.80E-05	Lin9	yes
ENSMUSG00000059820	546	0.47	2.17E-02	0.66	7.34E-04	-0.23	3.19E-01	AU01982 3	no
ENSMUSG00000061665	2223	0.54	1.08E-05	0.60	8.75E-07	-0.12	4.29E-01	Cd2ap	no
ENSMUSG00000062949	777	0.19	4.51E-01	0.45	3.14E-02	-0.38	7.78E-02	Atp11c	yes
ENSMUSG00000063558	431	1.61	1.36E-18	1.95	1.54E-27	0.27	2.63E-01	Aox1	no
ENSMUSG00000064120	420	0.94	2.83E-06	1.17	1.48E-09	0.30	2.22E-01	Mocs1	no
ENSMUSG00000066043	1014	0.09	5.67E-01	0.45	1.41E-04	-0.12	4.34E-01	Phactr4	no
ENSMUSG00000066568	3054	0.17	1.59E-01	0.20	8.42E-02	-0.40	9.56E-05	Lsm14a	yes
ENSMUSG00000068747	2534	0.37	1.60E-04	0.20	7.10E-02	-0.12	3.18E-01	Sort1	no
ENSMUSG00000070047	4637	0.80	3.44E-03	1.55	6.60E-10	-0.90	7.19E-04	Fat1	yes
ENSMUSG00000072501	1311	0.27	3.06E-02	0.35	3.84E-03	-0.15	2.76E-01	Phf20l1	no
ENSMUSG00000073702	21412	0.31	1.37E-03	0.16	1.35E-01	0.03	8.09E-01	Rpl31	no
ENSMUSG00000079614	1457	-0.02	9.51E-01	0.33	3.40E-02	-0.41	6.04E-03	Seh1l	yes
ENSMUSG00000085793	251	0.41	8.81E-02	0.54	2.07E-02	-0.29	2.56E-01	Lin52	no
ENSMUSG00000085925	212	0.55	2.21E-01	0.80	5.18E-02	-0.30	5.46E-01	Rtl1	no
ENSMUSG00000089715	7337	0.51	6.26E-07	0.22	5.85E-02	0.50	1.22E-06	Cbx6	no
ENSMUSG00000090115	193	0.47	1.53E-01	0.81	6.02E-03	-0.01	9.75E-01	Usp49	no

Table II-S4.

genes	base Mean	log2F oldC hang e.138 d0	padj.138 d0	log2F oldC hang e.138 d2	padj.138d 2	log2F oldC hang e.137 d0	padj.137 d0	log2F oldC hang e.137 d2	padj. 137d 2	cotarg et	SYMB OL
ENSMUSG00000000552	355	-0.59	3.01E-06	-0.29	3.99E-02	-1.12	3.86E-16	-0.63	8.84E-06	co-target	Zfp385a
ENSMUSG00000001156	141	0.36	7.10E-02	0.48	9.95E-03	-1.45	3.05E-10	-0.80	1.11E-04	co-target	Mxd1
ENSMUSG00000001911	3582	-2.13	8.12E-251	-1.91	1.37E-192	-0.57	1.34E-19	-0.65	2.18E-25	co-target	Nfix
ENSMUSG00000002222	2287	-0.23	4.81E-04	-0.43	1.55E-11	-0.77	2.46E-30	-0.46	1.55E-12	co-target	Rmnd5a
ENSMUSG00000008575	10418	-1.04	5.10E-103	-0.98	2.70E-92	-0.93	3.01E-79	-0.62	5.07E-38	co-target	Nfib
ENSMUSG00000015944	404	-0.33	2.26E-02	0.05	8.03E-01	-0.43	4.85E-03	0.06	7.43E-01	co-target	Gatsl2
ENSMUSG00000016239	306	0.38	2.57E-03	-0.13	4.46E-01	-0.40	4.29E-03	-0.30	6.05E-02	co-target	Lonrf3
ENSMUSG00000016559	7313	-0.73	1.24E-37	-0.62	1.76E-26	-0.74	2.33E-37	-0.34	1.10E-08	co-target	H3f3b
ENSMUSG00000016921	5591	-0.61	1.98E-26	-0.50	6.39E-17	-0.27	6.21E-06	-0.42	1.31E-11	co-target	Srsf6
ENSMUSG00000017774	1435	-0.03	7.62E-01	-0.16	5.00E-02	-1.06	3.02E-45	-0.57	2.80E-13	co-target	Myo1c
ENSMUSG00000017802	1035	0.18	3.96E-02	-0.03	8.11E-01	-0.55	1.31E-09	-0.39	9.40E-06	co-target	Fam134c
ENSMUSG00000018849	1731	-0.94	2.11E-50	-1.17	3.53E-64	-0.66	1.37E-23	0.00	9.74E-01	co-target	Wwc1
ENSMUSG00000019194	4	-0.69	NA	0.03	9.73E-01	-0.04	NA	0.96	4.07E-02	co-target	Scn1b
ENSMUSG00000019558	321	-0.80	4.90E-10	-0.40	7.79E-03	-0.42	3.45E-03	0.09	6.41E-01	co-target	Slc6a8
ENSMUSG00000020070	799	0.05	6.67E-01	-0.20	5.99E-02	0.33	9.06E-04	0.22	3.78E-02	co-target	Rufy2
ENSMUSG00000020653	350	-1.16	6.42E-21	-0.62	1.40E-06	-0.34	1.25E-02	0.19	1.93E-01	co-target	Klf11
ENSMUSG00000020661	1446	0.21	4.03E-03	0.28	1.25E-04	-0.69	6.98E-20	-0.54	1.20E-12	co-target	Dnmt3a
ENSMUSG00000021047	684	-0.86	3.05E-20	-0.77	8.59E-15	-0.30	4.56E-03	-0.35	9.71E-04	co-target	Nova1
ENSMUSG00000021156	2766	-0.63	5.21E-27	-0.67	5.44E-28	-0.64	6.49E-26	-0.46	2.94E-13	co-target	Zmynd11
ENSMUSG00000021725	1614	-0.10	2.06E-01	-0.16	2.74E-02	-0.03	7.93E-01	-0.22	2.50E-03	co-target	Parp8
ENSMUSG00000021962	611	-0.75	3.06E-13	-0.58	7.63E-08	-0.75	7.52E-12	-0.46	5.68E-05	co-target	Dcp1a
ENSMUSG00000022051	577	-0.38	3.03E-03	-0.61	6.93E-08	-1.25	2.71E-19	-0.16	2.39E-01	co-target	Bnip3l
ENSMUSG00000022708	2529	-1.17	1.39E-09	-0.97	6.18E-07	-0.11	6.90E-01	-0.04	8.82E-01	co-target	Zbtb20
ENSMUSG00000022811	1427	-0.10	2.24E-01	-0.38	6.55E-07	-0.51	1.03E-10	-0.52	2.17E-11	co-target	Zfp148
ENSMUSG00000023988	2369	0.28	2.05E-05	0.02	8.32E-01	0.08	3.03E-01	-0.32	2.72E-05	co-target	Bysl
ENSMUSG000000394	394	-1.36	3.02E-22	-1.41	2.13E-18	-0.84	1.10E-08	0.00	9.89E-01	co-	Cacn

24112									-01	target	a1h
ENSMUSG000000 24347	7	0.15	7.92E-01	1.24	7.07E-03	-0.06	9.32E-01	-0.15	8.20E-01	co-target	Psd2
ENSMUSG000000 24539	563	-0.75	1.04E-13	-0.84	2.69E-14	-0.16	1.83E-01	-0.16	2.27E-01	co-target	Ptpn2
ENSMUSG000000 25019	512	0.88	1.54E-14	0.85	2.46E-13	0.66	6.83E-08	0.70	7.09E-09	co-target	Lcor
ENSMUSG000000 26384	665	-0.09	4.83E-01	-0.27	2.02E-02	-0.12	3.95E-01	-0.33	6.63E-03	co-target	Ptpn4
ENSMUSG000000 26502	1216	-0.58	9.25E-14	-0.46	6.91E-08	0.13	1.52E-01	-0.10	3.33E-01	co-target	Desi2
ENSMUSG000000 26872	3344	-0.68	7.52E-22	-0.43	3.08E-09	0.17	2.74E-02	0.03	7.49E-01	co-target	Zeb2
ENSMUSG000000 27236	155	-0.36	4.49E-02	-0.53	9.95E-03	-0.24	2.59E-01	0.03	9.22E-01	co-target	Eif3j1
ENSMUSG000000 27692	682	0.07	5.90E-01	-0.36	4.21E-04	-0.33	7.31E-03	-0.37	5.51E-04	co-target	Tnik
ENSMUSG000000 27799	1404	0.09	2.88E-01	0.25	1.85E-03	-0.07	5.04E-01	-0.02	8.66E-01	co-target	Nbea
ENSMUSG000000 27864	5245	-0.95	5.94E-52	-1.38	2.52E-104	-1.06	3.71E-61	-1.00	9.15E-56	co-target	Ptgfrn
ENSMUSG000000 28565	133	0.12	6.46E-01	0.16	4.97E-01	-0.66	1.34E-02	-0.52	1.69E-02	co-target	Nfia
ENSMUSG000000 29651	407	0.45	1.53E-04	0.32	1.02E-02	-0.71	7.41E-08	-0.34	1.33E-02	co-target	Mtus2
ENSMUSG000000 29687	2517	-1.07	9.37E-48	-0.80	1.31E-23	0.00	9.81E-01	-0.05	6.55E-01	co-target	Ezh2
ENSMUSG000000 29772	1708	-0.60	1.10E-21	0.15	4.32E-02	-0.75	5.08E-29	-0.27	1.63E-04	co-target	Ahcyl2
ENSMUSG000000 30189	6210	-0.92	2.25E-51	-1.16	1.80E-74	-1.03	1.07E-62	-0.76	3.13E-32	co-target	Ybx3
ENSMUSG000000 30257	1617	0.00	9.96E-01	0.41	2.17E-07	-0.75	2.96E-17	-0.85	3.78E-25	co-target	Srgap3
ENSMUSG000000 30411	169	0.07	7.72E-01	0.93	2.63E-08	0.00	9.97E-01	0.83	2.21E-06	co-target	Nova2
ENSMUSG000000 30516	3158	-1.04	1.57E-63	-1.26	7.99E-88	-0.46	1.19E-12	-0.52	4.21E-16	co-target	Tjp1
ENSMUSG000000 30649	336	-0.67	5.97E-08	-0.22	1.99E-01	0.08	6.19E-01	-0.19	2.96E-01	co-target	Anapc15
ENSMUSG000000 30683	13	-1.11	1.22E-02	-0.19	7.57E-01	-0.93	4.92E-02	0.18	7.79E-01	co-target	Sez6l2
ENSMUSG000000 31783	409	-1.11	1.27E-23	-0.86	2.16E-11	-0.80	1.54E-11	-0.45	9.09E-04	co-target	Polr2c
ENSMUSG000000 31821	715	-0.71	7.01E-11	-0.33	9.66E-03	-0.95	4.71E-17	-0.38	4.47E-03	co-target	Gins2
ENSMUSG000000 32228	2686	-0.77	3.65E-38	-0.78	1.15E-36	-0.29	6.81E-06	-0.17	1.22E-02	co-target	Tcf12
ENSMUSG000000 32727	1735	-0.08	3.05E-01	-0.12	1.37E-01	-0.34	8.90E-06	-0.48	5.45E-11	co-target	Mier3
ENSMUSG000000 32890	802	-1.75	1.15E-92	-0.85	7.39E-11	0.19	4.66E-02	1.25	2.13E-32	co-target	Rims3
ENSMUSG000000 34575	1613	-0.09	2.33E-01	-0.24	1.04E-03	-0.22	2.79E-03	-0.26	5.18E-04	co-target	Papd7
ENSMUSG000000 34724	1813	-0.44	2.93E-09	-0.67	3.60E-21	-0.34	1.42E-05	-0.40	9.75E-08	co-target	Cnot6l
ENSMUSG000000 34751	381	-0.33	3.13E-02	-0.36	1.27E-02	-0.01	9.62E-01	0.34	2.38E-02	co-target	Mast4

ENSMUSG000000 35107	9699	-0.73	3.91E-49	-0.89	1.15E-73	-0.47	6.09E-20	-0.63	1.85E-37	co-target	Dcdbl2
ENSMUSG000000 35226	855	-0.58	7.23E-08	0.01	9.53E-01	-1.96	7.47E-45	-1.95	4.96E-92	co-target	Rims4
ENSMUSG000000 35392	441	-1.03	5.40E-17	-0.62	2.27E-06	-0.49	2.39E-04	-0.16	3.01E-01	co-target	Denn1a
ENSMUSG000000 35696	1479	-0.92	1.26E-43	-0.60	5.59E-19	-0.57	7.09E-16	-0.30	3.05E-05	co-target	Rnf38
ENSMUSG000000 36606	5250	-1.76	2.36E-208	-1.79	6.87E-202	0.12	5.69E-02	0.46	6.78E-16	co-target	Plxnb2
ENSMUSG000000 37235	1124	0.22	5.96E-02	-0.11	3.87E-01	-0.73	1.55E-09	-0.46	1.86E-05	co-target	Mxd4
ENSMUSG000000 37486	1498	-0.52	2.58E-08	-0.70	2.03E-13	-0.74	1.67E-14	-0.66	1.33E-11	co-target	Asxl2
ENSMUSG000000 37703	207	-0.57	1.12E-03	0.21	3.29E-01	-0.82	9.97E-06	-0.24	2.77E-01	co-target	Lzts3
ENSMUSG000000 37736	2853	-0.11	6.12E-02	-0.12	5.03E-02	-1.35	1.07E-107	-0.84	8.53E-47	co-target	Limch1
ENSMUSG000000 37750	591	-0.42	1.21E-04	-0.32	4.08E-03	0.24	4.64E-02	0.01	9.70E-01	co-target	Fam22b
ENSMUSG000000 38679	6332	-0.52	3.40E-17	-0.64	1.82E-25	-0.55	2.50E-18	-0.56	1.09E-19	co-target	Trps1
ENSMUSG000000 38764	762	0.10	3.95E-01	-0.53	6.70E-08	0.40	1.28E-04	-0.01	9.45E-01	co-target	Ptpn3
ENSMUSG000000 38780	1638	-0.09	2.74E-01	0.10	3.07E-01	-0.37	3.11E-06	0.02	8.73E-01	co-target	Smurf1
ENSMUSG000000 39738	757	-0.96	7.62E-24	-1.03	5.32E-24	0.08	5.53E-01	-0.01	9.28E-01	co-target	Slx4
ENSMUSG000000 40842	3710	-0.80	5.22E-50	-0.64	4.50E-30	-0.70	3.78E-36	-0.34	3.80E-09	co-target	Szrd1
ENSMUSG000000 41530	1354	-1.01	3.43E-36	-0.68	2.30E-17	-0.85	2.16E-23	-0.82	1.32E-23	co-target	Ago1
ENSMUSG000000 41741	806	-0.72	1.28E-09	-1.27	5.90E-43	-0.43	1.05E-03	-0.62	4.51E-11	co-target	Pde3a
ENSMUSG000000 42225	760	-1.16	1.94E-27	-0.65	7.00E-08	0.35	1.98E-03	0.47	7.39E-05	co-target	Ammecr1
ENSMUSG000000 42500	24	-0.03	9.58E-01	1.09	2.20E-03	-1.14	7.09E-03	-0.52	2.53E-01	co-target	Ago4
ENSMUSG000000 43241	1113	-0.98	1.12E-40	-0.53	1.89E-11	-0.37	3.06E-06	-0.17	5.46E-02	co-target	Upf2
ENSMUSG000000 43311	143	-0.34	9.37E-02	-0.34	9.14E-02	-0.09	7.39E-01	-0.22	3.24E-01	co-target	D17H6S53E
ENSMUSG000000 44950	1093	-0.23	1.31E-02	-0.37	3.47E-05	-0.07	5.74E-01	-0.31	9.75E-04	co-target	Pwwp2a
ENSMUSG000000 45817	2983	-1.65	1.18E-156	-2.03	7.38E-208	-1.00	4.23E-56	-0.71	2.55E-29	co-target	Zfp36l2
ENSMUSG000000 46709	439	-0.55	6.60E-06	0.13	4.29E-01	0.52	1.80E-05	1.53	3.51E-40	co-target	Mapk10
ENSMUSG000000 46873	1387	-0.44	1.08E-08	-0.84	8.31E-27	-0.82	9.53E-25	-0.58	5.98E-13	co-target	Mbtps2
ENSMUSG000000 47412	897	-0.26	3.23E-03	-0.40	3.46E-06	-0.26	5.55E-03	-0.44	4.78E-07	co-target	Zbtb44
ENSMUSG000000 47747	63	-0.13	7.01E-01	0.42	1.51E-01	-0.77	1.55E-02	-0.36	2.85E-01	co-target	Rnf150
ENSMUSG000000 47888	2841	-0.19	9.95E-03	-0.24	6.32E-04	-0.40	8.85E-08	-0.42	7.25E-10	co-target	Tnrc6b

ENSMUSG000000 48251	147	-0.30	1.22E-01	-0.74	1.91E-04	0.33	1.04E-01	-0.48	2.45E-02	co-target	Bcl11b
ENSMUSG000000 49281	17	-1.21	3.73E-03	-0.04	9.58E-01	-1.53	3.62E-04	0.76	1.32E-01	co-target	Scn3b
ENSMUSG000000 50295	215	-0.95	5.15E-08	-0.28	1.34E-01	0.37	4.75E-02	1.05	3.94E-12	co-target	Foxc1
ENSMUSG000000 50312	334	0.14	3.10E-01	0.21	1.55E-01	-0.78	1.24E-08	-0.24	1.39E-01	co-target	Nsun3
ENSMUSG000000 50910	1286	-0.50	3.15E-08	-0.51	2.18E-08	-0.35	3.70E-04	0.63	1.31E-12	co-target	Cdr2l
ENSMUSG000000 53477	7424	-0.83	1.02E-62	-1.15	1.17E-119	-0.94	5.56E-75	-0.91	1.45E-74	co-target	Tcf4
ENSMUSG000000 53838	2646	-0.12	6.23E-02	-0.33	7.94E-08	-0.61	1.77E-25	-0.43	2.13E-12	co-target	Nudcd3
ENSMUSG000000 54256	1056	-0.40	4.74E-05	0.13	2.36E-01	-0.95	8.52E-21	-0.74	5.85E-14	co-target	Msi1
ENSMUSG000000 56153	573	-0.01	9.67E-01	0.33	2.23E-03	0.25	4.97E-02	0.18	1.49E-01	co-target	Socs6
ENSMUSG000000 59602	192	0.11	6.08E-01	-0.46	7.47E-03	-0.61	3.03E-03	-0.93	9.69E-08	co-target	Syn3
ENSMUSG000000 59820	426	-0.39	5.37E-03	-0.20	2.35E-01	-0.83	5.89E-09	-0.46	3.36E-03	co-target	AU019823
ENSMUSG000000 61186	1167	-0.66	2.32E-13	-0.57	3.83E-10	0.00	9.81E-01	0.20	4.51E-02	co-target	Sfmbt2
ENSMUSG000000 61665	2309	-0.57	7.38E-19	-0.65	5.69E-23	-0.53	4.25E-15	-0.58	1.44E-17	co-target	Cd2ap
ENSMUSG000000 63273	4093	-0.31	9.42E-06	-0.52	1.61E-13	-0.35	6.21E-07	-0.31	2.18E-05	co-target	Naa15
ENSMUSG000000 79654	3	0.68	NA	0.93	3.22E-02	-0.09	NA	0.33	NA	co-target	Prmt4
ENSMUSG000000 84883	161	-0.61	7.85E-04	-0.95	1.25E-06	-0.71	2.84E-04	-0.48	2.51E-02	co-target	Ccdc85c

jennifer cherone

CELL (949) 525-8114 • E-MAIL jennifer@cherone.net • [linkedin.com/in/jcherone](https://www.linkedin.com/in/jcherone)

Molecular and computational biologist with a strong expertise in genome editing, high throughput sequencing data analysis, and post-transcriptional gene regulation with a focus in microRNAs.

EDUCATION

Massachusetts Institute of Technology

PhD Candidate in Biology

Expected Fall 2018

University of California at Berkeley

BA in Molecular and Cell Biology with Honors, emphasis in Genetics, Genomics and Development 2011

RESEARCH EXPERIENCE

The Burge Laboratory, Massachusetts Institute of Technology: PhD Candidate 06/2013 – Present

- Execute a multidisciplinary approach combining cutting-edge genome editing technology, genome-wide computational analyses, and molecular and cell biology techniques to study miRNAs in neuronal differentiation and their global overlap in targeting capability.
- Engineered protein and synthetic binding domain fusions for use in a tethered splicing reporter assay to generate an RNA map of RNA binding protein splicing.

MIT Graduate School Rotations

02/2013 – 05/2013

The Zhang Laboratory: Tested alternative Cas9 enzymes to improve cleavage efficiency and specificity of the CRISPR/Cas9 system.

The Young Laboratory: Improved chem-seq protocol to discover any drug's genomic interactions.

Sangamo Biosciences, Inc.: Research Assistant for therapeutic development

01/2010 – 06/2012

- Implemented and characterized novel DNA binding domains: including zinc finger nucleases, transcription activator-like effector nucleases, and zinc finger proteins for genetic engineering and gene therapy.
- Optimized assay for allele specific detection of repression of the Huntington's gene.
- Executed independent honors research investigating the transcriptional response to ZFN-specific DNA damage in human cells through a genome-wide expression profile comparison of ZFNs with varied specificity.

Tissue Culture Facility, University of California Berkeley: Laboratory Technician

09/2008 – 12/2009

- Maintained over 50 cell lines and prepared orders for UC Berkeley labs.

TALKS & PRESENTATIONS

RNA Society, Poster

June 2018

Cold Spring Harbor Labs: Eukaryotic mRNA Processing, Talk

August 2017

MIT Biology Graduate Retreat, Talk

May 2017

Gordon Research Conference: Post-transcriptional Gene Regulation, Poster

July 2016

Keystone Symposia: Axons: From Cell Biology to Pathology, Poster

January 2015

RNA Society, Poster

June 2014

PUBLICATIONS

- Jennifer M. Cherone, Vjola Jorgji, Christopher B. Burge. **Cotargeting among microRNAs is widespread, and is highly enriched in the brain** (Manuscript in preparation.)
- Eric T Wang, Amanda J Ward, Jennifer M Cherone et al. Antagonistic regulation of mRNA expression and splicing by CELF and MBNL proteins. Genome Research. 2015 Jun; 25(6):858-71. Epub 2015 Apr 16.
- D Hockemeyer, H Wang, S Kiani et al. Genetic Engineering of human pluripotent cells using TALE nucleases. Nature Biotechnology. 2011 Jul; 29(8):731-4. Epub 2011 Jul 7.
- John J. Young, Jennifer M. Cherone et al. Efficient targeted gene disruption in the soma and germ line of the frog *Xenopus tropicalis* using engineered zinc-finger nucleases. Proc Natl Acad Sci. 2011 Apr; 108(17):7052-7. Epub 2011 Apr 6.
- Jeffrey B. Doyon, Bryan Zeitler, Jackie Cheng et al. Rapid and efficient clathrin-mediated endocytosis revealed in genome-edited mammalian cells. Nature Cell Biology. 2011 Mar; 13(3):331-7. Epub 2011 Feb 6.

AWARDS & SCHOLARSHIPS

MIT \$100K Pitch Competition Semi-finalist; Data Analytics Prize Finalist	2017
Spencer W. Brown Award in Genetics, Genomics, and Development	2011
Rose Hills Foundation Science and Engineer	08/2010 – 05/2011
May J. Koshland Scholarship	08/2010 – 05/2011
Dean's Honor List	Fall 2009
ELK National Foundation Scholarship	08/2007 – 05/2011
James R. Hoffa Memorial Scholarship	08/2007 – 05/2011
Cheng Scholarship	08/2007 – 05/2008
California School Employees Association Scholarship	2007
California State Parent Teacher Student Association Scholarship	2007
Orange County Teachers Federal Credit Union Scholarship	2007

COMMUNICATION SKILLS

- MIT Resource for Easing Friction and Stress (REFS), BioREFS Representative** 02/2017 – Present
- Completed 40-hour Conflict Management Training.
 - Act as a resource to help fellow graduate students manage stress and maintain a healthy lifestyle.
- Office of the Dean for Graduate Education Fellow, Graduate Accomplishments Writer** 09/2014 – 07/2016
- Independently researched and wrote articles for MIT news on graduate student work and accomplishments.
 - Coordinated Graduate Appreciation Week, including inspirational faculty seminars and student reception.
- Berkeley Scientific Journal, Interviews Editor** 01/2009 – 05/2011
- Produced a fully encompassing online journal featuring undergraduate research, editorials, and interview profiles with professors.

MANAGEMENT & LEADERSHIP SKILLS

- Cydan Development, Inc. Consultant** 10/2017 – 04/2018
- Worked directly under the CEO and CSO to help them explore an area of interest for investment.
- Broad Biomedical Entrepreneurship Course** 01/2017 – 03/2018
- 2018 Course Organizer: structured curriculum, selected participants, and coordinated public pitch night event.
 - 2017 Course Participant: developed and pitched business plan for StratiFYRE to a panel of venture capitalists.
- Biology Career Lunch Series, Founder and Organizer** 01/2017 – Present
- Founded and moderate department events hosting individuals from careers outside of academia to share their experiences and career insights with a group of graduate students over monthly lunches.
- MIT *Committed to Caring* Program Coordinator** 08/2016 – 09/2017
- Led production of photo-shoots and written material to celebrate faculty who are nominated and selected by graduate students for excellent mentoring.
- Sloan School of Management Healthcare Certificate** 08/2015 – 03/2017
- Designed real world solutions for complex operational problems within multi-disciplinary teams.
 - Innovation Teams: Developed a commercialization strategy for a new MIT technology, Aluminum fuel.
 - Healthcare Lab: Solved critical care delivery inefficiencies at Lahey Health Cancer Institute.

TEACHING EXPERIENCE

- Massachusetts Institute of Technology, Graduate Student Instructor**
- Introductory Biology & Genetics** Fall 2013; Spring 2016
- Led biweekly sections, drafted problem sets and exams with fellow course instructors.
- UC Berkeley Student Learning Center, Organic Chemistry Study Group Leader** 08/2009 – 05/2011
- Lectured two-hour biweekly review course with subsequent problem-solving session.
 - Created and customized lesson plans, lectures, problem sets, and mock exams based off of lecture.
 - Hosted mock exam session for midterms and final with more than half the course in attendance.